PROCEEDINGS

of an

INFORMAL MEETING

on

LINKS BETWEEN WEAK AND ELECTROMAGNETIC

INTERACTIONS

Held at Rutherford High Energy Laboratory
on 24 and 25 February 1973.

W. T. Toner)
) Editors
R. K. P. Zia)

CONTENTS

FOREWORD

This proceedings contains the text of talks given at an informal meeting
on

        'Links between weak and electromagnetic interactions'

which was held at the Rutherford Laboratory on 24th and 25th February 1973.

In the interests of speedy publication, editing has been limited to
ensuring that the figures appear in the text of the talks. Otherwise,
where possible, no changes have been made to the scripts kindly provided
by the authors.

We would like to thank Mr. P. Nicholls and Mr. F. Harden for their help
in organising the meeting.

                                        W. T. Toner
                                        R. K. P. Zia

An Introduction to Renormalizable Theories of Weak

Interactions and their Experimental Consequences.

C.H. Llewellyn Smith

CERN, Geneva.

Caution:

These notes are an extended transcript of the view graph
transparencies for the talk I gave at the Rutherford Laboratory
Meeting on "Links between Weak and Electromagnetic Interactions"
(February 24-25, 1973). They were rapidly compiled at the insistence
of the organisers in the hope that they may be useful to the
participants; they are rough, incomplete and unreliable. The
references are inadequate but a short bibliography is included
at the end. A detailed write up of courses of lectures on the same
subject which I shall give at CERN and various summer schools may
be available later as a CERN preprint.

Problems with the Phenomenological Theory of Weak Interactions

In the "phenomenological theory", weak interactions are described by the Lagrangian

$$\mathcal{L} = \frac{G}{\sqrt{2}} J_\lambda^\dagger(x) J_\lambda(x)$$
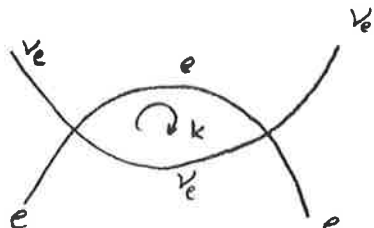
where

$$G = \frac{10^{-5}}{M_p{}^2}$$

$$J_\lambda = J_\lambda^{\text{hadronic}} + J_\lambda^{\text{muonic}} + J_\lambda^{\text{electronic}}$$

$$J_\lambda^{\text{hadronic}} = \text{Cabibbo current}$$

$$J_\lambda^{\text{muonic}} = \bar{\mu}(x)\, \gamma_\lambda(1-\gamma_5)\nu_\mu(x)$$

$$J_\lambda^{\text{electronic}} = \bar{e}(x)\gamma_\lambda(1-\gamma_5)\nu_e(x)$$

In lowest order this Langrangian gives an excellent description of all known leptonic and semileptonic processes (apart from T violation; there is also some trouble for non-leptonic processes eg. with the $\Delta I = \frac{1}{2}$ rule). In next order divergent integrals are encountered:

$$\longrightarrow \qquad \int \frac{d^4k}{k^2} = \infty \quad !$$

Unlike the case in QED, we cannot absorb these infinities by re-defining the "bare" masses and coupling constants so as to reproduce the correct physical values in each order. To render all matrix elements finite new arbitrary constants (which can, however, be determined by experiment) must be introduced in each order i.e. the theory is non-renormalizable.

Sometimes <u>an effective Lagrangian philosophy</u> is adopted and higher orders are simply ignored. This must fail at high energies. In (e.g.) the amplitude
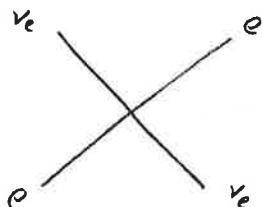
the electron mass can be safely neglected at high energy so that, on dimensional grounds,

$$\sigma \sim G^2 s$$

But this is an S wave process (it takes place at a point with zero impact parameter); hence, by unitarity,

$$\sigma \leq const / s$$

and the theory must fail at the "unitarity limit" $S \sim \frac{1}{G} \sim 10^5$ GeV^2. That this "bad high energy behaviour" is connected with the non renormalizability becomes clear when we consider calculating second order processes in terms of lowest order cross sections using dispersion relations e.g. in order G^2 the amplitude for forward νe scattering is given by

$$A(\nu e \to \nu e)\Big|_{t=0} \sim \int_0^\infty \left(\frac{\sigma^{\nu e}(s')}{s'-s} - \frac{\sigma^{\bar\nu e}(s')}{s'+s} \right) ds'$$

Since $\sigma^{\nu e} \sim 3\sigma^{\bar{\nu}e} \sim G^2 s'$, two (arbitrary) subtraction constants must be introduced. We therefore seek a theory with "good" high energy behaviour which seems desirable 1) because of the connection with renormalizability 2) because perturbation theory must be totally misleading when it violates unitarity.

For the particular process considered above the situation is improved by <u>introducing a vector meson</u> - W:-

$$\frac{G}{\sqrt{2}} = \frac{g_w^2}{M_w^2}$$
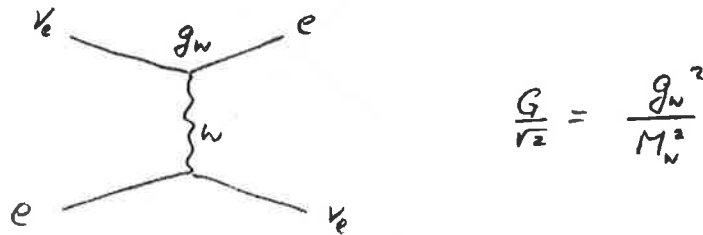
g_w is dimesionless and hence

$$\frac{d\sigma^{\nu e \to \nu e}}{dQ^2} \sim \frac{g_w^4}{(Q^2+M_w^2)^2} \quad , \quad \sigma \sim \frac{g_w^4}{M_w^2}$$

The partial wave amplitudes now only voilate unitarity logarithmically (at energy $S \sim M_w^2\, e^{1/GM_w^2}$) and the forward dispersion relation now needs only one subtraction (note that $\sigma^{\bar{\nu}e \to \bar{\nu}e} \sim g_w^4/s$).*

However, the situation is as bad as ever in the process:
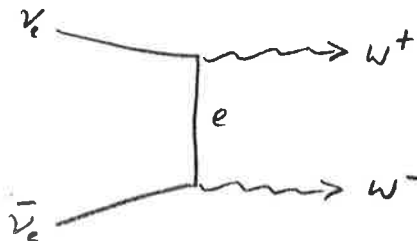
In its rest frame the possible polarization states of the W are
described by the vectors

$$
\begin{matrix} t \\ x \\ y \\ z \end{matrix}
\underbrace{\begin{pmatrix} 0 \\ 1 \\ 0 \\ 0 \end{pmatrix}, \begin{pmatrix} 0 \\ 0 \\ 1 \\ 0 \end{pmatrix}}_{\epsilon_T}, \underbrace{\begin{pmatrix} 0 \\ 0 \\ 0 \\ 1 \end{pmatrix}}_{\epsilon_L}
$$

----

* Footnote to page 3.

In a renormalizable theory we must ensure that to lowest
order __either__ $\sigma_{tot}^{\nu e}$ and $\sigma_{tot}^{\bar{\nu} e}$ vanish asymptotically
__or__, if they tend to constants, in order that

$$
\sigma_{tot}^{\nu e} / \sigma_{tot}^{\bar{\nu}e} \rightarrow 1
$$

the forward dispersion relation converges. The latter possibility is
realised in the models discussed below. It is not hard to see that
this requires the existence of neutral bosons (Z) and/or heavy leptons.
We will follow a slightly different approach in motivating the existence
of these objects and "deriving" their properties but it is instructive
to think about the role they play in the process considered here.

Under a Lorentz boost along OZ

$$\epsilon_T \rightarrow \epsilon_T$$

$$\epsilon_L \rightarrow \left(|\vec{k}|, 0, 0, \frac{k_o}{M_W} \right)$$

$$= \frac{k}{M_W} + O\left(\frac{M_W}{k_o}\right)$$

Hence, dimensionally,

$$\sigma(\nu\bar{\nu} \rightarrow W_T W_T) \xrightarrow{\ s \rightarrow \infty\ } \text{const}$$

but

$$\sigma(\nu\bar{\nu} \rightarrow W_L W_L) \xrightarrow{\ s \rightarrow \infty\ } g_W^4 s / M_W^4$$

which rapidly violates unitarity and makes two subtractions necessary
in the forward dispersion relation for
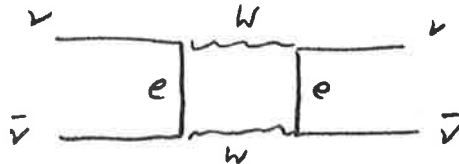
(the total cross section in the crossed channel — $\sigma(\nu\nu)$ — is zero in
lowest order in the phenomenological model).

Alternatively, the W propagator is

$$\frac{\sum\limits_{pol} \epsilon_\mu^* \epsilon_\nu}{k^2 - M_W^2} = \frac{-g_{\mu\nu} + \frac{k_\mu k_\nu}{M_W^2}}{k^2 - M_W^2} \xrightarrow{\ k \rightarrow \infty\ } \text{const.}$$

which makes loop integrals diverge.

To <u>repeat</u>: There seems to be more hope of making a sensible theory where we introduce W's because g_w is dimensionless. However, serious trouble occurs with longitudinal W's because

$$\epsilon_\mu^L = \frac{k_\mu}{M_w} + O\left(\frac{M_w}{k_o}\right)$$

at high energies. To keep the dimensions of cross sections etc. correct the factor $1/M_w$ is accompanied by powers of E. What happens with longitudinal (virtual) γ's in QED? Do not similar problems occur? The answer is no, because of gauge invariance. S matrix elements are invariant under the replacement

$$\epsilon_\mu^{\gamma_i} \longrightarrow \epsilon_\mu^{\gamma_i} + \lambda k_\mu^{\gamma_i} \quad ;$$

this suggests pieces of ϵ_μ proportional to k_μ are impotent.

It would obviously be desirable to generalize gauge invariance to massive charged vector fields; we return to this later.

Motivation for Elements of Renormalizable Models

In a renormalizable perturbation theory the offending
high energy behaviour of the amplitude corresponding to
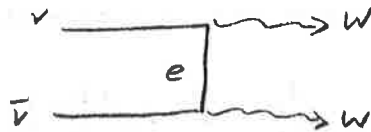
must be cancelled by other contributions in the same order.
The only possibilities are to introduce new exchanges in the s
channel (neutral current) or t or u channels (heavy leptons):
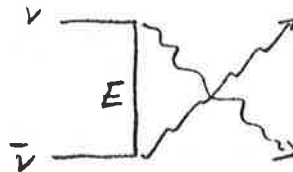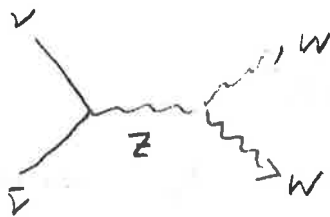
Thus there must be neutral currents and/or heavy leptons (the reason
why we have drawn the heavy lepton in the u channel will become clear later).

Trouble also occurs in the amplitudes
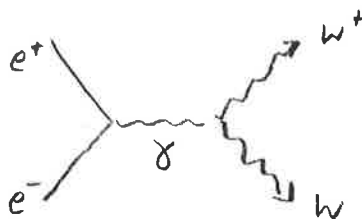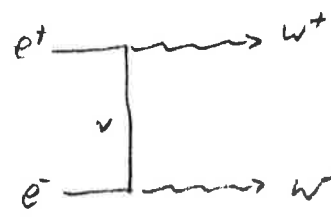
Complete cancellation of the undesirable terms using only these diagrams is impossible because parity is violated in one but not the other (we can polarize the electrons so that the second diagram does not contribute). Cancellation requires new exchanges:-
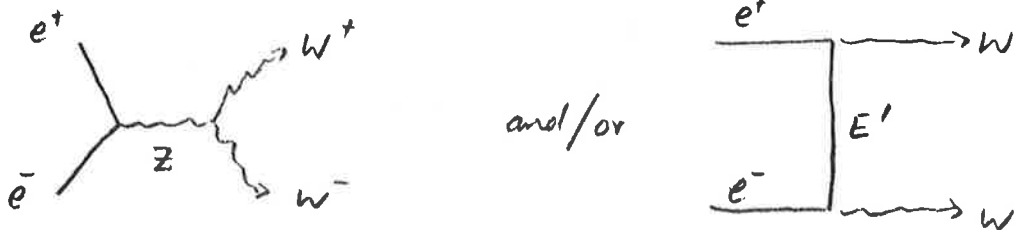
It is economical (but not necessary) to use the same mechanism to cancel the "bad" behaviour of diagrams A and B simultaneously and the same (related) neutral boson (heavy lepton) to achieve cancellation in $\bar{\nu}\nu \rightarrow$ WW and $e^+e^- \rightarrow$ WW; this leads us to <u>unify weak and electromagnetic interactions</u>. Note that in this case we expect $g_W \sim e$ and hence

$$M_W \sim \left[\frac{e^2 \sqrt{2}}{G} \right]^{\frac{1}{2}} \quad = 106 \text{ GeV.}$$

An example; the Georgi-Glashow Model.

We consider explicitly a model with only heavy leptons (Georgi-Glashow), rather than the other "minimal model" with only a neutral current (Weinberg-Salam), because it is probably the simplest and you are probably all bored with the Weinberg model by now.

Clearly
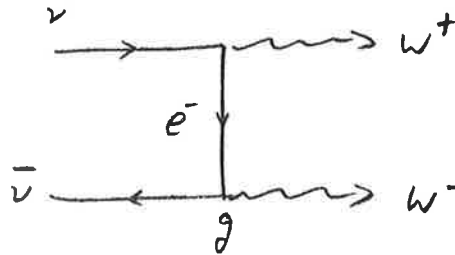
cannot be cancelled with
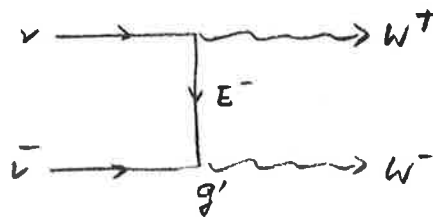
since the e and E masses can be neglected at high energy and the sum of the amplitudes must be proportional to $g^2 + g'^2$. Rather we must try to cancel with
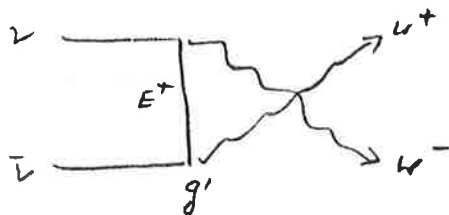
i.e. ν_e, e^- and E^+ (and likewise ν_μ, $\mu-$ and M^+) have the same lepton number. Diagrams C and D differ only in a labelling of the particles if the lepton masses are neglected and the amplitudes can differ at

most by a sign. This happens in fact and cancellation requires

$$g^2 - g'^2 = 0$$

Diagrams A and B above must be combined with:

$$g_L \gamma_\mu (1 - \gamma_5) + g_R \gamma_\mu (1 + \gamma_5)$$
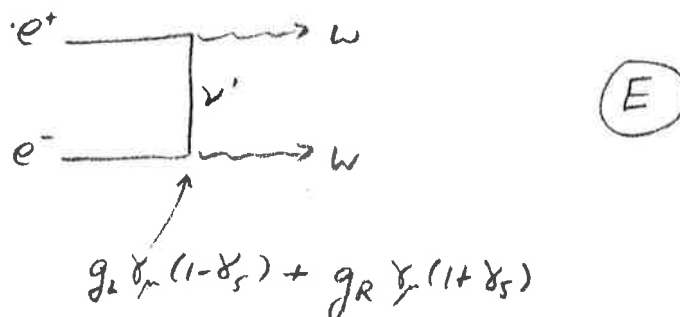
where ν' is a "heavy neutrino" (heavy neutral lepton).

A little algebra shows that cancellation of the worst part of the right and left handed amplitudes between A, B and E requires:

$$\frac{1}{4} e^2 = g_R^2$$

$$\frac{1}{4} e^2 = g^2 + g_L^2$$

(Hence $M_W^2 = \frac{\sqrt{2} g^2}{G} \leq \frac{\sqrt{2} e^2}{4G} = (53 \text{ GeV})^2$)

Similarly the $E^+ \nu' W$ coupling is adjusted to give cancellations in $E^+ E \rightarrow W^+ W^-$ and $\nu' \bar{\nu}' \rightarrow W^+ W^-$. The resulting interaction can be written in the compact form:

$$\mathcal{L} = e \vec{W}_\lambda \cdot (\vec{\Psi} \times \gamma_\lambda \vec{\Psi})$$

12.

where $W^{\pm}$ and γ form the "isovector" $\vec{W}$ and

$$\vec{\psi} = \vec{\psi}_R + \vec{\psi}_L$$

with

$$\vec{\psi}_L = \frac{1}{2}(1-\gamma_5)\begin{pmatrix} E^+ \\ \nu\cos\theta + \nu'\sin\theta \\ e^- \end{pmatrix}$$

$$\vec{\psi}_R = \frac{1}{2}(1+\gamma_5)\begin{pmatrix} E^+ \\ \nu' \\ e^- \end{pmatrix}$$

$$g = \frac{e\cos\theta}{2}$$

Similarly we can "derive" the Weinberg model. In that case we also get an "isospin invariant" type of interaction such as occurs in Yang-Mills (or general gauge invariant) theories, to which we shall turn after considering the general case.

Cancellation of leading divergences in the general case

Let all fundamental spin $\frac{1}{2}$ leptons be placed in a vector

$$\psi = \begin{pmatrix} \nu_e \\ e \\ \nu_\mu \\ \mu \end{pmatrix}$$

(where ν_μ and μ^- could be replaced by $\bar{\nu}_\mu$ and μ^+ depending on what conservation laws we want to embody in the theory) and let there be an arbitrary number of vector mesons $W\mu^i$ ($i = 1, 2 \ldots\ldots$). Suppose we collide beams of left handed leptons and antileptons; the lowest order amplitude for producing two W's is described by:
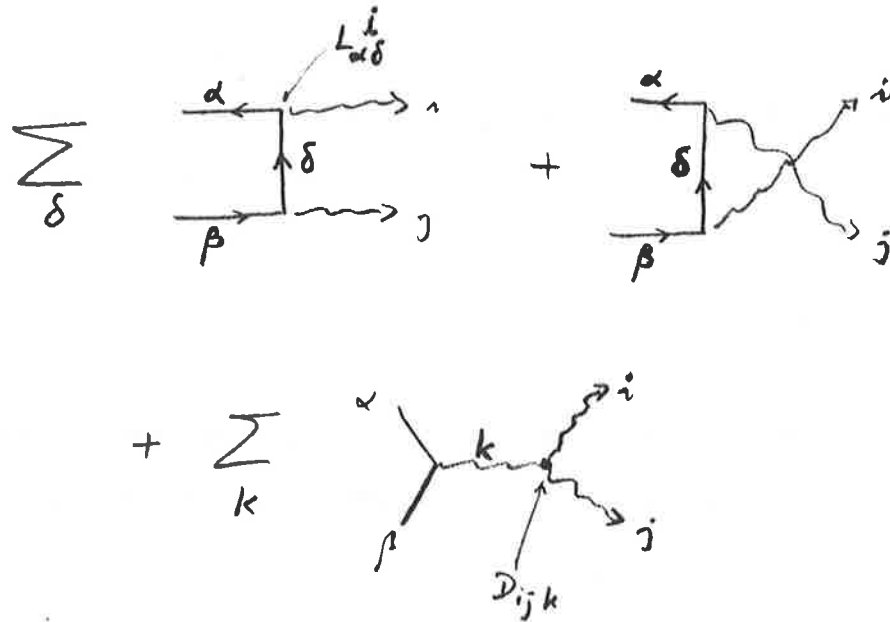
From the discussion of the Georgi-Glashow model it should be clear that the sum of the worst contributions of the first two diagrams is proportional to

$$\sum_\delta \left(L^i_{\alpha\delta} L^j_{\delta\beta} - L^j_{\alpha\delta} L^i_{\delta\beta} \right)$$

This must cancel a piece proportional to $\quad \sum \mathcal{D}_{ijk} L^k_{\alpha\beta}$

In fact the cancellation condition is

$$[L^i, L^j] = \sum_k i \mathcal{D}_{ijk} L_k$$

A similar condition can obviously be derived for the couplings of right handed leptons. We see that an underlying group structure (which is characteristic of a Yang-Mills theory) is required to achieve desirable high energy behaviour to leading order (the next to leading order "bad behaviour" must also be eliminated; we return to this below).

Gauge Invariance

We recall that charge conservation is expressed formally by saying that the Lagrangian is invariant when the phase of every field (i) with charge e_i is changed thus

$$\psi_i \longrightarrow e^{ie_i \chi} \psi_i$$

This ensures that in (e.g.) a vertex described by an interaction $\phi_A \bar{\psi}_B \psi_C$ the charges satisfy $e_A + e_C = e_B$. Can we make a theory which is invariant when we replace the constant χ by a function $\chi(X)$, i.e. invariant under local phase changes which differ at different points of space-time? Under these transformations the kinetic energy term in the Lagrangian changes thus

$$\bar{\psi}\gamma^\mu \partial_\mu \psi \longrightarrow \bar{\psi}\gamma^\mu(\partial_\mu + ie\partial_\mu \chi)\psi$$

Nevertheless, as you all know, invariance can be achieved if (as a minimal requirement) we replace ∂_μ by $\partial_\mu - ie A_\mu$, where A_μ is a massless vector field (the photon) which is supposed to transform as follows

$$A_\mu \longrightarrow A_\mu + \partial_\mu \chi$$

This is gauge invariance. In momentum space, the gauge transformation changes the polarization vectors of all photons from $\epsilon_\mu^{\gamma\wedge}(k)$ to

$\epsilon_\mu^{\gamma i}(k) + i k_\mu^{\gamma i} \hat{\chi}(k)$; because S matrix elements are independent of χ, it turns out that pieces of ϵ proportional to k can be ignored effectively. We would like to generalize this transformation to allow for charged vector fields, with mass if possible.

Generalized Gauge Invariance

We wish to mimic the discussion above for some transformation which connects particles with different charge; we consider isospin as an example. Isospin invariance is expressed formally by requiring the Lagrangian to be invariant under

$$\psi_i \longrightarrow e^{ig \frac{\vec{\tau_i} \cdot \vec{\Lambda}}{2}} \psi_i \,,$$

where i labels different isospin multiplets and $\vec{\tau_i}$ are the appropriate generalized Pauli matrices. Can we let $\vec{\Lambda} \to \vec{\Lambda}(x)$? i.e. can we find a theory which is invariant when we make different isospin rotations at different points of space time? This questions was posed by

Yang and Mills. The answer is yes-provided we introduce an isospin multiplet of massless fields $\vec{W}_\mu{}'x)$ which are coupled invariantly to themselves and transform as

$$\vec{W}_\mu \longrightarrow \vec{W}_\mu + \partial_\mu \vec{\Lambda}(x) + g\, \vec{\Lambda}(x) \times \vec{W}_\mu(x)$$

and replace ∂_μ by $\partial_\mu - ig\, \dfrac{\vec{\tau}\cdot\vec{W}_\mu}{2}$ in the fermion kinetic energy term. This is Yang-Mills theory. As before we can make a gauge transformation which changes pieces of $\vec{\epsilon}_\mu(k)$ proportioned to $k\mu$ while leaving S matrix elements invariant. It is believed that massless Yang-Mills theory is renormalizable (however it is hopelessly infrared divergent); from the point of view adopted here, there is a cancellation between badly behaved terms which occurs systematically order by order because of the high degree of symmetry of the theory. In fact the isospin matrices $\vec{\tau}$ satisfy precisely the cancellation condition derived in the previous section.

This is all very nice except that generalized gauge invariance requires $M_W = 0$ in the Lagrangian, and that fermion masses are zero (unless parity is conserved and the fermions in a given multiplet are exactly degenerate). This disagrees with the only fact known about the W; namely that if it exists at all, then $M_W > 2.5$ GeV. The only hope seems to be that the mass is generated "spontaneously" i.e. that we can find a field theory whose solution has $M_w \neq 0$ although the original Lagrangian has $M_w = 0$. Similarly we would like fermion mass differences (and masses, at least in part) to be generated spontaneously .

Before we discuss a model which shows how this may come about,
we try to motivate it by returning to the cancellation strategy.

Motivation for the "Spontaneous Mass Generating Mechanism"

We consider as an example the Georgi-Glashow model discussed
above. In lowest order, $W^+W^+ \rightarrow W^+W^+$ is described by the diagrams:-
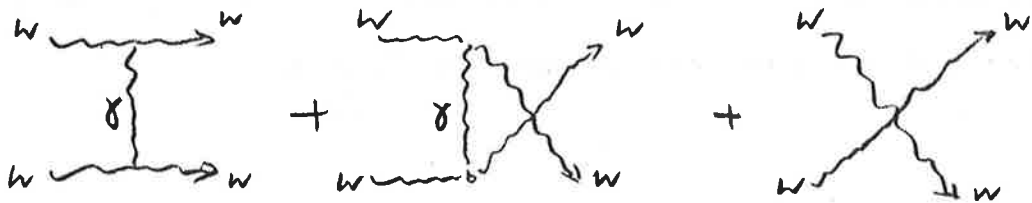
On dimensional grounds we might fear that the amplitude grows
as S^2/M_W^4 as $S \rightarrow \infty$ (in the fixed c.m. angle limit) when all
four W's are longitudinal. In fact, however, the Yang Mills
structure ensures a cancellation of S^2 terms between the seagull and
the first two terms (we could turn the argument around and derive the
form of the W-W interaction by demanding cancellation; see my forth-
coming paper listed in the bibliography). However a term which
grows like S/M_W^2 remains and violates unitarity; it cannot be
removed without introducing new exchanges. The simplest possibility
is
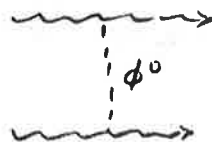
with a vertex: $g_\phi \phi W_\mu W^\mu$. This gives a contribution

$\sim g_\phi^2 s / M_W^4$ which must cancel the $\frac{g^2 s}{M_W^2}$ contribution from the

original diagrams;   hence $g_\phi \sim g M_W$.

The ϕ is also needed to remove some residual terms in

$\bar\nu \nu \to W_L^+ W_L^-$ and other processes of this type; the commutator

condition removes a term which grows like $\frac{s}{M_W^2}$ but terms like $\frac{m_\ell \sqrt{s}}{M_W^3}$

persist stubbornly. They can only be removed by introducing new

exchanges. Using the ϕ we soon find that it can do the job provided

it coupled to leptons with strength $\sim g \frac{m_{lepton}}{M_W}$.

Thus we learn from the cancellation condition that well

behaved theories must involve scalar fields ϕ coupled to W's with

strength $\sim g\, M_W$ and to leptons with strength $\sim g \frac{m_{lepton}}{M_W}$ (the

coupling to leptons could be avoided if parity were conserved and all

leptons in a given multiplet were degenerate). Thus there seem to be

an intimate connection between the ϕ's and the masses which we

wish to generate spontaneously.

An example of spontaneous mass generation

Higgs studied the Lagrangian:

$$\mathcal{L} = -\tfrac{1}{4} F_{\mu\nu} F^{\mu\nu} - (\partial_\mu + ie A_\mu)\phi^* (\partial_\mu - ie A_\mu)\phi - m^2 |\phi|^2 - \lambda |\phi|^4$$

where ϕ is a complex field and, as usual,

$$F_{\mu\nu} = \partial_\mu A_\nu - \partial_\nu A_\mu$$

If $M^2 > 0$, this is just QED for a charged scalar particle.
What if $M^2 < 0$? In this case (if h>o) the classical potential
$V(\phi) = M_1^2|\phi|^2 + h|\phi|^4$ has the form
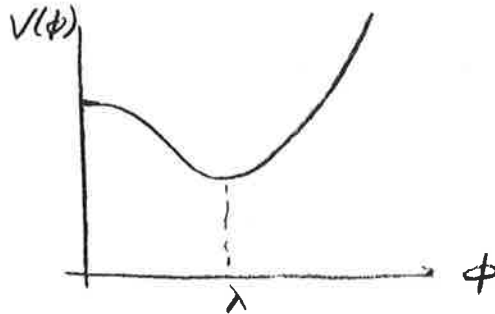
The classical ground state is at $\phi = \lambda$. This suggests that
perturbation theory about $\phi = 0$ would be unstable and it would be
better to change variable to $\phi^1 = \lambda + \phi$. Doing this the term $e^2 A_\mu A^\mu \phi^2$
becomes

$$e^2\lambda^2 A_\mu A^\mu + 2e^2\lambda A_\mu A^\mu \phi' + e^2 A_\mu A^\mu \phi'^2$$

The vector field acquires a mass $M_\omega \sim e\lambda$ and we find a $A_\mu A^\mu \phi'$
interaction with strength eM_ω, such as we encountered in the previous
section, where its necessary role was already discussed.

If we rewrite ϕ^1 in terms of two real fields ϕ_1 and ϕ_2 thus

$$\phi^1 = \phi_1 + i\phi_2$$

we find that ϕ_2 has zero mass — we seem to have traded one
undesirable massless particle for another (ϕ_2 is the Goldstone boson
which, as the erudite reader knows, is supposed to accompany any
"spontaneously broken" symmetry). However ϕ_2 is actually spurious

and effectively decouples from physical processes. One way to see this is to use the new real fields χ, θ and B_μ defined by

$$\phi = (\lambda + \chi) e^{ie\theta}$$

$$A_\mu = B_\mu + \partial_\mu \theta \ .$$

This change of variables is a gauge transformation which therefore leaves the Lagrangian independent of θ, as can easily be checked explicitly. Thus one degree of freedom of the scalar field vanishes; that this must happen is clear intuitively since the vector field (which has only two degrees of freedom when massless) acquires a degree of freedom when it becomes massive – the new state must come from somewhere since we do not expect the number of degrees of freedom to change when we change variables.

The new Lagrangian is supposed to be renormalizable, like the original one with $M^2 > 0$. The proof of renormalizability is hard. A clue to why it works is that using χ and B_μ the theory is manifestly unitary (the B propagator is

$$\frac{- g_{\mu\nu} + k_\mu k_\nu / M_w^2}{k^2 - M_w^2}$$

and the residue has the desired positivity) but not manifestly renormalizable while using A_μ , ϕ_1 and ϕ_2 it is manifestly renormalizable but not manifestly unitary (the A propagator turns out to be $-g_{\mu\nu}/(k^2 - M_w^2)$ and ϕ_2 turns out to be a ghost); if we can prove the naive expectation that the S matrix is the same in the manifestly unitary and the manifestly renormalizable gauge then it must be both renormalizable and

unitary.

The "spontaneous" part of fermion masses (mass differences) m^s is introduced by writing a coupling

$$\kappa \phi \bar{\psi} \psi \longrightarrow \kappa (\lambda + \phi') \bar{\psi} \psi$$

Hence $\kappa = m^s/\lambda = e\, m^s/M_W$ ————— a result whose

"phenomenological origin" (and necessity) was already discussed in the last section.

Problems With Models

The basic problem in model building is that it seems to be impossible to construct satisfactory models with three quarks and the usual Cabibbo current. The bad high energy behaviour of the quark – antiquark $\to W^+W^-$ amplitude:
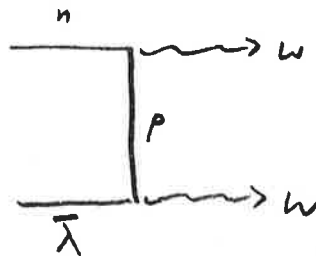
cannot be cancelled by a new S channel exchange since $\Delta S = 1$ neutral currents seem to be highly suppressed experimentally; therefore a new t or u channel exchange is required and the number of "quarks" must be increased to at least four (one might imagine that the neutral boson decouples from leptons; however, if it is self conjugate, it can couple back to $\bar{n}\lambda$ and hence induce (e.g.) a $K_L - K_S$ mass difference

in order G - in gross contradiction to experiment - this happens
in the otherwise ingenious "red white and blue" quark model
considered by Tonin).

One way out is to let the $p\bar{\lambda}W$ coupling be righ handed, in
which case there is no S/M_W^2 term from this amplitude; this
possibility was considered by T.C. Yang in a model based on $SU(2) \times U(1)$
which unfortunately needs θ cabibbo = 45°. Very recently Georgi
and Glashow have considered a model based on $SU(2) \times SU(2) \times U(1)$ in
which a "pseudo-Cabibbo" structure emerges very naturally; there
is no obvious conflict with experiment except that the sign of g_A
in $\Lambda \beta$ decay is opposite to the value obtained in the usual theory
and hence in bad disagreement with the experimental value (a study
of the history of weak interaction theory suggests that the model
should not necessarily be dismissed on account of this). There is a
potential oddity in this model which we mention to illustrate
possible dangers in model building. There is a residual $m_p\sqrt{s}/M_W^2$
term in the $n\bar{\lambda} \rightarrow W_L^+ W_L^-$ which must be cancelled by ϕ exchange(s).
This implies the existence of:-

if ϕ° is self conjugate.
We expect the $\phi\lambda\bar{n}$ amplitude to be of order $g m_p/M_W$ and hence
this amplitude may be of order $g^2 m_p^2 /(M_W M_\phi)^2$.
The observed value of the $K_L - K_S$ mass difference would then require
$M\phi > 100$ Mp. Perhaps this bizarre result can be avoided in some
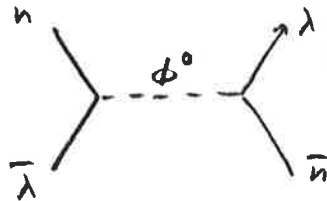
sufficiently ingenious scheme (otherwise we must check that it does not lead to unacceptably large contributions from loop integrations involving ϕ's).

Going beyond Gell-Mann-Zweig quarks, it is natural to consider 3 triplet models of the Han-Nambu (HN) type, which reproduce the results of the GMZ model for low lying un-charmed particles. Several schemes based on the HN model have been proposed; all are somewhat arbitrary - in particular weak universality has to be put in by hand in models based on the Georgi-Glashow scheme by adjusting the parameter Θ introduced above so that $g_{leptonic} = \dfrac{e \cos \Theta}{2} = g_{hadronic}$ (for that matter electromagnetic universality must be put in by hand in models of the Weinberg type). Various other more or less ad hoc schemes involving 5, 8, 11 ... "quarks" have been proposed.

To <u>summarise</u>: there are no entirely satisfactory models at the moment but all involve charmed particles and/or breakdowns of the Cabibbo theory and, in some cases, current (light-cone) algebra-all of which should be sought experimentally.

Two attractive theoretical features of gauge theories should be mentioned. First, electromagnetic mass differences are finite and calculable in many models - (see the reference in the bibliography). Second, these models provide the possibility of understanding the universality of both weak and electromagnetic interactions, because of the non-linearity of the coupling constant commutation relations which do not allow interactions to be scaled independently in general (technically this is so for models involving only non-abelian groups);

surely any "final model" must exploit this.

One further difficulty should also be mentioned. In higher order processes which diverge like $G(G\Lambda^2)$ in the phenomenological theory, the role of the cut off Λ is generally played by M_W. $\Gamma(K_L \to \mu^+\mu^-)$ and $M_{K_L} - M_{K_S}$ suggests that Λ is of order 10 GeV and not of order 100 GeV (the value of M_W in these models). In fact, experimentally $\Gamma(K_L \to \mu^+\mu^-) \lesssim G^2\alpha^2 M_K^5$ and not $\sim G^2\alpha M_K^5$ as we would naively expect in "unified models" and $M_{K_L} - M_{K_S} \sim G^2 M_K^3$ and not $G\alpha M_K$. Therefore the traditional cut off estimates must be evaded by suppressing these amplitudes; in many models this is done in an ad hoc way.

Experimental Consequences

1. **W's must exist ($M_W \sim 50$ GeV?)**

W's might be detected in

a) $e^+e^- \to W^+W^-$, which is very clean but obviously limited by the machine energy.

b) $pp \to W+ \quad \ldots$; the cross section could be estimated from $\sigma(pp \to \gamma(\to \mu^+\mu^-) + \ldots)$ but it has not yet been measured at very high energy. If Drell-Yan sealing holds for this process, W's of up to 15 or 20 GeV might be seen in this way at the ISR.

c)
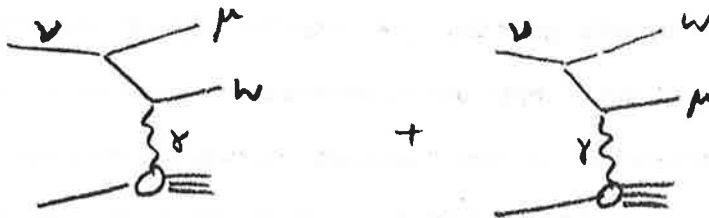
This has been used to get the present limit Mw > 2.5 GeV;
it could be extended to about 15 GeV at CERN II and NAL.

d)
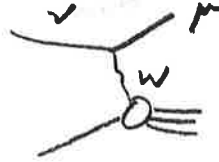
The W leads to an apparent violation of scaling in a very
characteristic way which could even be sensitive to W's
as heavy as 70 GeV in counter experiments at CERN II and NAL
if scaling persists.

2.   Neutral Currents

The coupling of neutral currents to neutrinos has obvious
consequences which have been widely discussed in the literature.   The
present experimental situation is reviewed in the accompanying paper
by Cundy.

It is especially interesting to consider the coupling of neutral
currents to electrons and muons since there is a neutral current which
decouples from neutrinos in some models.

Consider:
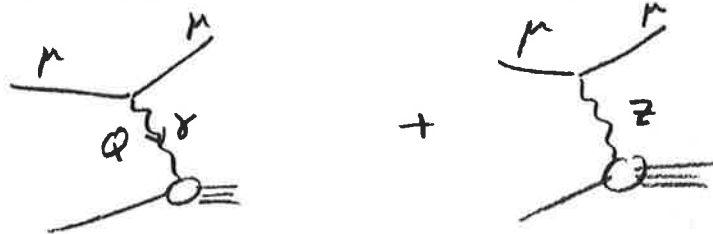
in which we expect:

$$\frac{|\text{ Interference Term }|}{|\text{ }\gamma\text{ exchange }|^2} \sim \frac{G}{4\pi\alpha} Q^2 = 10^{-4} \frac{Q^2}{m_p^2}$$

The signature of this disappointinly small effect might be:

a)   A characteristic (apparent) violation of scaling.

b) $\sigma^{\mu^+} \neq \sigma^{\mu^-}$. This is also expected from two photon exchange which, however, can violate the Rosenbluth formula in a more dramatic way.

c)   Parity violation e.g. $\sigma^{\mu(\text{lefthanded})} \neq \sigma^{\mu(\text{right handed})}$

If high energy circularly polarized γ's could be produced this effect could also be seen in
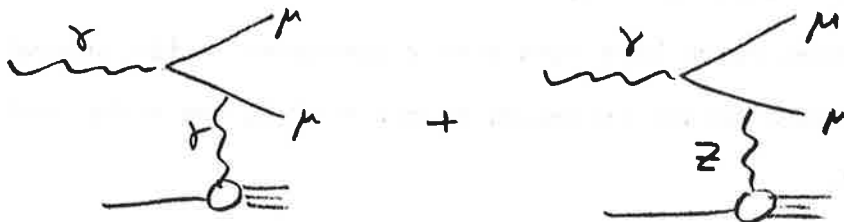
for example.

3.   <u>Heavy leptons</u>

The decays of (e.g.) the heavy muon M^+ required by renormalizable theories are

$$M^+ \rightarrow \nu_\mu \; \mu^+ \nu_\mu$$

$$\rightarrow \nu_\mu \; e^+ \nu_e$$

$$\rightarrow \nu_\mu + \text{hadrons}$$

The life time is too short for the tracks to be visible for masses $\gtrsim$ 800 MeV.

Ideas which are currently orthodox suggest:

$$\frac{\Gamma(M^+ \to \text{leptons})}{\Gamma(M^+ \to \nu + \text{hadrons})} \quad \sim 1$$

Heavy leptons could be produced in

a)
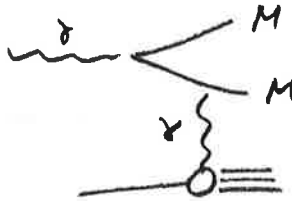
M's of up to $\sim$ 3.5 GeV could perhaps be seen in this way at CERN II
and NAL.

b) $e^+e^- \to M^+M^-$; this is clean but obviously limited by present
machine energies (Frascati experiments of this sort give $M_{\text{Heavy lepton}} >$
900 MeV)

c)
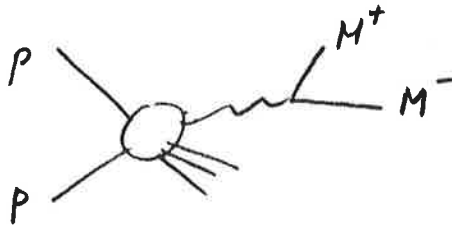
The cross section can be calculated from the unknown high energy
$pp \to \mu^+\mu^- + \dots$ cross section; Drell-Yan scaling suggests that
M's of up to about 5 GeV might eventually be seen in this way at the ISR.

d)

Which has a spectacular signature bearing in mind that the conventional

process is $\nu_\mu A \rightarrow \mu^- +$

The cross section has been estimated by Bjorken and myself; our

curve for $\dfrac{\sigma(\nu \rightarrow M^+)}{\sigma(\nu \rightarrow \mu^-)}$ as a function of $S/_M 2$ for e.g. M = 5GeV (assuming

$$g_{\nu\mu^- W^+} = g_{\nu M^+ W^-})$$

$\qquad\qquad\qquad\qquad\qquad\qquad\qquad\qquad$ gives:

$\qquad$ Eν = 50, 100, 150, ∞ Gev

$\dfrac{\sigma(\nu \rightarrow M^+)}{\sigma(\nu \rightarrow \mu^-)} \sim$ 0.1, 0.3, 0.4, 1. (the ratio can be scaled for other

masses since it is a function of $S/_M 2$). Heavy leptons with masses

up to about 20 GeV could perhaps be seen in this way in counter

experiments at CERN II and NAL.

4. Scalar mesons $\emptyset$

The properties of the $\emptyset$'s are extremely model dependent and

no realistic model independent tests of their existence have been

devised. In most models their coupling to e(μ) is extremely feeble

($\sim$ $e\, m_e (m_\mu) / M_w$) but this is not necessarily so; in the Georgi

Glashow model, as may be deduced from the discussion above, the coupling

is $\sim e\, m_{Heavy\,lepton} / M_w$ and they might be seen in $e^+ e^-$ experiments.

In any case we should bear them in mind; they could be invoked to

account for any unexpected anomalous phenomena.

5.   Charmed Particles and/or Failures of Cabibbo theory etc.

In the section on "Problems with Models" we discussed a model in which the Cabibbo theory is changed. Improved tests (e.g. with hyperon beams at the new accelerators) are desirable in any case. As discussed above, we expect that in all gauge theories either the Cabibbo theory is changed or charmed particles exist (or both); in many models SU(3) looses its fundamental position.

How could "charmed particles" be seen? Recall that "charm" is like a new strangeness. These particles have leptonic and non-leptonic decays. If they are heavy enough ($\stackrel{\sim}{>}$ 2 GeV?) we expect

$$\frac{\Gamma(C \to \text{leptons} + \text{hadrons})}{\Gamma(C \to \text{hadrons})} \sim 1 \text{ (within a factor of 10?)}$$

If they are light enough ($\stackrel{\sim}{<}$ 2 GeV?) they might be long lived enough to leave visible tracks in very high energy experiments.

There can be associated production (e.g. in $pp \to C\bar{C}' \, X \, .., \, e^+e^- \to C\bar{C}' + .., \, p\bar{p} \to C\bar{C}' + ..$) or single production by neutrinos ($\nu A \to C + ..$). These processes might manifest themselves through the leptonic decays or a sudden increase in strange particle production above threshold (C's decay predominantly into strange particles in some models) but they would be very hard to detect.

Final Remark

Even if gauge models have nothing to do with the real world, we think they have already played a seminal role in reactivating weak interaction theory and throwing doubt on existing hypotheses (prejudices). The experiments suggested by the models have an importance which transcends them.

Acknowledgements

I am grateful to Cecilia Jarlskog and John Bell for comments on the manuscript and to R. K. P. Zia for editing it.

Brief Bibliography

References to the original literature can be traced from the (somewhat random) list of papers below, which were chosen for their relevance to the presentation in my talk (rather than priority or originality).

Reviews

B.W. Lee   Invited paper presented at the 1972 Batavia Conference
                 (the comprehensive list of references includes papers
                 on the renormalization problem which we do not consider here).

B. Zumino   Lectures at the Cargese Summer School 1972 (CERN preprint
                 TH). (This paper contains a clear introduction to
                 Yang Mills theory and the "Higgs mechanism" as well as
                 a discussion of several models).

J.C. Taylor   "An introduction to Gauge Fields and Renormalizable
Theories of Charged Vector Mesons" (Rutherford preprint
RPP/T/29 1972) (goes into Feynman rules from Yang-Mills
fields, Faddeev Popov ghosts etc. etc. in some detail).

Models

References to models can be traced from B.W. Lee's review;
The contents of the following papers were referred to explicitly
in the text:

S. Weinberg   Phys. Rev. Lett. 19, 1264, 1967 and 27, 1688, 1971.

A. Salam   in Elementary Particle Theory ed. N. Svartholm
(Almouist and Forlag A.B. Stockholm, 1968).

H. Georgi and S.L. Glashow Phys. Rev. Letters 28, 1494, 1972.

T.C. Yang   Physics Letters 41B, 62, 1972.

H. Georgi and S.L. Glashow "Pseudo-Cabibbo Structure in a Gauge Theory
of Weak Interactions and Electromagnetism" (Harvard
preprint 1972).

Properties of Heavy Leptons

J.D. Bjorken and C.H. Llewellyn Smith

SLAC PUB 1107 (to be published in Phys. Rev).

Neutral Currents

Bounds on the effects in neutrino reactions in certain models are given in NAL preprint THY - 86B - 1973 by C.H.Albright, B.W. Lee, E.A. Paschos and L. Wolfenstein (see also references therein).

Neutral currents in electromagnetic processes:

A. Love, D.V. Nanopoulos and G.G. Ross

Rutherford preprint RPP/T/26 1972.

E.Derman Columbia preprint CO-2271-2, 1972.

R. Petronzio Rome University preprint 411, 1972.

Charmed Particles

G.A. Snow   Inst. de Phys. Nucleaire, Fac., des Sciences, Paris

preprint PAP-LPTHE 11, 1972.

Finite mass differences

The most recent paper containing a brief review is H.M. Georgi and S.L. Glashow "Attempts to Calculate the Electron Mass". Harvard preprint, 1973.

The idea of the cancellation strategy followed in the text seems to be part of the folklore.   Several people seem to know that elimination of S terms in $\overline{FF} \to WW$ leads to Yang Mills theory but the role of the ϕ in removing $\sqrt{S}$ terms in $\overline{FF} \to WW$ and improving $WW \to WW$ does not seem to have been investigated systematically; it will be considered in a forthcoming CERN preprint which I am now writing.

Search for Weak Neutral Current Processes
at CERN using Gargamelle

D.C. Cundy

Since the start of the neutrino experiments at CERN in 1963, systematic searches have been carried out for weak neutral current processes. With the introduction of Gargamelle an order of magnitude gain in sensitivity has been obtained for some processes. This for example is the case for the process $\nu_\mu + e^- \rightarrow \nu_\mu + e^-$ which was looked for previously to set a limit on the magnetic moment, and now is so interesting with relationship to unified theories of weak interactions.

Search for $\left(\genfrac{}{}{0pt}{}{\nu_\mu}{\bar{\nu}_\mu} + e^- \rightarrow \genfrac{}{}{0pt}{}{\nu_\mu}{\bar{\nu}_\mu} + e^-\right)$

Of the various unified models of weak interactions only the Weinberg model [1] gives specific cross-section for the above process. The cross-section is a function of the ratio of the electric coupling constant e^2 and the lepton coupling constant g^2 to the intermediate boson. This variation is shown in Fig. 1. For comparison the four-fermion charged current process $\nu_e + e^- \rightarrow \nu_e + e^-$ is shown. However due to the fact that the ν_e flux is $\sim 1/100$ of the ν_μ flux this process cannot be detected in the present experiment. In fact the neutral current process is just about at the level of detection.

The minimum predicted Weinberg cross-section for $\bar{\nu}_\mu + e^- \rightarrow \bar{\nu}_\mu + e^-$ is $\sim 0.1\ E_\nu \times 10^{-41}\ cm^2$/electron. As $2 \times 10^5\ \bar{\nu}$ pictures gave ~ 1000 events in πm^3 fiducial volume and $\sigma_{\bar{\nu}} = 0.27\ E_\nu \times 10^{-38}\ cm^2$/nucleon, then in $7\ m^3$ one expects a minimum of ~ 0.25 events or a maximum of ~ 5 events.

FIG 1

NEUTRINO-ELECTRON SCATTERING CROSS-SECTIONS IN WEINBERG MODEL
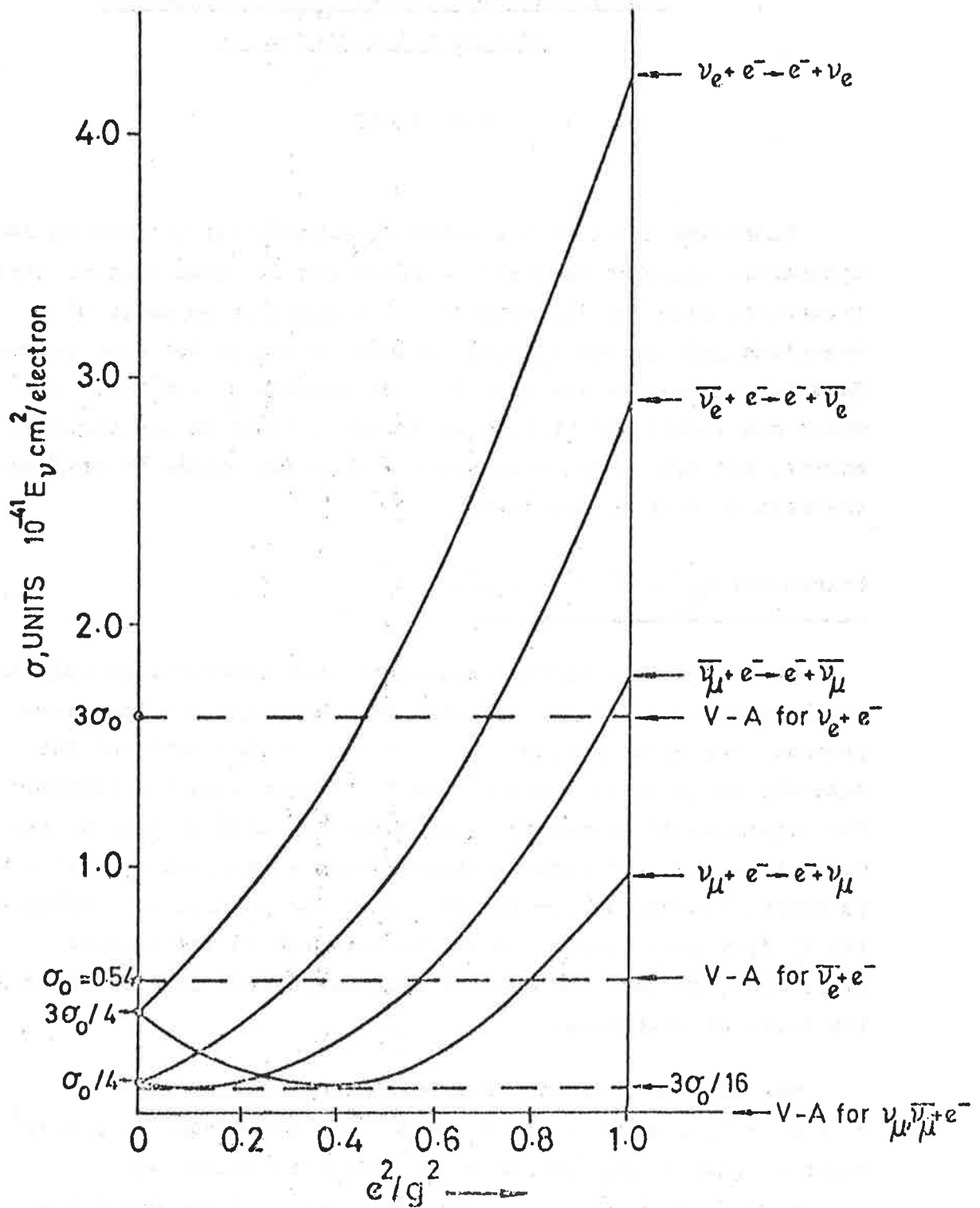
Similarly 2×10^5 ν pictures would give a __minimum__ of ~ 0.4 events and a maximum of ~ 4 events. Such events would be very characteristic in Gargamelle, being high energy single electrons, very close to the beam direction (ie $\theta < \sqrt{\dfrac{2m_e}{E_\nu}} < 5°$).

In fact one such event has been found in the $\bar{\nu}$ film, having an energy of ~ 400 MeV and an angle of 1° to the beam.

The obvious question to ask is what are the background levels ?

Essentially the only background comes from the process

$$\nu_e + n \rightarrow e^- \ (\theta < 5°) + (p)$$

$\qquad\qquad\qquad\qquad\quad$ ⌐— retained ·in nucleus
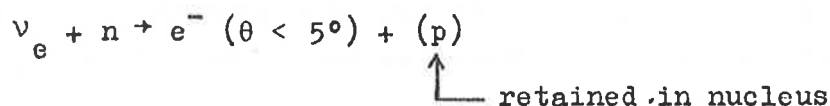
The above process should follow exactly the same behaviour as :

$$\nu_\mu + n \rightarrow \mu^- \ (\theta < 5°) + p$$

$\qquad\qquad\qquad\qquad\quad$ ⌐— retained
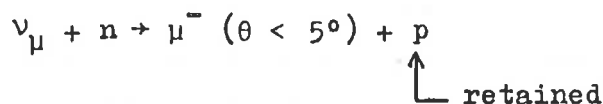
This process was found to be 3 ± 2 % of all events with μ^- + protons.

In the 2×10^5 ν pictures 10 events with e^- + protons were found in the fiducial volume. Hence we expect a background of ~ 0.6 ± 0.5 events due to above process. For $\bar{\nu}$ the situation is much more favourable due to the ν_e flux being about 10x less. As no events of the type e^- + protons were found in the $\bar{\nu}$ film, we estimate from the ν_e flux prediction a background of ~ 0.06 events, compared to a minimum signal of ~ 0.3 events (ie signal : noise of ~ 5:1).

From the one event obtained no conclusions can be drawn other than this type of experiment should be continued with anti-neutrinos. In the near future a further 10^6 $\bar{\nu}$ pictures will be taken at the PS, if possible with the booster, giving at least 3x the intensity. Such a run will yield 12 events on the basis of the one event found or a minimum of 3 events if the cross-section is minimal.

Search for hadronic neutral currents

Previous experimental limits on such processes are :

1) $$\frac{\nu_\mu + p \to \nu_\mu + p}{\nu_\mu + n \to \mu^- + p} < 0.21 \quad 90\ \%\ \text{C.L.} \quad \text{CERN } 67 \quad [2]$$

2) $$\frac{\nu_\mu + p \to \nu_\mu + \Delta^+}{\nu_\mu + p \to \mu^- + \Delta^{++}} \quad \begin{array}{l} < 0.31 \quad \text{ANL } (p\pi^o)\ 72 \quad [3] \\ < 0.46 \quad \text{CERN } (n\pi^+)\ 67 \quad [2] \end{array}$$

Unfortunately these limits are just that bit too high to really test the Weinberg theory, as can be seen from Fig. 2 and 3.

However the situation has been much improved for the limits of neutral current π^o production.

In a restricted fiducial volume neutral events with 1 or 2 γ's have been noted and compared with similar events accompanied with a μ^-. If one excludes charge exchange processes (which by the way are not negligible), the result can be thought of as the measurement of :

$$\frac{\sigma(\nu n \to \nu n\pi^o) + \sigma(\nu p \to \nu p\pi^o)}{2\,\sigma(\nu n \to \mu^- p\pi^o)} < 0.21 \quad 90\ \%\ \text{C.L}$$

This limit is somewhat inferior to the Columbia [4] result of < 0.14 90 % C.L.

In Fig. 4 the results are compared with the predictions of Pachos and Wolfenstein. The theoretical predictions are somewhat uncertain, but at least all have the common feature that the cross-section falls rapidly with increasing e^2/g^2. Hence it would seem that low values of e^2/g^2 are excluded, which would certainly be compatible with the observation of one $\bar{\nu}_\mu + e^- \to \bar{\nu}_\mu + e^-$ event. However, this conclusion is certainly incompatible with the recent experiment of Reines [5] on $\nu_e + e^- \to \nu_e + e^-$ scattering which

FIG.2

$$R = \frac{\sigma(\nu + p \longrightarrow \nu + p)}{\sigma(\nu + n \longrightarrow \mu^- + p)}$$

$\begin{cases} 0.3 < q^2 < 1.0 \, GeV^2 \\ 1 \; < \; E_\nu < 4 \; GeV \end{cases}$

WEINBERG
THEORY
(MYATT 1972)

90% C.L.
(CUNDY ET AL 1970)

$e^2/g^2 \longrightarrow$

FIG. 3

$$R_1 = \frac{\sigma(\nu p \rightarrow \nu \Delta^+)}{\sigma(\nu p \rightarrow \mu^- \Delta^{++})}$$

FIG 4

$$R = \frac{\sigma(p\pi^0 + n\pi^0)}{2\sigma(\mu^- p\pi^0)}$$

Reines $\bar{\nu}_e e \to \bar{\nu}_e e$??

CERN $\bar{\nu}_\mu e \to \bar{\nu}_\mu e$

Paschos & Wolfenstein (pure $I = \frac{3}{2}$)

CERN

Columbia
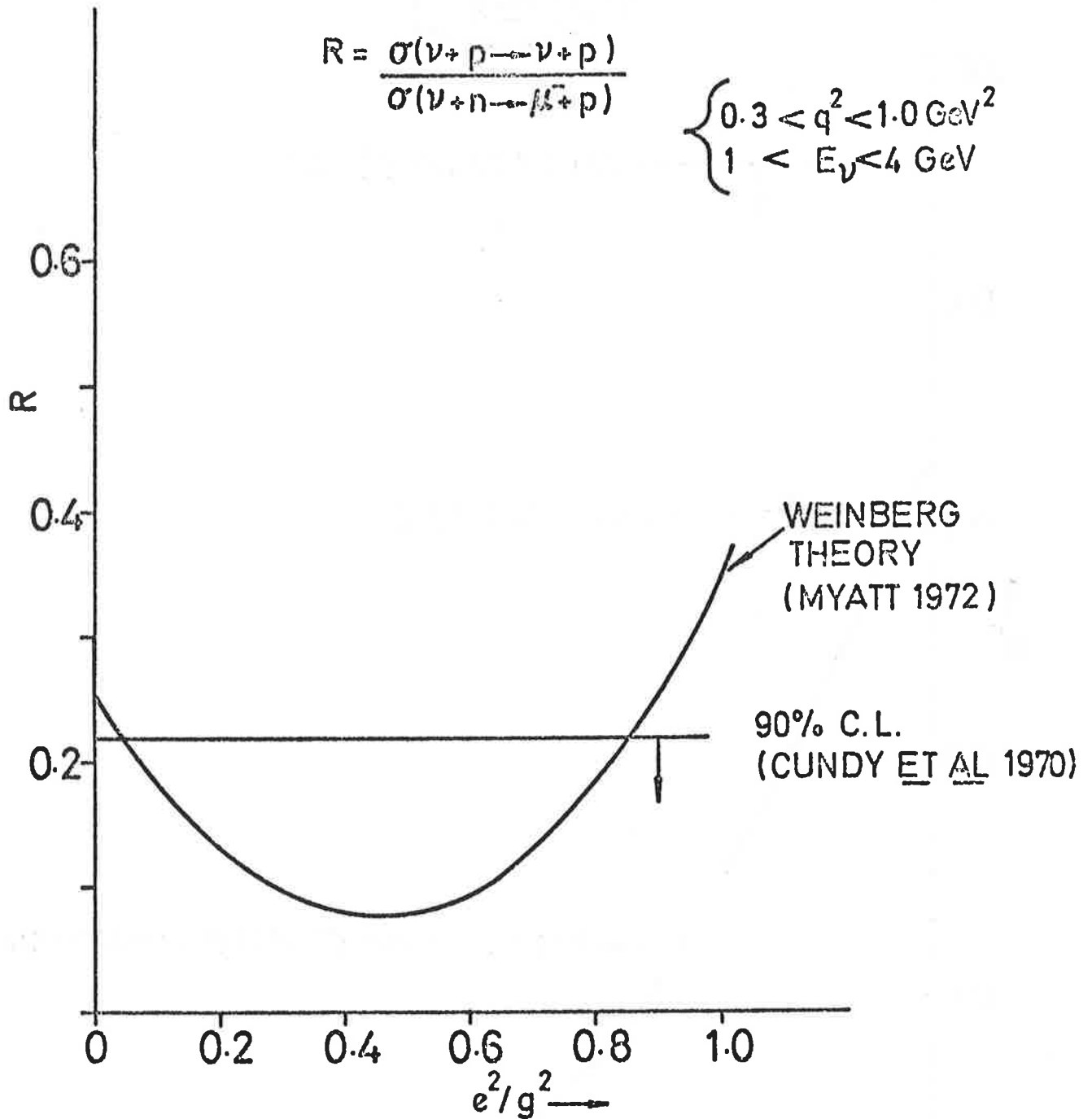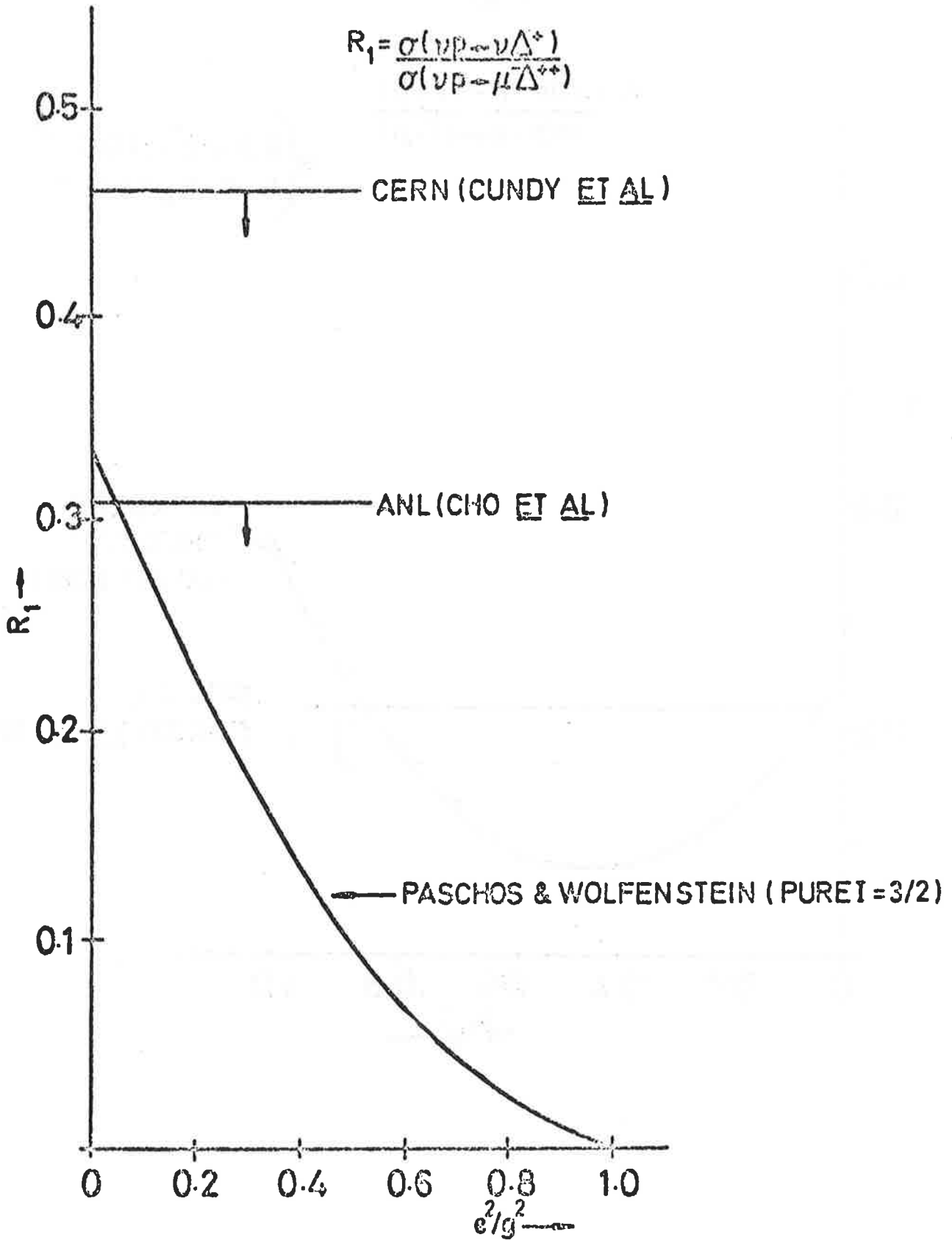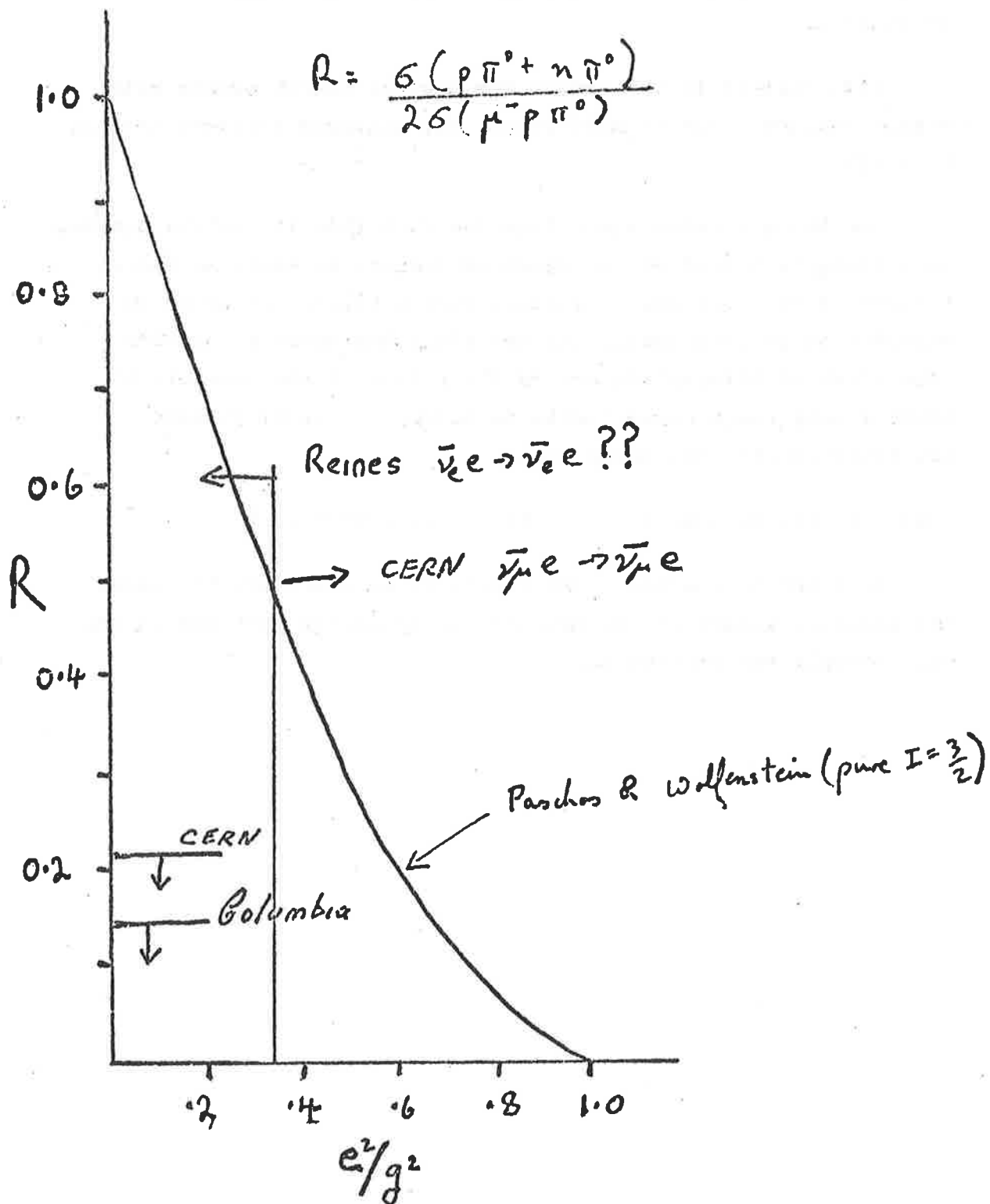
excludes high values of e^2/g^2. The Reines experiment was certainly very difficult and must be confirmed before firm conclusions can be reached.

With respect to the search for neutral hadron events with single charged pions or multipions, the analysis problems are not negligible.

The basic problem comes from the fact that the bubble chamber is sitting in a neutron gas which is induced by neutrino interactions in the surrounding matter. Such a background would be expected to be essentially uniform along the chamber but show some signs of attenuation across the radius of the chamber. At present only rough upper limits on hadronic neutral current processes can be put, these are

a) < .25, 90 % CL ν b) < .55, 90 % CL $\bar{\nu}$

In order to improve these limits it is necessary to reduce the fiducial volume of the chamber, apply energy cuts and increase considerably the statistics.

References

1) S. Weinberg, PRL 19, 1264, 1967.

   G. t'Hooft, Phys. Lett. 37B, 195, 1971.

2) D.C. Cundy et al., Phys. Lett. 31B, 479, 1970.

3) Y. Cho et al., presented at Batavia Conference 1972.

4) W.Y. Lee, Phys. Lett., 40B, 425, 1972.

5) H.S. Gurr et al., PRL 28, 1406, 1972.

LEPTON PRODUCTION AT THE ISR

(B.G. Duff, University College London)

A)   INTRODUCTION

We are mainly interested in the production of leptons, in p-p collisions, which arise from electromagnetic and weak processes. We may consider the following possibilities:

<u>Lepton pair production</u> by electromagnetic processes.

$$p + p \longrightarrow \mu^+ \mu^- + \text{ANYTHING} \qquad \dots\dots 1$$

$$\text{or} \quad p + p \longrightarrow e^+ e^- + \text{ANYTHING} \qquad \dots\dots 2$$

<u>Heavy lepton production</u>

$$p + p \longrightarrow L^+ L^- + \text{ANYTHING} \qquad \dots\dots 3$$
$$\big|\!\longrightarrow \mu\text{'s, e's etc.}$$

<u>Weak Interaction processes</u>

$$p + p \longrightarrow e \; \nu + \text{ANYTHING} \qquad \dots\dots 4$$

$$\text{or} \quad p + p \longrightarrow \mu \; \nu + \text{ANYTHING} \qquad \dots\dots 5$$
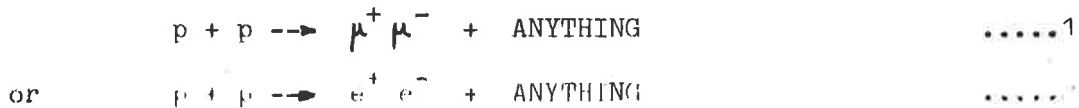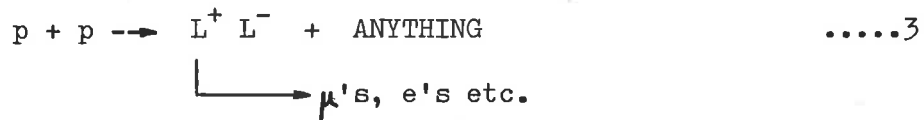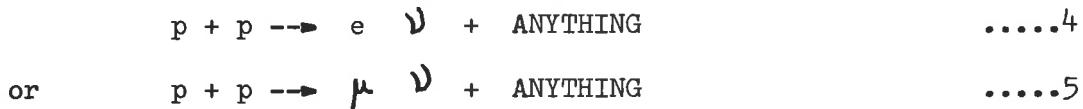
<u>Real Intermediate Vector Boson (W) production</u>

$$p + p \longrightarrow W^{\pm} + \text{ANYTHING} \qquad \dots\dots 6$$
$$\big|\!\longrightarrow \mu, \nu \text{ or } e\nu$$

$$\text{or} \quad p + p \longrightarrow W^{o} + \text{ANYTHING} \qquad \dots\dots 7$$
$$\big|\!\longrightarrow e^+ e^- \text{ or } \mu^+ \mu^-$$

$$\text{or} \quad p + p \longrightarrow W^+ W^- \qquad \dots\dots 8$$
$$\big|\!\longrightarrow e^+ e^-, \mu^+\mu^- \cdots$$
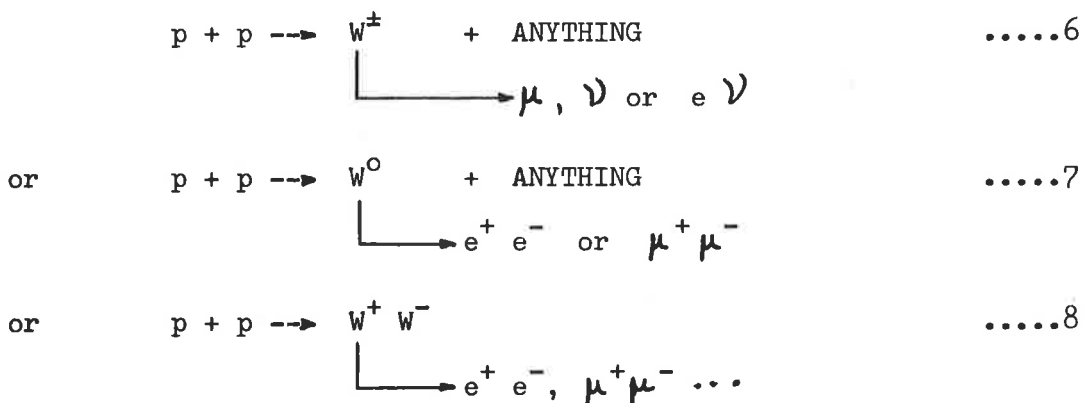
These processes will have to compete, from an experimental point of view,

with leptons produced in decays of π's and K's and we will first attempt to estimate the cross sections.

B) CROSS-SECTION ESTIMATES

Two experimental pieces of information can help to estimate the various leptonic cross sections. First, the Columbia - BNL[1] measurement of the reaction

$$p + NUCLEUS \longrightarrow \mu^+ + \mu^- + ANYTHING$$
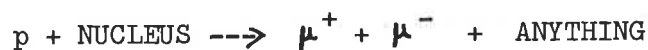
at beam energies between 22 and 29.5 GeV. Secondly, the SLAC inelastic lepton-hadron data can give a handle on how to scale up from BNL ($s \sim 50$ GeV^2) to the ISR ($s \sim 2500$ GeV^2). (For example, by using a parton model.)

The cross section for reaction ① can be written in the form

$$\frac{d\sigma}{dm} = \frac{\alpha^2}{m^3} \quad F(m,s)$$

where m is the mass of the heavy virtual photon, s is the square of available energy in the CM system and F is a dimensionless structure function (which allows for the hadron-photon vertex). For large m and s, for F to be dimensionless we must have $F = F(m^2/s)$. (This is the condition for scale invariance.) it has been pointed out[2] that the BNL data approximately fits

$$\frac{d\sigma}{dm} = \frac{\alpha^2}{m^3} e^{-10\, m^2/s} \approx \frac{2 \cdot 10^{-32}}{m^3} e^{-10\, m^2/s} \quad cm^2 GeV^{-1} \text{ (where m is in GeV)}$$

$$\text{for} \quad .03 \lesssim m^2/s \lesssim .5 \qquad\qquad .....9$$

and this form can be used to make estimates for ISR energies.

If we consider a parton model, then there are two important terms[3]. First, there is the Drell-Yan[4] term which corresponds to the parton-antiparton annihilation process
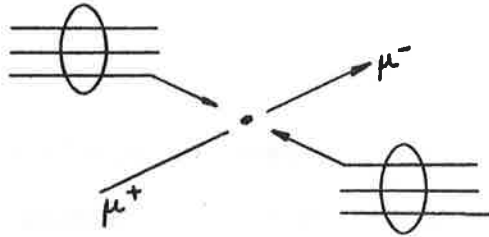
This term goes as $1/m^3$. Secondly, the rest of the hadron system may interact via pomeron exchange. This second term goes as $1/m^5$ and is probably only important at rather small m (say, < 2 GeV).

One particular parton model of Landshoff and Polkinghorne[3] gives rise to a cross section

$$\frac{d\sigma}{dm} \approx \frac{10^{-32}}{m^3} \quad \log (E/m) \quad cm^2 \ GeV^{-1} \qquad \qquad \dots 10$$

where E is the beam energy. We may now use ⑨ or ⑩ , (which give similar numerical results) to make estimates for reactions ① and ② at ISR energies. (See table 1.)

Heavy lepton pairs can also be produced (if any exist!) and an estimate can be made by integrating ⑨ or ⑩ from a threshold of $2m_L$ to $(\sqrt{s} - 2m_L)$, provided a threshold factor is included which has the form[5]

$$\left[\frac{(m^2 - 4 m_L^2)}{m^2} \right]^{\frac{1}{2}} \left[1 + \frac{2m_L^2}{m^2} \right] \qquad \qquad **$$

It will be seen in table 1 that the resulting cross sections[2] are of

---

** If the photon yields two real W's, equations 9 or 10 can predict the cross section, but now the multiplicative factor is

$$\frac{(m^2-4Mw^2)^{3/2}}{4m^3 \ Mw^4} \left[\tfrac{1}{4} g^2 m^2 (m^2 + 4Mw^2) - \tfrac{1}{2} g m^2 (m^2 - 2Mw^2) + (\tfrac{1}{2} m^2 - Mw^2)^2 + 2Mw^4 \right]$$

where g is the g-factor of the W (1 or 2?)

TABLE 1

PRODUCTION OF:	MASS IN GeV		
	10	20	30
$(\mu^+ \mu^-)$ or $(e^+ e^-)$	$\left(\dfrac{d\sigma}{dm}\right) \sim 10^{-35}$	$\sim 10^{-36}$	
$(L^+ L^-)$	$\sigma_{L^+L^-} \sim 10^{-35}$	$\sim 10^{-36}$	
Single W	$\sigma_w B \sim 10^{-33}$	$\sim 5 \cdot 10^{-34}$	$\sim 5 \cdot 10^{-35}$ [2] or ~ 0 [3]

Cross sections (in cm^2 GeV^{-1} or cm^2) for leptonic production processes in p-p collisions at $s \approx 2500$ GeV^2. (Orders of magnitude and with assumptions given in text.)

the same order of magnitude as the μ or e pair case. By CVC and other simple assumptions[6] it is possible to relate the μ pair predictions to the reaction in which a real W (if one exists!) is produced. The cross section times the leptonic branching ratio then takes the form

$$. \; \sigma_W \; B_{leptonic} \approx \frac{3}{8\sqrt{2}} \quad \frac{G}{\alpha^2} \quad M_W^3 \left(\frac{d\sigma}{dm}\right) \text{(for virtual photon)}$$

.....11

$$\text{i.e.} \quad \sigma_W \; B_e \approx 0.1 \; M_W^3 \left(\frac{d\sigma}{dm}\right)$$

For large values of M_W ($\geqslant$ 10Mp) this implies comparitively large cross sections for W production. (See table 1.)

Direct observation of weak interaction effects, without a real W, seems to be unlikely. (The order of magnitude is the cross section (11) multiplied by G.m.[6].)

However, Lederman[7] has suggested that there could be a possiblity of seeing first order interference effects between a virtual neutral W and the electromagnetic current, in which both couple to e^+e^- or $\mu^+\mu^-$ pairs. This cross term is of the order G/α and could be as large as 10%.

C) WHAT CROSS SECTIONS ARE OBSERVABLE AT THE ISR?

First, let us see what is possible currently at the ISR. The design luminosity of 4.10^{30} $s^{-1}cm^{-2}$ has recently been acheived. Suppose that a reasonable running time is 2000 hours, and suppose that the solid angle of the equipment is $\Omega \approx \pi$. If we assume that $\sim$ 100 events are required, this implies a sensitivity given by

$$\sigma B \approx 10^{-35} \; cm^2$$

where B is the branching ratio, where appropriate. (As an absolute limit we could assume 4π coverage, an increased luminosity $\approx 10^{-31} s^{-1} cm^{-2}$ and 10,000 hours of running corresponding to $\sigma B \approx 10^{-37} cm^2$.)

Assuming the more practical figure of $10^{-35} cm^2$, reference to Table 1 suggests that, in principle:

1) it is likely that one can only see heavy lepton effects for $M_L < \sim 7$ GeV

2) μ and e pairs should be observable to masses ~ 15 GeV

3) W production cross sections are sufficiently high to ~ 30 GeV, or ~ 20 GeV using ref. 3. (Assuming $B \approx \frac{1}{4}$).

However, the main uncertainty in all work with leptons at the ISR is the enormous "background" of leptons from the decays of π's and K's, and the possibility of lepton simulation by a small fraction of the copiously produced hadrons.

The situation is not helped at the present time by the considerable uncertainties about high transverse momentum hadron production spectra and the problems of separating π's and K's at large momentum, (> 5 GeV/c).

D) CURRENT EXPERIMENTS AT THE ISR

There are two relevant experiments at the ISR, neither of which is at the stage of final analysis and results have only been reported in a very preliminary form at conferences and meetings.

I Search for electrons and electron pairs

(CERN-COLUMBIA-ROCKEFELLER)

This experiment has been searching for pairs of electrons, which

might arise from heavy virtual photons, neutral W's (or even heavy
vector mesons). The equipment is also capable of detecting high
transverse momentum single electrons which could have originated from
the decay of charged W's.

Figure 1 shows the equipment. Wire spark chambers were used to
show up the electron tracks (which must come from the intersection
region). The triggering system included dE/dx counters to help
eliminate nearly colinear electron pairs from photons converting in
the vacuum pipe, or from Dalitz pairs. Lead glass Čerenkov counters
were used to measure the electron energies. An additional array of
lead glass was used to discriminate against pions that might interact
in the large glass blocks giving rise to pulses of comparable height
to those from genuine electrons.

The resulting spectrum of single electrons (based on $\sim \frac{1}{4}$ of the
data taken) is of very approximately exponential form[9]

$$E \ \frac{d^3\sigma}{dp^3} \sim A e^{-B p_\perp} \quad \text{(where, by eye, } A \sim 10^{-30} \text{cm}^2/\text{GeV}^2.\text{s}^2\text{r}$$
$$B \sim 2.3 \text{ for } P_\perp > 2.5 \text{ GeV/c)}$$

E, being the electron energy, and shows no obvious structure at large
transverse momenta. This spectrum should only be considered as an
upper limit, as it is thought that a considerable fraction (and
possibly even all) of these events are from background effects. (An
important background simulation arises from the chance coincidence of
a charged pion satisfying the track conditions with an uncharged pion
satisfying the energy requirements.) To set limits on W production will

SIDE VIEW

LEAD GLASS
ČERENKOV COUNTERS

PLASTIC SCINTILLATORS

50 cm

WIRE SPARK CHAMBERS

CALIBRATING BOX

TOP VIEW
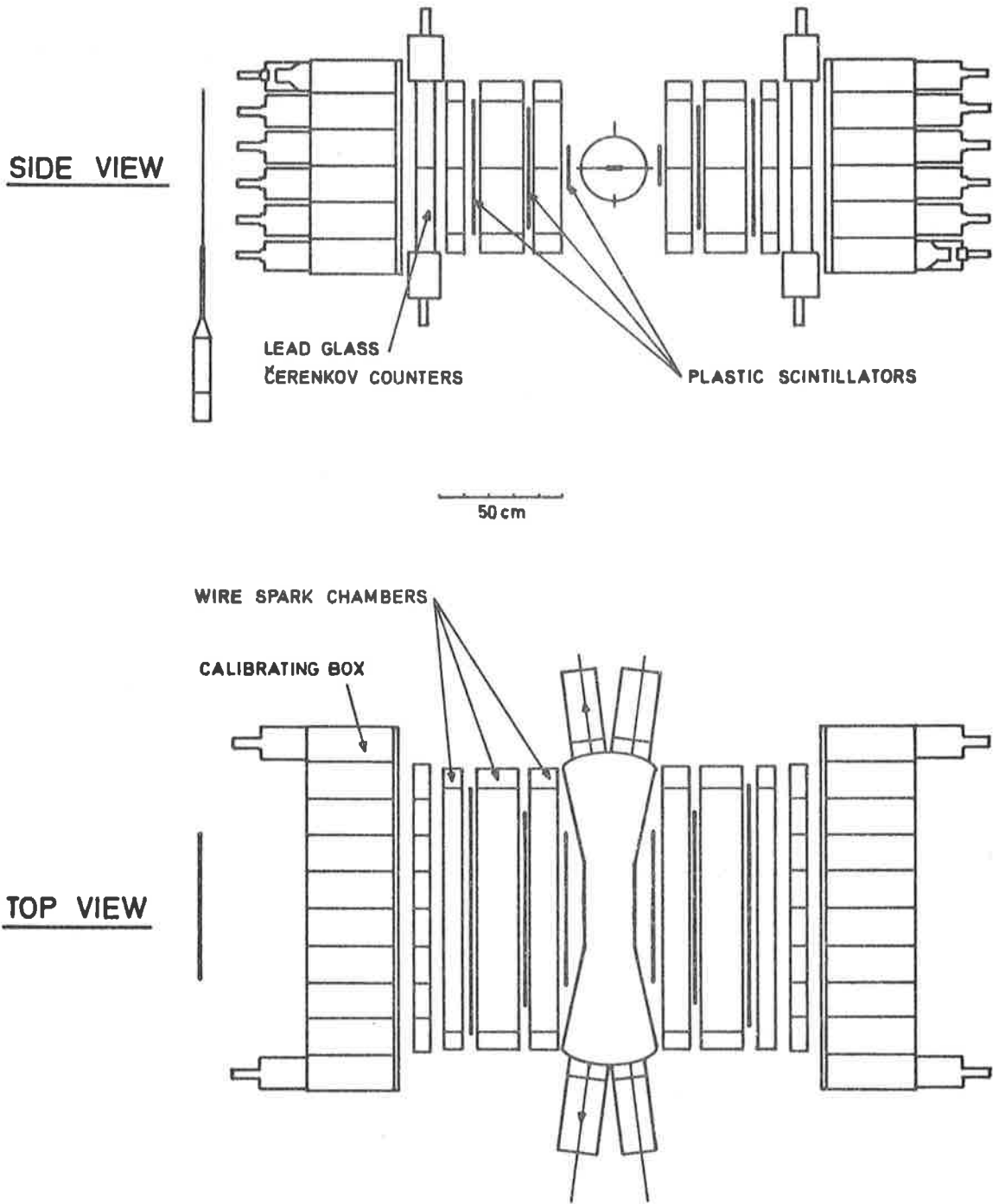
CERN - COLUMBIA - ROCKEFELLER COLLABORATION

Figure 1   ELECTRON DETECTOR

require not only an understanding of the background but a Monte Carlo study of the W production and decay processes, which is model dependent.

The position with electron pairs is more straightforward and the equipment should be sensitive to σB's $\approx 10^{-34}$ cm^2 for neutral W production. Analysis of the data has yielded a small number of candidates which are now under careful scrutiny to see if they could originate from a background process.

II   SEARCH FOR MUONS AND MUON PAIRS

(British Collaboration)

A search is being carried out for muons with large transverse momenta, again as evidence for heavy virtual photon production or as an indication of W production. In this experiment it is expected that the main backgrounds come from decays of π's and K's and from cosmic radiation.

The detector (see figure 2) consists of a set of large optical spark chambers which are interleaved between magnetised steel plates (with fields ~ 15 k G). Four counter planes are used in the trigger and this requires a minimum transverse momentum, for the muon, of ~ 1.6 GeV/c. In order to emerge from the far end of the detector, a muon must have at least 2.1 GeV/c transverse momentum.

Backward-going cosmic rays are rejected by time-of-flight and forward downward-going cosmic rays are vetoed in directionally sensitive perspex Čerenkov counters. Magnetostrictive chambers in the neighbourhood of the intersection region enable any remaining cosmic ray muons to be

SCINTILLATION COUNTERS

MAGNET

— 5 metres

ČERENKOV COUNTERS

MAGNETOSTRICTIVE
SPARK CHAMBERS

LEAD ABSORBER

OPTICAL SPARK CHAMBERS

BRITISH COLLABORATION

Figure 2 MUON DETECTOR (PLAN)
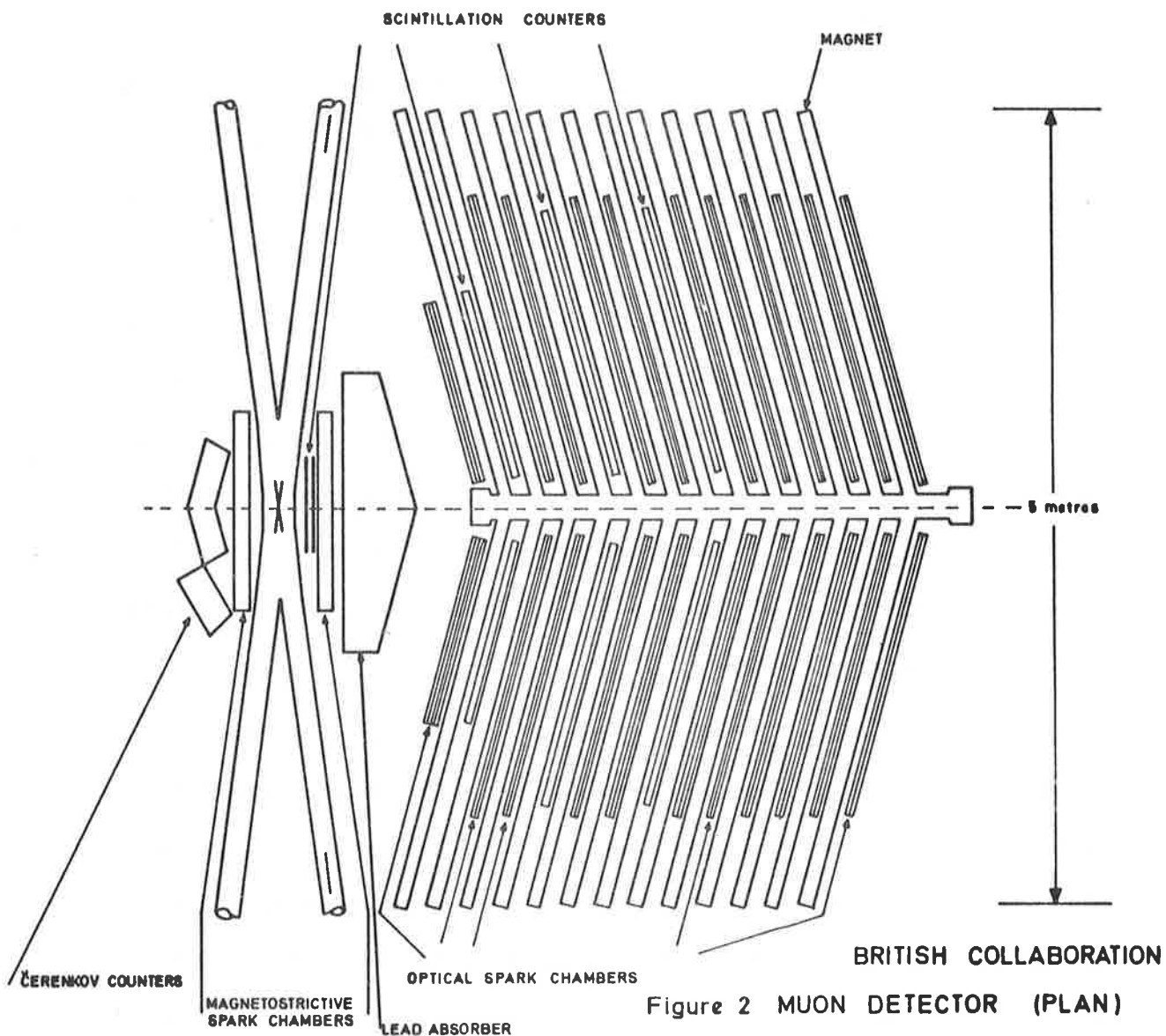
rejected by co-linearty.

The lead absorber in front of the detector (see figure 2) can be moved in such a way as to vary the decay path for π 's and K's and the part of the muon spectrum resulting from these decays can then be separated from any remaining signal.

A preliminary analysis of a small sample of the data was undertaken for the Chicago conference[10]. At that time it was reported that the upper limit for the production of muons with momenta $\geqslant$ 6 GeV/c was ~ 4 . 10^{-33} cm^2/sr, and it was also stated that a certain fraction of these events seemed to correspond to stopping tracks (which, if they were muons, would require momenta $\leqslant$ 2.1 GeV/c). A number of possible explanations were discussed[10].

There are two main difficulties, at present, in the interpretation of the data. First, there is a technical problem in the detailed understanding of the measurement of muon momenta using the solid magnet. Monte Carlo studies suggest that a momentum resolution Δp/p $\sim$ 15% should be obtainable when proper allowance is made for the multiple scattering. However, it only requires a few per cent of low momentum muons (from hadron decays) to somehow simmulate a high momentum particle to account for the observed 'signal' of high momentum muons and also for the stopping tracks. The problem is being tackled both with further Monte Carlo studies and experimentally. An air magnet has been set up near the muon detector in such a way that samples of cosmic ray muons can pass through the air magnet and the solid magnet and direct calibrations can be made.

The second problem concerns the lack of detailed knowledge of the hadron spectra at high transverse momenta. However, measurements are now in progress at the ISR which should help to understand the hadron induced backgrounds.

A great deal of data has been taken in the last few months, at a variety of energies and absorber configurations and provided the momentum measurement problem is solved, a sensitivity of the order of $\sigma B = 10^{-35} cm^2$ should be attainable.

REFERENCES

1   J.H. Christenson et al. Phys. Rev. Letts., $\underline{25}$, 1523 (1970).

2   L.M. Lederman. Paper read at Muon-Electron Puzzle Conference
        Dubna, 1972.

3   P.V. Landshoff and J.C. Polikinghorne. Nucl. Phys., $\underline{B33}$, 221 (1971).
                                        and   Phys. Letts., $\underline{40B}$, 463 (1972).

4   S.D. Drell and T.M. Yan. Phys. Rev. Letts., $\underline{25}$, 316 (1970).

5   S.S. Gerstein et al. IHEP Report 71 - 54.

6   L.M. Lederman and B.G. Pope. Phys. Rev. Letts., $\underline{27}$, 765 (1971).
        Can be derived from: Y. Yamaguchi. Il Nuovo Cim. $\underline{XLIII}$ A, 193 (1966).

7   L.M. Lederman. Talk given at CERN.

8   P.V. Landshoff. Private communication.

9   B.G. Pope. Private communication.

10   British ISR Collaboration. Contribution to XVIth. Int. Conf. on
        High Energy Physics, Chicago, 1972.

WHAT HAVE WE LEARNED FROM ELECTRON SCATTERING?

F.E. Close

Daresbury Nuclear Physics Laboratory,
Daresbury, Warrington, Lancashire.

CONTENTS

Fig. 1   Inelastic electron scattering.

R = 0.18
W ≳ 2 GeV

νW_2

- • $1 \le q^2 \le 2$
- × $2 < q^2 \le 4$
- □ $4 < q^2 \le 8$
- ▲ $8 < q^2 \le 12$
- ● $12 < q^2$

$\omega' = (W^2 + q^2)/q^2$

Fig. 2 $\nu W_2(W^2, Q^2)$ for $W^2 > 4$ (GeV)^2, $Q^2 > 1$ (GeV)^2 plotted against ω'.

1   KINEMATICS FOR INCLUSIVE ELECTROPRODUCTION

A target (proton) of mass M sits in the laboratory and an electron of energy E emerges from the accelerator. The target sees the electron by receiving from it one photon whose energy ν and mass squared q^2 are given by

$$\nu = E - E'; \qquad q^2 = -4EE'\sin^2\theta/2 \equiv -Q^2 \tag{1}$$

where E' is the energy of the final electron with θ the angle through which the beam has been scattered (fig. 1). Averaging over the spins in the initial state and summing over the final state spins, then the cross section for observing the electron in an element $d\Omega$ of solid angle and dE' of energy may be written[1]

$$\frac{d^2\sigma}{d\Omega dE'} = \frac{4\alpha^2 \, E'^2 \, \cos^2\theta/2}{Q^4} \left(W_2(\nu, Q^2) + W_1(\nu, Q^2) \, 2\tan^2\theta/2 \right) \tag{2}$$

$W_{1,2}$ are structure functions which summarise our lack of knowledge of the dynamics in the vertex "$\gamma_V p \to$ anything" of fig. 1.

Given a dynamical theory of the nucleon we could calculate $W_{1,2}$ and hence the cross section. In practice we do the reverse - measure the cross section and hence determine $W_{1,2}$. Knowledge of these structure functions then tells us something about the substructure of the proton, the only problem is to decipher the meaning of the data once you have them. The data[2] for νW_2 with $Q^2 > 1$ and $W^2 > 4$ (GeV)^2 are shown in fig. 2, and the apparent Q^2 independence at fixed ω' suggested that we might be seeing evidence for a "pointlike" structure within the proton - commonly called partons. This popular interpretation will be discussed in Dr. Landshoff's talk and I shall not trespass on his territory further. My purpose here is to examine the data, to note and hopefully correlate various phenomena without, so far as is possible, recourse to particular models. In this way we might hope to extract from the abundance of data just a few "essential" phenomena which require explanation in a dynamical model.

We can simplify our conception of the problem by treating the electron beam as a very expensive source of a beam of photons whose mass as well as energy can be tuned by varying the energy and scattering angle of the electron

"source". We are then studying total photoabsorption cross sections as a function not only of the photon's energy but also as a function of its mass (viz. the fig. 1 with the electron lines removed). The photon being virtual can be scalar (helicity 0) in addition to transverse (helicity±1) and the photoabsorption cross sections $\sigma_{S,T}$ for scalar and transverse photons are related to $W_{1,2}$ as follows

$$W_1 = \frac{K}{4\pi^2\alpha} \sigma_T \tag{3a}$$

$$W_2 = \frac{K}{4\pi^2\alpha} \frac{Q^2}{Q^2 + \nu^2} (\sigma_T + \sigma_S) \tag{3b}$$

where the choice of the (arbitrary) flux factor K defines the cross sections. When $Q^2 = 0$ then $K = \nu$ unambiguously. However, for $Q^2 \neq 0$ one might choose[3] for example $K = |\vec{q}|$ (Gilman) the three momentum of the photon, or $K = \nu - Q^2/2M$ (Hand). This latter choice is widely adopted but is no more or less fundamental than Gilman or for that matter any other that you may invent yourself. The $W_{1,2}$ are well defined in terms of measurable quantities (eq. 2), the absorption cross sections are then defined modulo this arbitrary flux factor (eq. 3).

Substituting the relations between $W_{1,2}$ and $\sigma_{T,S}$ (eq. 3) into the form (2) for the electroproduction cross section we obtain the following frequently quoted expression relating the photoabsorption cross sections to the double differential cross section

$$\frac{d^2\sigma}{d\Omega dE'} = \Gamma \Sigma$$

with

$$\Sigma \equiv \sigma_T + \epsilon \sigma_S$$

$$\epsilon \equiv \left[1 + 2 \frac{Q^2 + \nu^2}{Q^2} \tan^2\theta/2 \right]^{-1} \tag{4}$$

$$\Gamma = \frac{K\alpha}{2\pi^2 Q^2} \frac{E'}{E} \frac{1}{1 - \epsilon}$$

The structure functions $W_{1,2}$ and cross sections $\sigma_{T,S}$ are functions of the two variables ν, Q^2 or equivalently s, Q^2 these being related by

$$s \equiv W^2 = M^2 + 2M\nu - Q^2 \qquad (5)$$

(s being the square of the mass of the final hadronic system $\equiv W^2$). Conventionally we define for future reference[4-6] $\omega = \dfrac{2M\nu}{Q^2}$, $\dfrac{W^2}{Q^2} = \omega' - 1$ (hence $\omega' = \dfrac{2M\nu + M^2}{Q^2}$) and $\omega_W = \dfrac{2M\nu + a^2}{Q^2 + b^2}$. The kinematic region being explored is then shown in fig. 3 where contours of fixed ω, ω' and ω_W as well as fixed W^2 are shown.
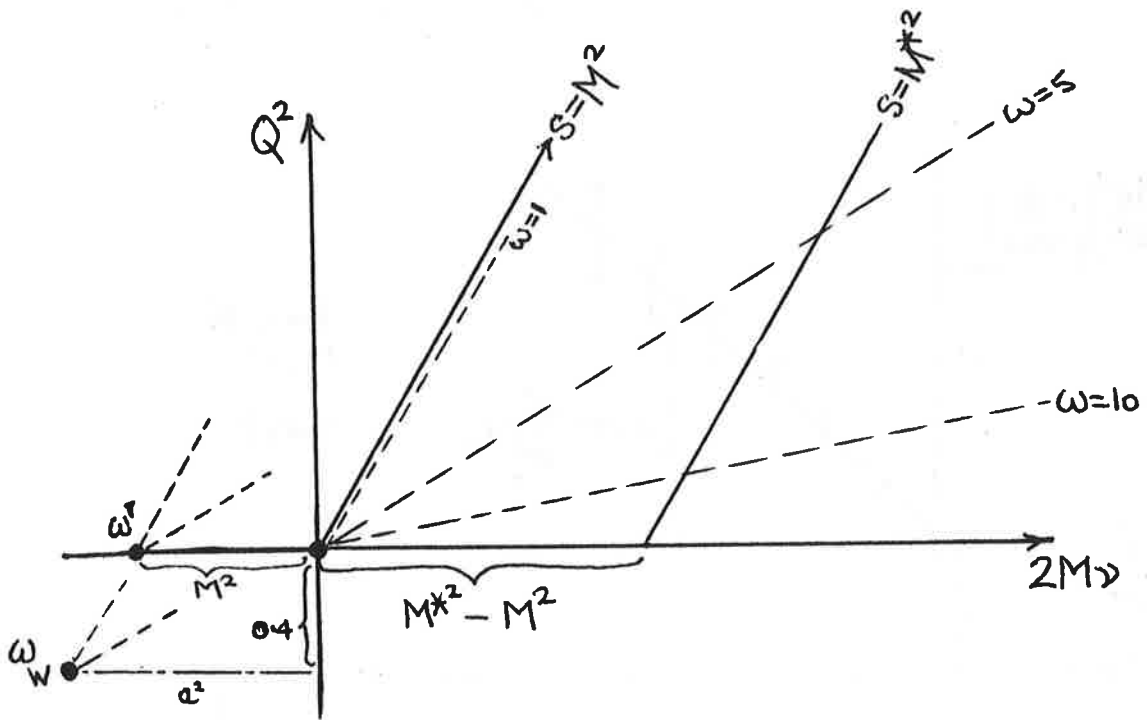
Fig. 3   Kinematic region in $\nu - Q^2$ plane available to electron scattering. Contours of fixed ω, ω', ω_W and W are indicated. The fixed ω radiate from the origin, ω' and ω_W radiate from the indicated points.

2 ELASTIC SCATTERING AND THE Q^2 BEHAVIOUR AT FIXED W^2

If we hold $s(W^2)$ fixed $= M^2$ then we will be studying elastic scattering for which

$$\frac{d^2\sigma}{d\Omega dE'} = \frac{4\alpha^2 \, E'^2 \, \cos^2\theta/2}{Q^4} \, \delta\left(\frac{Q^2}{2M} - \nu\right) \left(\frac{G_E^2 + \frac{Q^2}{4M^2} G_M^2}{1 + Q^2/4M^2} + \frac{Q^2}{4M^2} G_M^2 \, 2\tan^2\theta/2 \right) \quad (6)$$

where $G_{E,M}(Q^2)$ are the electric and magnetic form factors of the proton[7], and the delta function arises due to our constraining the final state to elastic scattering. Thus

$$W_2^{el} = \delta\left(\frac{Q^2}{2M} - \nu\right) \left\{ \frac{G_E^2 + \frac{Q^2}{4M^2} G_M^2}{1 + Q^2/4M^2} \right\} ; \quad W_1^{el} = \frac{Q^2}{4M^2} G_M^2 \, \delta\left(\frac{Q^2}{2M} - \nu\right) \quad (7)$$

Fig. 4   Schematic plot of $(d\sigma)/(d\sigma)_{MOTT}$ against $\tan^2\theta/2$.

Integrating over the electron energy dE' we obtain the Rosenbluth formula

$$\frac{d\sigma}{d\Omega} = \left(\frac{d\sigma}{d\Omega}\right)_{MOTT} \left[\frac{G_E^2 + \frac{Q^2}{4M^2} G_M^2}{1 + Q^2/4M^2} + \frac{Q}{4M^2} G_M^2 \, 2\tan^2\theta/2 \right] \tag{8}$$

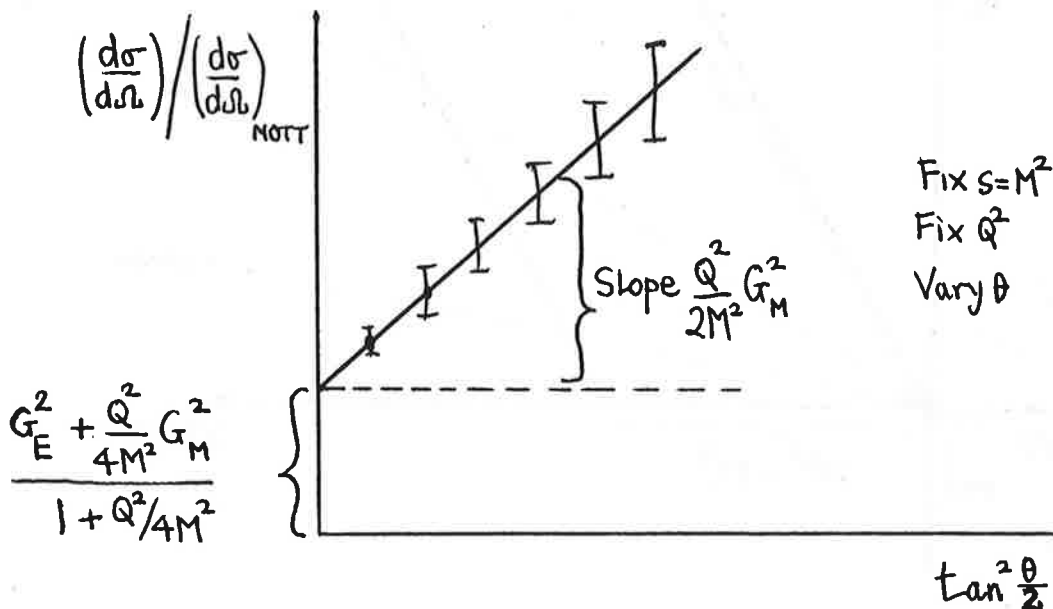where $\left(\dfrac{d\sigma}{d\Omega}\right)_{MOTT} = \dfrac{4\alpha^2 \, E'^2 \, \cos^2\theta/2}{Q^4 \left[1 + \dfrac{2E}{M} \sin^2\theta/2 \right]}$ is the cross section for an electron

scattering from the Coulomb field of a "structureless" proton of mass M. Hence the quantity is parentheses in eq.(8) arises from the proton's structure. We note that

$$\frac{d\sigma}{d\Omega} \bigg/ \left(\frac{d\sigma}{d\Omega}\right)_{MOTT} = A + B \, \tan^2\theta/2 \tag{9}$$

and so varying θ while holding Q^2 fixed and $W^2 = M^2$ we can separate A, B and hence $G_{E,M}$ (or $W_{1,2}^{el}$) (fig. 4).

As is familiar to you all, $G_{E,M}(Q^2)$ die at large Q^2 and are <u>approximately</u> fitted by a dipole behaviour $(1 + Q^2/.71)^{-2}$, their ratio being <u>approximately</u> constant, $G_M \sim \mu G_E$. This "dipole fit" is not theoretically motivated, not understood and does not fit the data further than a first approximation[7]. It is however a useful parametrization for <u>illustrative purposes only</u>. (Experimentalists - with your powerful machine at CERN II - please do not forget "mundane" elastic scattering out to as large Q^2 as you can get - there is still a lot to be learned here). In fig. 5 we show[5] the combination $G_E^2 + \frac{Q^2}{4M^2} G_M^2$ plotted against Q^2/M^2 this being the elastic analogue of $\sigma_T + \sigma_S$ (eqs. 8 and 3b). At small Q^2 we note the cross section falls as Q^{-2}, at large $Q^2 \gg .71$ GeV^2 the dipole behaves as Q^{-4} and hence the cross section as Q^{-6} ($\sim Q^2 \, G_M^2$).
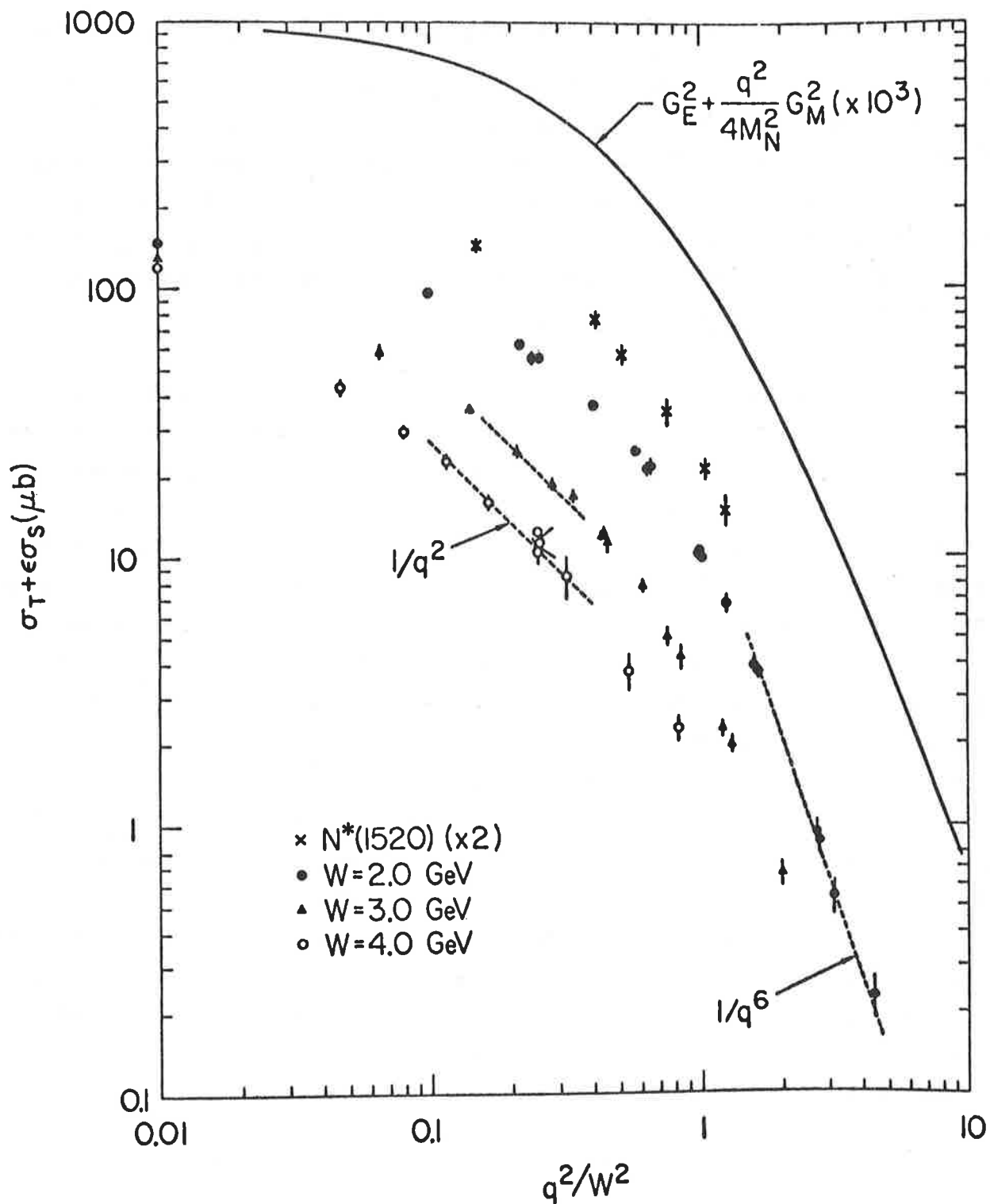
Fig. 5 $\sigma_T + \epsilon\,\sigma_S$ for various hadron masses W plotted against Q^2/W^2. The solid line is for elastic scattering assuming dipole form factors (after ref. 5).

From the data on $\frac{d^2\sigma}{d\Omega dE'}$ one can extract Σ (eq.4) and for various fixed W = 1.52, 2, 3,4 GeV we obtain the Q^2 dependences shown in fig. 5. We note that these various fixed W cross sections exhibit similar behaviours in Q^2/W^2, falling like Q^{-2} for .1 < Q^2/W^2 < .4 whereas at larger Q^2/W^2 they fall like Q^{-6}. Thus whereas the deep inelastic cross sections (W $\gtrsim$ 2 GeV) <u>do</u> fall more slowly with Q^2 than does elastic scattering <u>at the same value of Q^2</u> (at least, for Q^2 < W^2) eventually at <u>large</u> Q^2 the fixed W cross sections turn over to Q^{-6} <u>even in the deep inelastic region</u>[8].

Just as in the elastic scattering example where we had to vary θ at fixed W^2, Q^2 to separate $W_{1,2}^{elastic}$, so in the inelastic case we must vary θ at fixed W^2, Q^2 to separate $W_{1,2}$ or equivalently $\sigma_{T,S}$. This being done one defines R $\equiv \sigma_S/\sigma_T$ and experimentally this ratio is small in the kinematic region examined up to the present time[2]. Having separated W_1 and W_2 (W^2, Q^2) we may now plot the quantity νW_2 $(Q^2)_{W^2\ fixed}$ and for W^2 > resonance region we show in fig. 6 the data for W^2 = 4, 9 and 16 $(GeV)^2$. When plotted against Q^2/W^2 these three data sets appear to be on top of each other. Indeed, for <u>any</u> fixed $W^2 \gtrsim$ 4 $(GeV)^2$ the Q^2 dependence is consistent with lying on the single "universal" curve (fig. 7). Hence νW_2 $(Q^2/W^2, W^2) \rightarrow \nu W_2$ (Q^2/W^2) for each and every $W^2 \gtrsim$ 4 $(GeV)^2$. Thus we have obtained the familiar result that for W^2 > 4, Q^2 > 1 νW_2 exhibits the phenomenon of scale invariance though the direction from which we have approached (i.e. concentrating on fixed W^2 behaviours) is perhaps different from that which one normally uses. To see this curve plotted against W^2/Q^2 instead of Q^2/W^2 the choice of log plot means that all the reader need do is to turn the page, hold the page to the light and view from behind (alternatively hold a mirror perpendicular to the page aligned along the νW_2 axis). The resulting curve will be νW_2 versus W^2/Q^2 and may be compared with fig. 2.

The phenomenon of scale invariance gets its most popular interpretation in the parton model where the inelastic scattering is the incoherent sum of the elastic scattering from the constituents or "partons" in the proton (fig. 8a) (see P.V. Landshoff, these proceedings).

1.   How does this universal Q^2 dependence of νW_2 at large values of W^2 compare with that at small W^2 where resonance excitation is present?
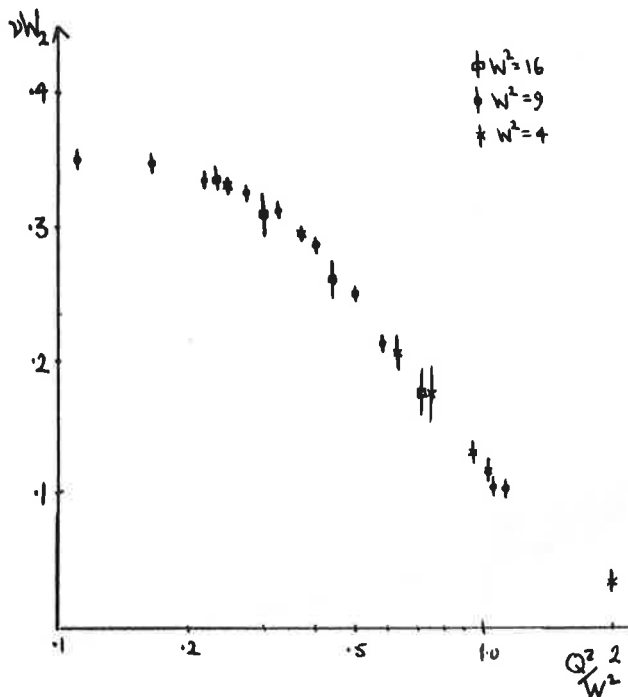
Fig. 6 νW_2 as a function of Q^2 at fixed $W^2 = 4, 9, 16$ (GeV)^2

from refs. 5, 8.
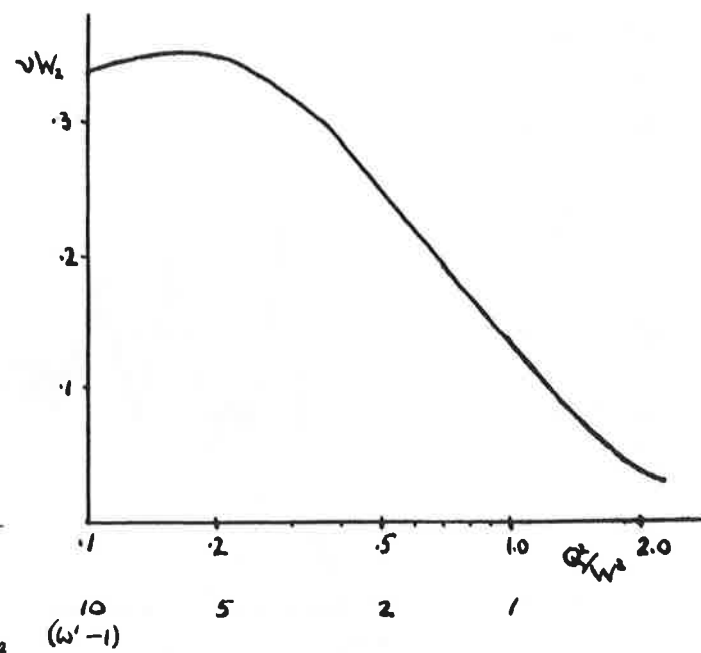
Fig. 7   Best fit to νW_2 (Q^2, W^2) for any $W^2 \geq 4$ (from G. Miller, ref. 8)
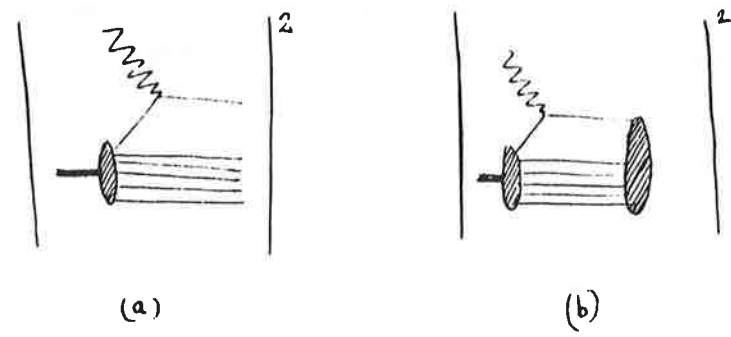
Fig. 8   a) Incoherent scattering from partons.

b) Coherent excitation of nucleon in the parton picture.
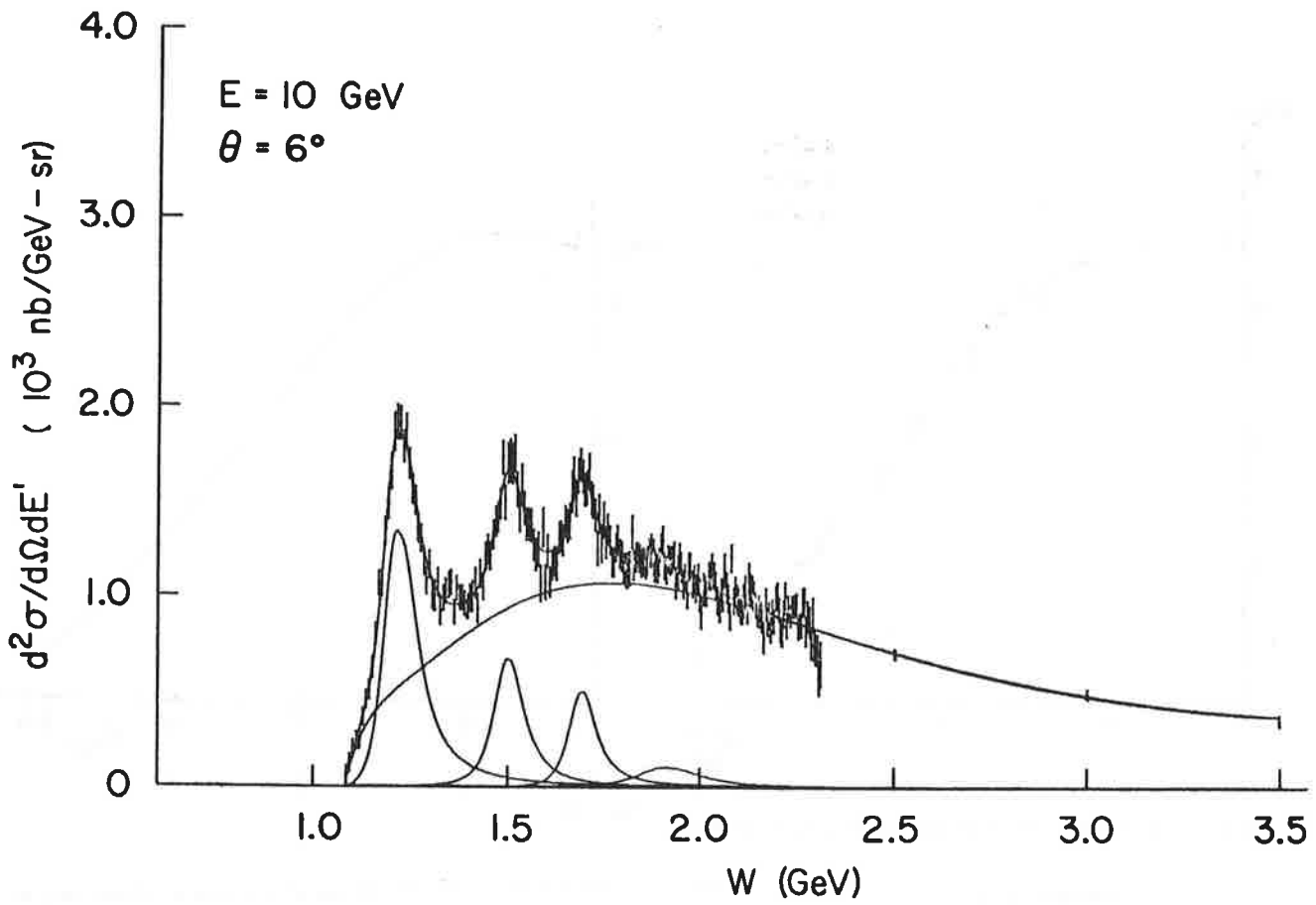
Fig. 9   Resolution of the 10 GeV, 6° electron spectrum (ref. 9) into four modified Breit-Wigners and a smoothly varying background.
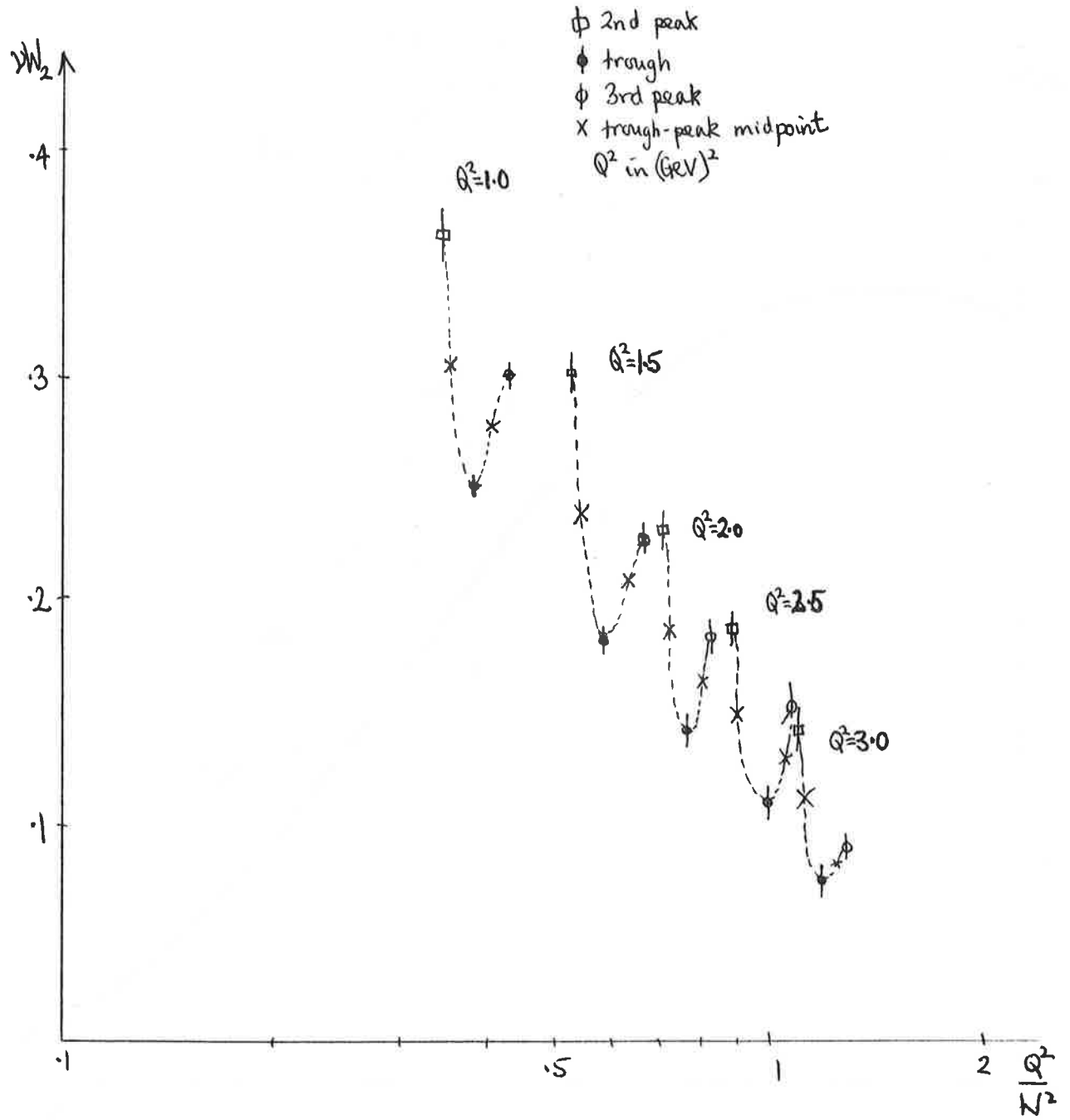
Fig.10   a) Contribution to νW_2 (Q^2) from the second and third resonance regions plotted against Q^2/W^2.
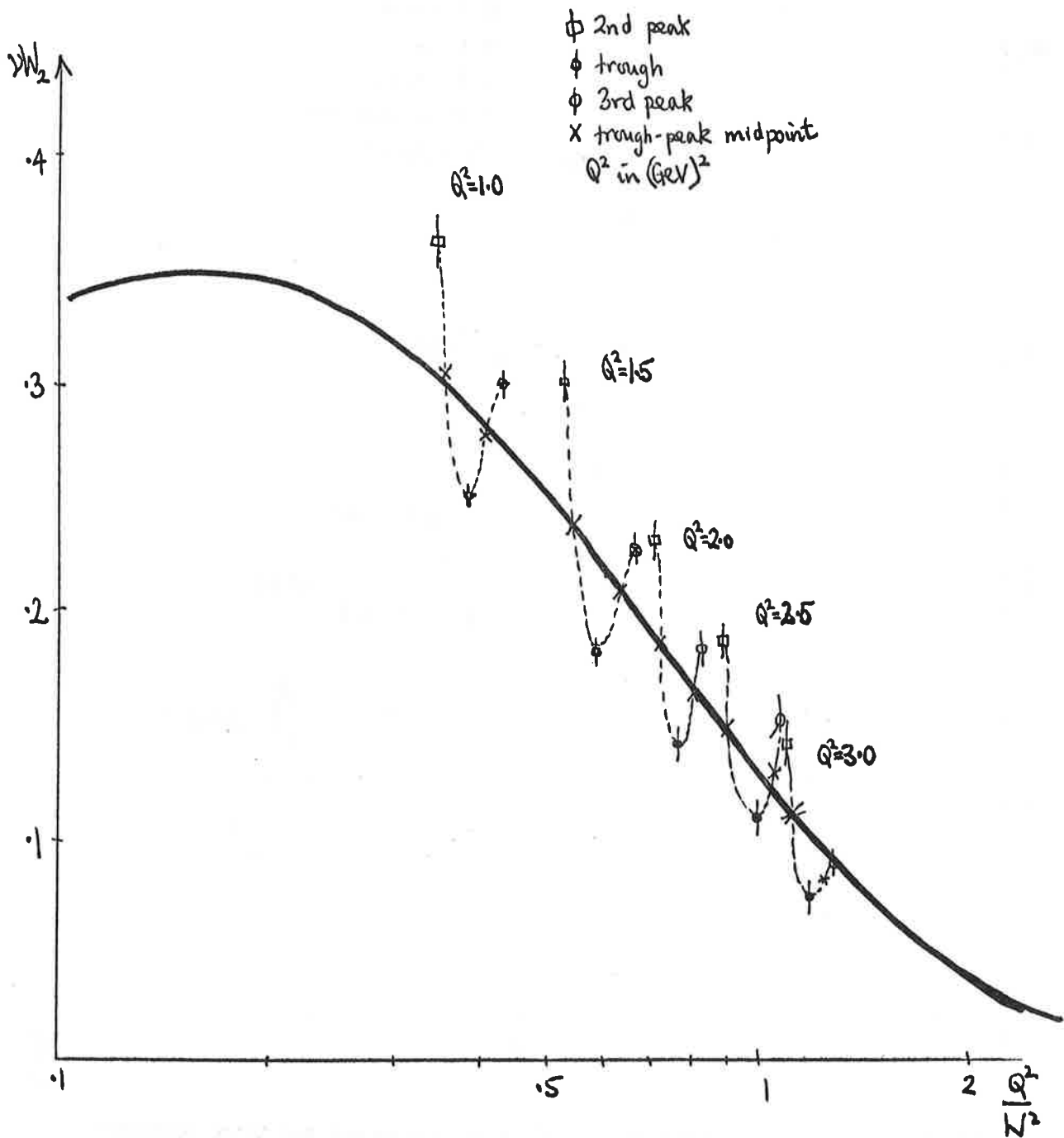
b) and compared with νW_2 (Q^2) for $W^2 \gtrsim 4$ $(GeV)^2$.

(2)   What happens if we include data for $Q^2 < 1$ $(GeV)^2$?

We shall study question (2) in section 4 and concentrate here on the question of the behaviour in the resonance region. A typical excitation data set is shown[9] in fig. 9 where bumps corresponding to the 1st, 2nd, 3rd and possibly even 4th resonance regions can be seen. Combining data at various angles one can interpolate to obtain fixed q^2 cross sections and we can then extract νW_2 (W^2, Q^2) through the resonance region. For the moment we shall make no attempt to separate resonance from background and in fig. 10a we show the νW_2 contribution from the peak of the second resonance, the peak of the third and also the trough between them plotted against Q^2/W^2 for $Q^2 = 1$, 1.5, 2, 2.5 and 3 GeV^2. The crosses which fall midway between crest and trough follow almost exactly the universal behaviour found at large W^2 (fig. 10b). Thus were it not for modulations caused by the resonating partial waves it would appear that the universal behaviour at large W would also obtain at small W. This is essentially Bloom-Gilman duality[5] (note that Bloom-Gilman duality does not, contrary to a popular misapprehension, extend scaling to smaller values of Q^2 - see section 4 in this respect).

At this point it is interesting to make a remark about parton models. I am trespassing on Dr. Landshoff's territory here - but as he is bound to claim that we have learned something from electron scattering in his talk and hence trespass on mine - I feel free to take this liberty. The universal curve for the large W, large Q^2 behaviour is generated in such models by the incoherent impulse diagrams, fig. 8a. Resonance excitation on the other hand is coherent excitation of the whole nucleon and may be represented by fig. 8b. Since we know nothing about the blob ("final state interactions") there is no a priori reason for this diagram to exhibit scaling behaviour (nor, for that matter, for it not to). However, the scaling seems to persist empirically even in to the small W region where N^* excitation (and hence this latter diagram) is present.

Two possibilities emerge:

(a)   This diagram does not scale - the "apparent" scaling of the data is due to the non-scaling N^* excitation being small and super-imposed upon a very large scaling background (fig. 8a).
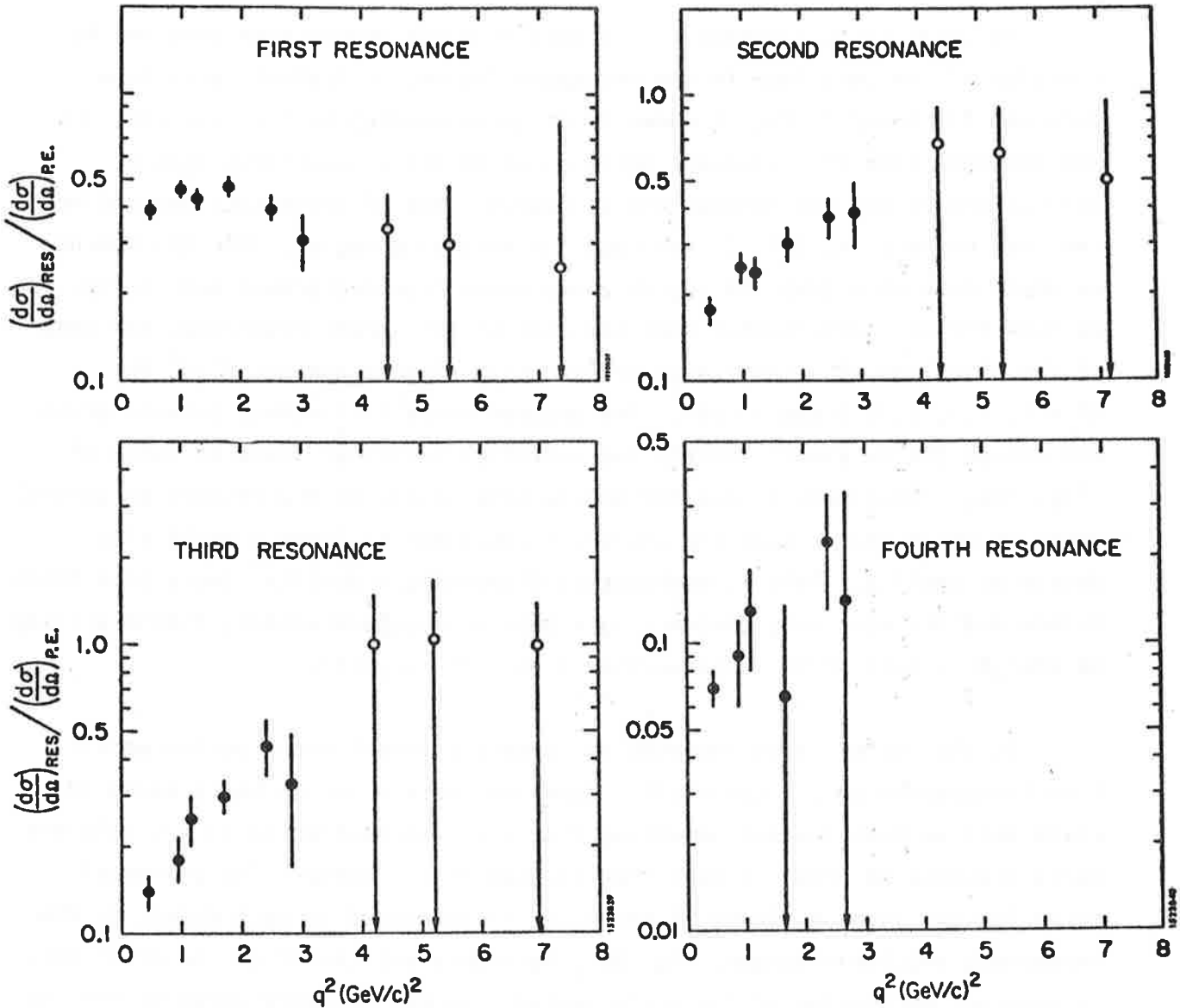
Fig.11   a) Ratio of resonance excitation cross section to elastic cross
              section in electron proton scattering (ref. 9) versus Q^2.

         b) Indication that data of fig. 11a may be consistent with
              resonance excitation being a function of Q^2/W^2. For a function
              of Q^2 the resonance to elastic ratio is a constant (upper
              figures) while for Q^2/W^2 the ratio increases due to the higher
              mass of the resonance the slope increasing as W^2 increases
              (lower figure).

$$\sigma(N^*) \text{ OR } \sigma(\text{ELAST.})$$

$$Q^2$$

$$Q^2/W^2$$

$$\frac{\sigma(N^*)}{\sigma(\text{ELAST})}$$

$$Q^2$$

----- "ELASTIC, $W^2 \sim 1$"

⎯⎯ "N^*" $W^2 \sim 2$

$$\boxed{f(Q^2)}$$

$$\sigma(N^*) \text{ OR } \sigma(\text{ELAST})$$

$$Q^2$$

$$Q^2/W^2$$

$$\frac{\sigma(N^*)}{\sigma(\text{ELAST})}$$

$$Q^2$$

$$\boxed{f\left(Q^2/W^2\right)}$$

fig 11b

(b)   This diagram does scale - the N^* themselves have "universal form factors", i.e. are functions of Q^2/W^2.

To attempt to settle which of these is realised in Nature requires a separation of N^* from background in the small W^2 data.

In fig. 11a we show $(d\sigma)^{N^*}/ (d\sigma)^{ELASTIC}$ obtained from Briedenbach's fit[8] to the small W data as four Breit-Wigner's plus a smooth background. That this behaviour is possibly consistent with being a function of Q^2/W^2 rather than Q^2 is shown in fig. 11b where universal behaviour in Q^2/W^2 would lead to $\sigma(N^*)/\sigma(ELASTIC)$ rising with Q^2 as against being constant if the excitation were universal in Q^2.

Encouraged by this qualitative suggestion we take Briedenbach's fits and plotting the 2nd and 3rd resonances against Q^2/W^2 we find they appear to be consistent with universal behaviour in Q^2/W^2 (fig. 12). The first resonance, however, appears to fall more rapidly. This conclusion coincides with the figure 13 taken from Bloom and Gilman (ref. 5), supplemented by $Q^2 < 1$ $(GeV)^2$ data, where the resonant fraction in νW_2 at 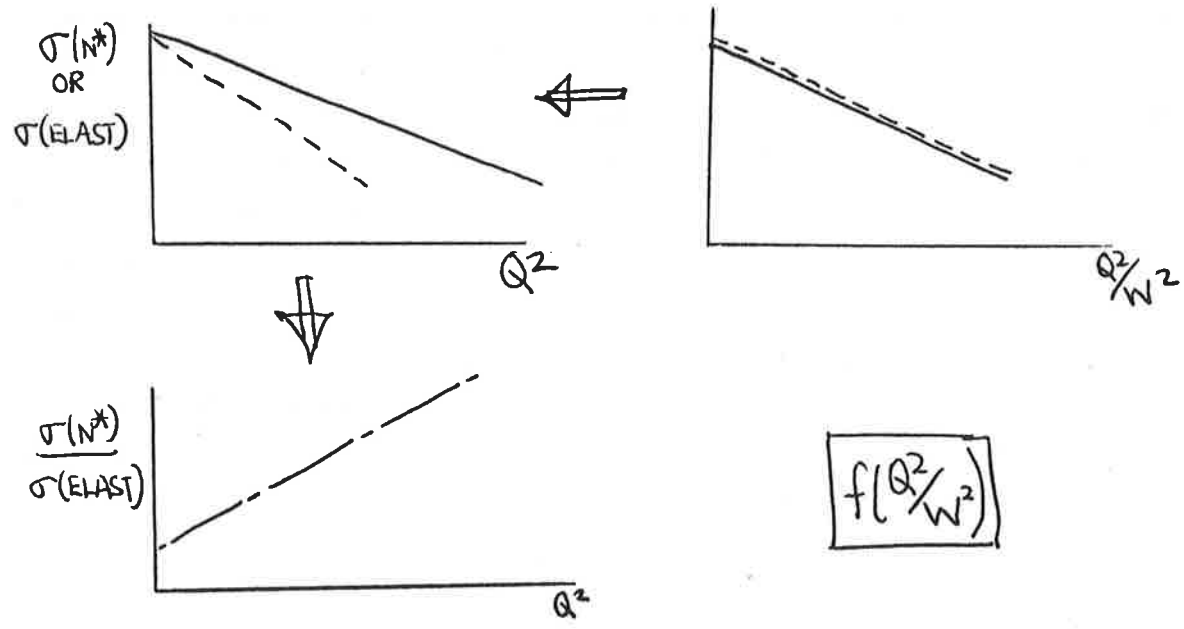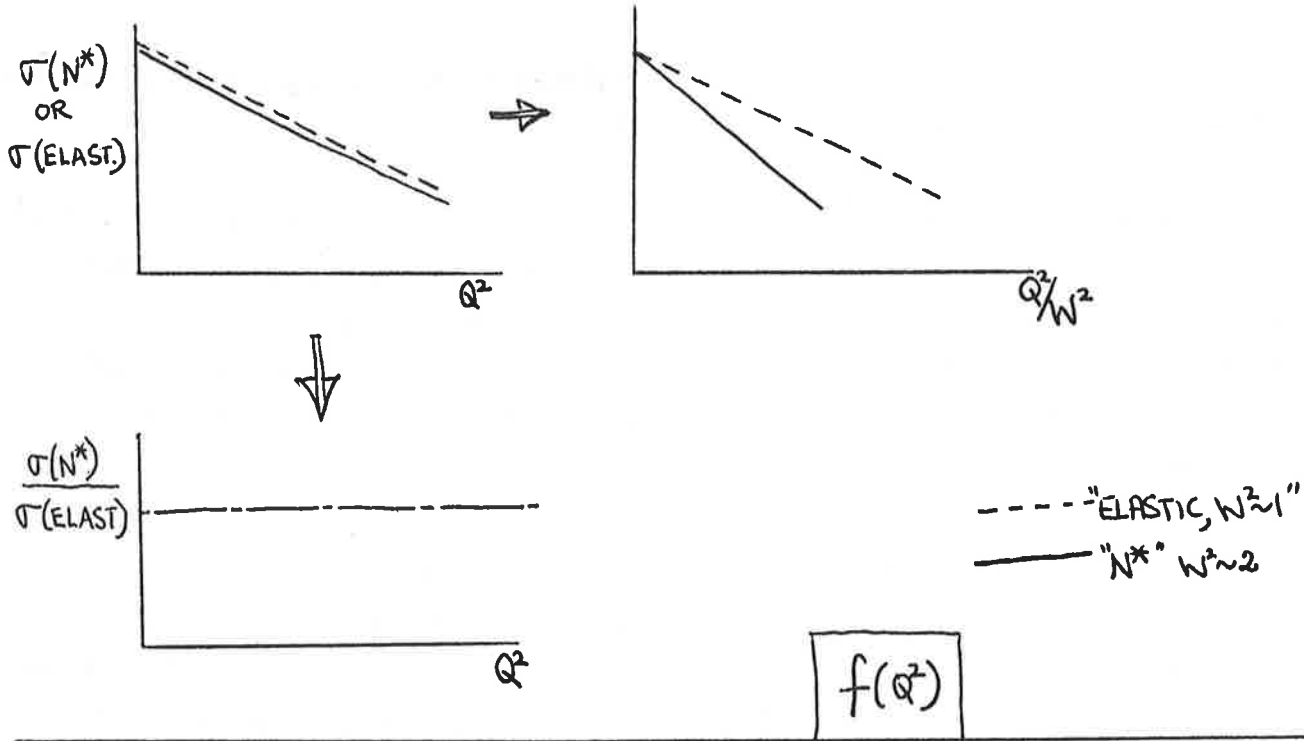a given ω' is compared with the universal behaviour of νW_2 (fig. 7) at the same ω' as Q^2 varies. The second and third resonances appear to be a constant ratio of the νW_2 scaling curve (fig. 7) as Q^2 varies and hence themselves scale. The possibility that the first resonance sinks into a scaling background as Q^2 increases while the second becomes more prominent (?) with the third staying roughly constant is suggested by the DESY data[10] (fig. 14) where as Q^2 increases the prominence of the second bump becomes marked while the first bump is becoming less noticeable above the background. Could it be that the $I = 3/2$ states are becoming less important than the $I = 1/2$ as Q^2 gets large ($\omega' \to 1$)? This at least is a possibility and although further study is needed to confirm this it is interesting to note that one effect of such a behaviour would be to reduce the value of $\nu W_2^{en}/\nu W_2^{ep}$ in the limit $\omega' \to 1$ from what it would have been if the $I = 1/2$ and $3/2$ states were "equally"[11] excited.

The data for this ratio is shown in fig. 15. Bloom and Gilman predict this ratio $\to 4/9$ as $\omega' \to 1$. As the error bars are large, and as the ratio need not approach $4/9$ monotonically, this prediction is still realisable by
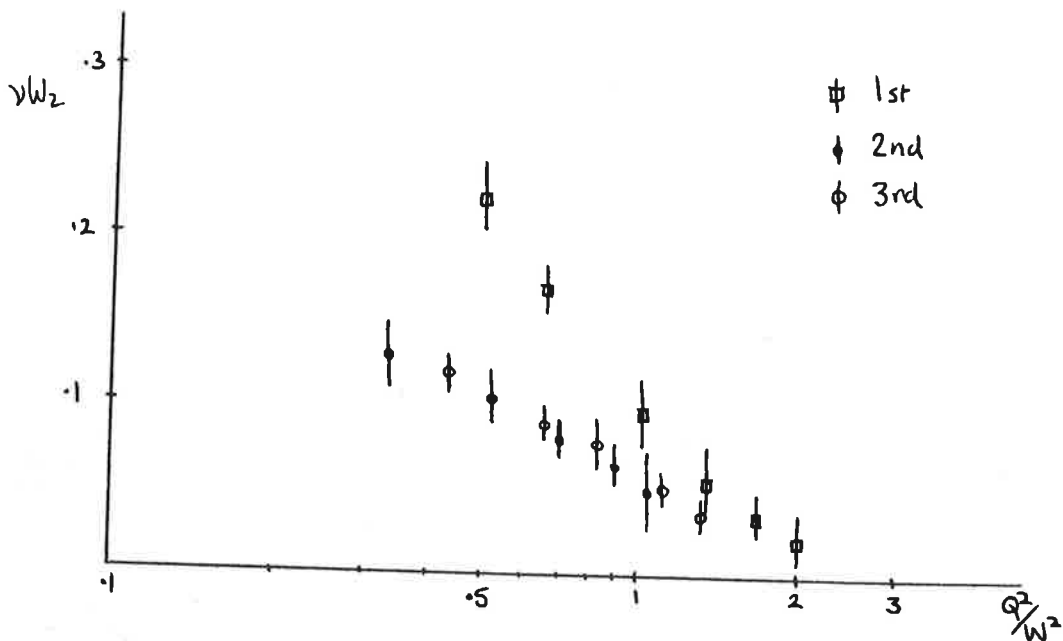
Fig.12 νW_1^{Res} against Q^2/W^2 for first, second and third resonance regions.
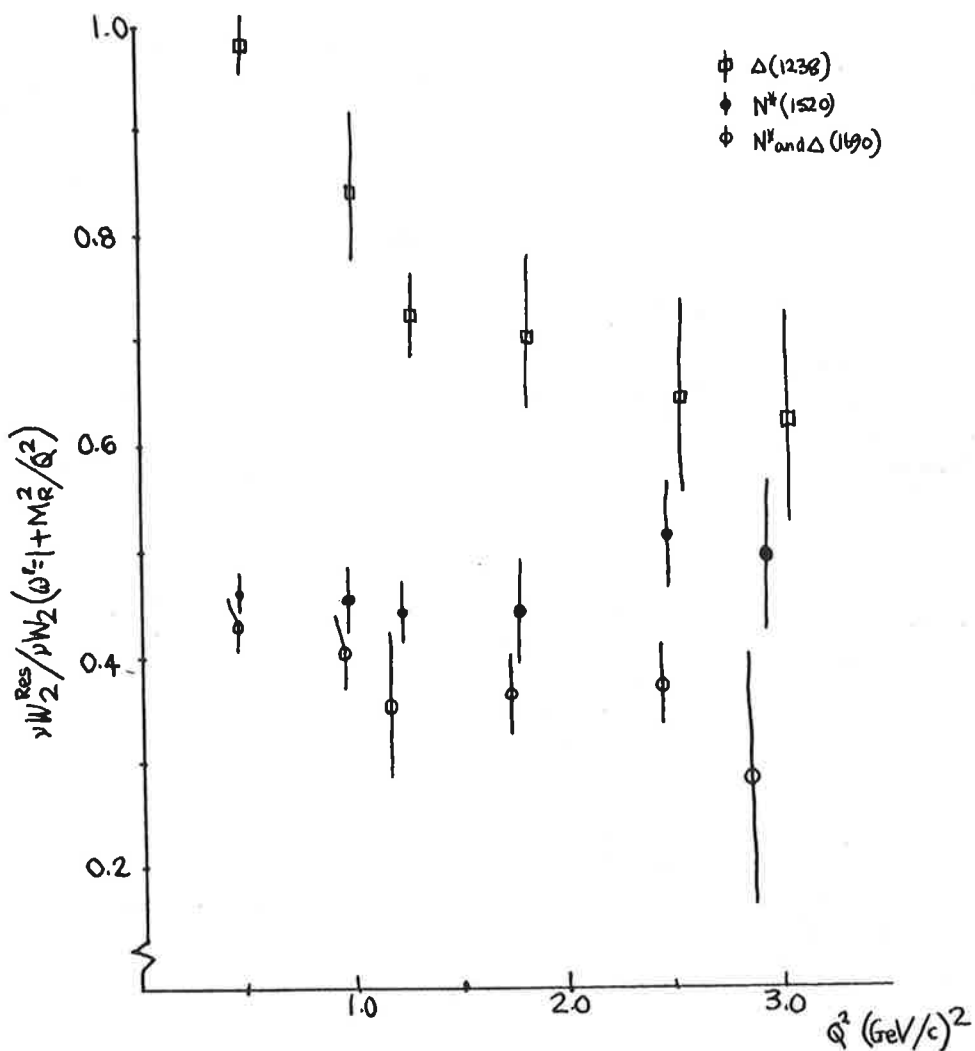
Fig.13   The ratio of the height of the resonance bumps in νW_2 to the value
of the scaling limit curve $\nu W_2(\omega')$ at the corresponding value of
$\omega' = 1 + M_{N*}^2/Q^2$ (from ref. 5 supplemented by $Q^2 < 1$ (GeV)^2 points –
F.J. Gilman (unpublished)). Values for the height of the
resonance bump are taken from fits to the 6° and 10° inelastic
spectra by M. Briedenbach, the $\nu W_2(\omega')$ values from G. Miller (ref.8).
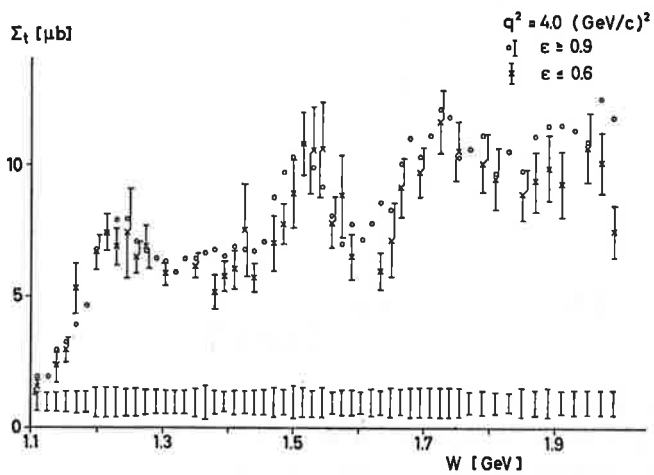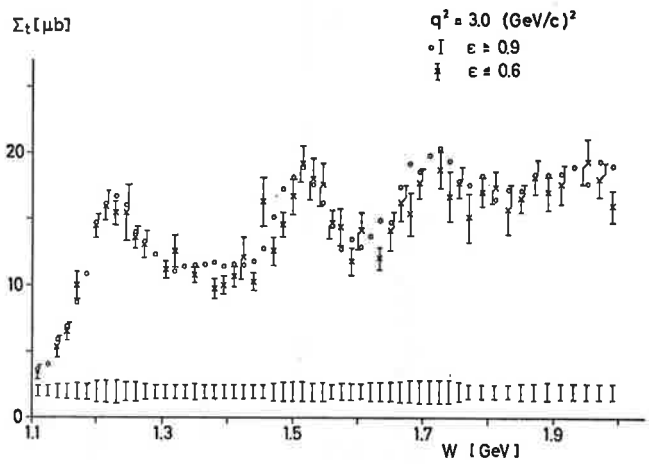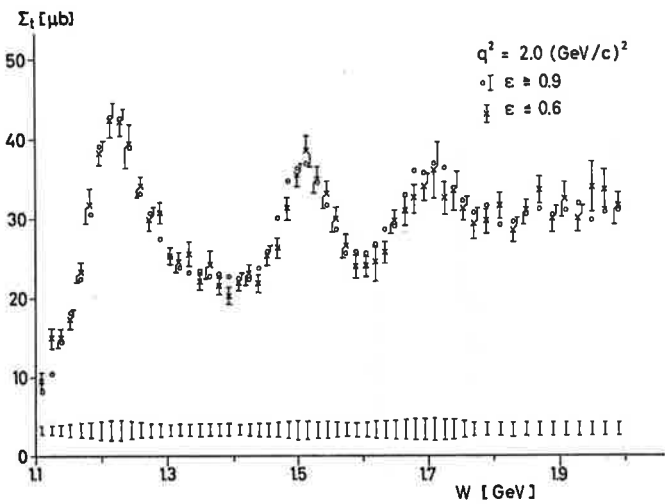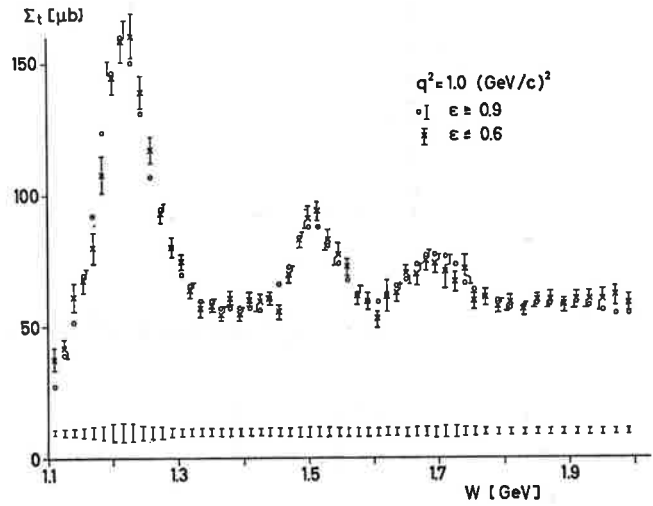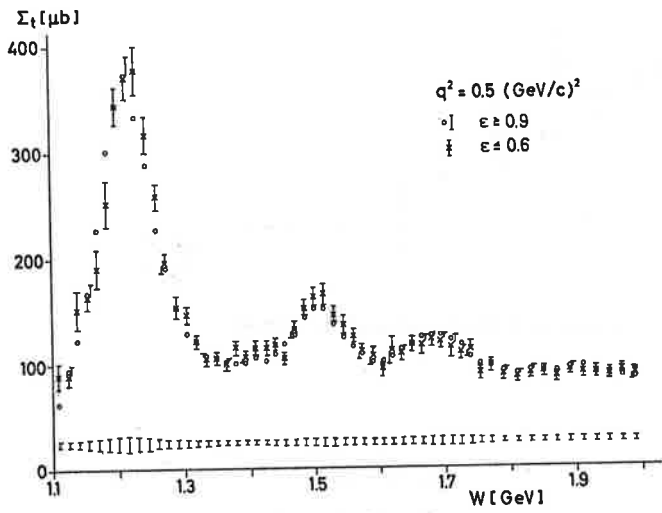
Fig.14 Σ (eq.4) data from ref. 10 for Q^2 = 0.5, 1.0, 2.0, 3.0 and 4.0 (GeV)^2.
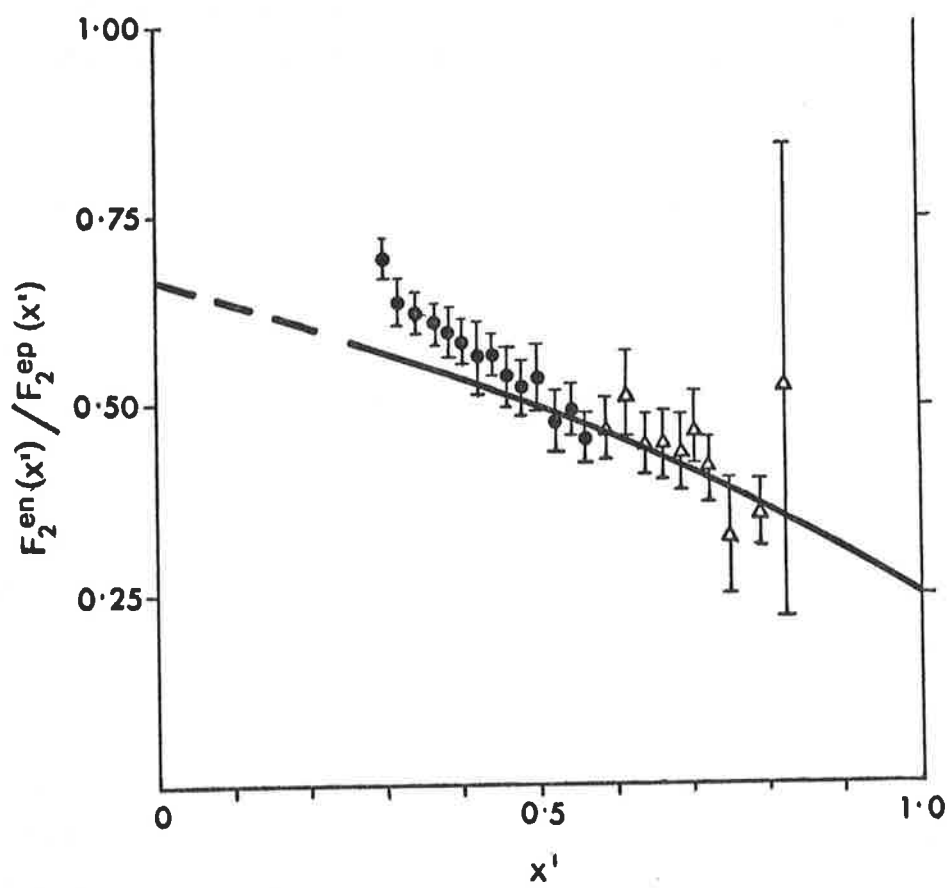
Fig.15 νW_2^{en} ratio with νW_2^{ep} against $x' = 1/\omega'$.   The curve is from ref.15.

the data. In quark-parton models this ratio cannot fall below 1/4. Ways in which attainment of this bound might connect with Δ suppression at large Q^2 have been discussed in refs. 12 - 14 where it seems that these effects might be quantitatively rather than just qualitatively correlated (ref. 14 and fig. 15). Further tests of this idea will be obtained in the neutrino experiments which I will discuss in the next section.

Before leaving this section two comments are called for. In fig. 11a one notes that the $\sigma(N^*)/\sigma(\text{elastic})$ gets progressively steeper as one proceeds to the higher mass N^* and as shown in fig. 11b this is what one would expect if the data were a function only of Q^2/W^2. However, the higher the resonance mass then the higher its spin and so the steepening of the slope in $\sigma(N^*)/\sigma(\text{elastic})$ could be in part not so much a scaling effect as a kinematic effect arising from the higher angular momentum barriers that need to be overcome in exciting the higher spin resonances. One could then ask oneself whether at even larger W^2, into the deep inelastic region, whether the ever higher partial waves present means that the "scaling" of νW_2 has an origin, in part, in the higher angular momentum barriers[15].

Alternatively one may accept that the scaling is real, over and above angular momentum barrier effects, even down into the resonance region. As mentioned briefly earlier, in the deep inelastic (large W) region the scaling arises in the parton model from the incoherent impulse diagrams (fig. 8a). The resonance excitation is coherent excitation of the whole nucleon (fig. 8b) and empirically also exhibits scaling behaviour. Thus, in some sense, the diagram 8a is dual to 8b. Hence one might summarise this by concluding that the final state interactions don't change things much from the incoherent situation (8a). Thus numerical predictions and sum rules derived in the incoherent quark parton model (8a) may well work but no partons are seen due to the final state interaction which does not affect the scaling nor the essential underlying quark quantum numbers. The final state then consists of the decay products of hadrons (for a derivation of quark-parton model results by summing over s-channel hadron states[*] - fig. 8b - see ref. 22).

---

[*]It is possible that a complete picture might develop from marrying the quark-parton "intrinsic scaling" with the s-channel sum, fig. 8b and ref. 22, where the "scaling" obtains from angular momentum barrier effects discussed previously.

3 NEUTRINO SCATTERING AND ITS RELATION TO ELECTRON DATA

We can gain further information on the nucleon sub-structure by probing with a charged current instead of the photon. This we can do by using neutrino (anti neutrino) beams. Neglecting terms of order of the final lepton mass and assuming that the weak interaction proceeds by W exchange (with mass m_W) then the cross section may be written[16]

$$\frac{d^2\sigma(\nu,\bar{\nu})}{d\Omega dE'} = \frac{G^2 E'^2}{2\pi^2} \left[\frac{m_W^2}{m_W^2 + Q^2}\right]^2 \left\{\widetilde{W}_2 \cos^2\frac{\theta}{2} + 2\widetilde{W}_1 \sin^2\frac{\theta}{2} \mp \widetilde{W}_3 \frac{(E + E')}{M} \sin^2\frac{\theta}{2}\right\} \quad (10)$$

and if $m_W^2 \gg Q^2$ this collapses to the familiar current-current interaction at a point (with which we shall subsequently work). This cross section may be compared with the analogous expression in the electromagnetic case

$$\frac{d^2\sigma}{d\Omega dE'} = \frac{4\alpha^2 E'^2}{Q^4} \left\{ W_2 \cos^2\frac{\theta}{2} + 2W_1 \sin^2\frac{\theta}{2} \right\} \quad (2)$$

The similarity and difference with the electromagnetic case is obvious and arises as follows. Defining $\sigma_{R,L,S}$ as the "W absorption" cross sections (in analogous fashion to the electron case in section 1) for right handed, left handed and scalar W then

$$\widetilde{W}_1 = \frac{K}{\pi G \sqrt{2}} (\sigma_R + \sigma_L)$$

$$\widetilde{W}_2 = \frac{K}{\pi G \sqrt{2}} \frac{Q^2}{Q^2 + \nu^2} (\sigma_R + \sigma_L + 2\sigma_S)$$

$$\widetilde{W}_3 = \frac{K}{\pi G \sqrt{2}} 2(\sigma_R - \sigma_L) \frac{M}{\sqrt{Q^2 + \nu^2}}$$

The comparison with the electromagnetic case now follows: the photon propagator has gone; $\frac{G^2}{2\pi} \leftrightarrow 4\pi\alpha^2$ and finally by parity $\sigma_R = \sigma_L$ and hence $W_3^{e.m.}$ is zero (hence equation 2), and $\sigma_T = 1/2 (\sigma_R + \sigma_L)$. The $\widetilde{W}_{1,2}$ contain now

78.

both vector-vector (VV) and axial-axial (AA) pieces in contrast to the electro-magnetic which is purely VV. The vector axial interference is given by $\widetilde{W}_3$ and hence the sign change in eq.(10) upon replacing a neutrino beam by anti-neutrino.

Questions to be answered include:

(i) Do the weak structure functions scale analogously to their electromagnetic counterparts?

(ii) What are the magnitudes of the weak as compared to the electromagnetic structure functions?

The first question is investigated as follows. Assume that the W boson, if it exists, has $M_W^2 \gg Q^2$ so that we may drop the bracket involving m_W in the eq.(10). Defining $x = \dfrac{Q^2}{2M\nu} \equiv 1/\omega$ and $y = \nu/E$ then (10) is rewritten as

$$\frac{d^2\sigma}{dxdy} \left(\equiv \frac{2M\nu E^2 E'}{\pi} \frac{d^2\sigma}{d\Omega dE'} \right) = \frac{G^2 ME}{\pi} \left\{ \nu W_2(x,y) \left[1 - y - \frac{Mxy}{2E} \right] \right.$$

$$\left. + M\overset{?}{y}x \;\; W_1(x,y) \mp y(1 - \frac{y}{2}) \, x\nu W_3(x,y) \right\} \tag{11}$$

If the $\widetilde{W}_i$ scale as[17]

$$M\widetilde{W}_1(x,y) \;\to\; F_1(x)$$
$$\nu\widetilde{W}_2(x,y) \;\to\; F_2(x) \tag{12}$$
$$\nu\widetilde{W}_3(x,y) \;\to\; F_3(x)$$

then on substituting into (11) we have

$$\underset{E \to \infty}{\text{Lim}} \;\; \sigma(E) = \frac{G^2 ME}{\pi} \int_0^1 dx \left\{ \frac{1}{2} F_2(x) + \frac{x}{3} F_1(x) \mp \frac{x}{3} F_3(x) \right\} \tag{13}$$

where $E \to \infty$ means E large enough that our formulae apply while not so large that the current-current form of the interaction breaks down (see C.H. Llewellyn-Smith, these proceedings). Hence, if the $\widetilde{W}_i$ scale as in (12),

the cross section will increase linearly with neutrino energy. The data on propane indeed show such a linear behaviour[18]

$$\sigma(E) = (0.51 \pm 0.13) \frac{G^2 ME}{\pi} \text{ per nucleon} \qquad (14)$$

suggesting that the structure functions do scale (though much more work is needed to make this conclusive).

This brings us to the second question, namely the magnitude of these structure functions. We define:

$$R,L \equiv \sigma_{R,L}/\!\left(\sigma_R + \sigma_L + 2\sigma_S\right) \qquad (15)$$

so that $0 \leqslant R,L \leqslant 1$. One can show that in the large energy limit in which we are working

$$\frac{xF_1}{F_2} = \frac{R + L}{2} \; ; \qquad \frac{xF_3}{F_2} = R - L \qquad (16)$$

Hence eq.(13) may be written

$$\underset{E \to \infty}{\text{Lim}} \frac{\pi}{G^2 ME} \sigma^{\nu,(\bar{\nu})}(E) = \int \frac{F_2(\omega)\, d\omega}{\omega^2} \left\{ \frac{1}{2} + \frac{R + L}{6} \pm \frac{L - R}{3} \right\} \qquad (17)$$

which may be further simplified by assuming $\sigma_S \approx 0$ (as suggested in the electron data) and hence $R + L = 1$ in which case

$$\underset{E \to \infty}{\text{Lim}} \frac{\pi}{G^2 ME} \sigma^{\nu,(\bar{\nu})}(E) = \int \frac{F_2(\omega)\, d\omega}{\omega^2} \left\{ \frac{2}{3} \pm \frac{1 - 2R}{3} \right\} \qquad (18)$$

Data with both ν and $\bar{\nu}$ beams are now available and hence the relative magnitudes of R and L can be obtained since from eq.(18) the ratio of cross sections for $\bar{\nu}$ to ν is

$$\underset{E \to \infty}{\text{Lim}} \frac{\sigma^{\bar{\nu}}}{\sigma^{\nu}} \approx \frac{1 + 2R}{3 - 2R} \qquad (19)$$

and hence lies between $1/3$ $(R = 0)$ and 3 $(R = 1)$. Parity conservation $(R = L = 1/2)$ would yield $\sigma^{\bar{\nu}} = \sigma^{\nu}$. Experimentally this ratio appears to be 0.38 ± 0.02 suggesting $R = (5 \pm 2)\%$ (more information may be found in the talk by W. Venus[19]) and hence $\tilde{W}_3$ is maximal and negative, which is a good thing if the Gross-Llewellyn Smith sum rule[20] is to be saturated

$$\int_1^\infty \frac{d\omega}{\omega^2} (F_3^{\nu p} + F_3^{\nu n}) = -6 \tag{20}$$

Taking the experimental magnitude eq.(14) and inserting into the left hand side of (18) with $R = (5 \pm 2)\%$ yields*

$$\frac{1}{2} \int \frac{F_2^{\nu n} + F_2^{\nu p}}{\omega^2} \, d\omega = 0.55 \pm 0.16 \tag{21}$$

In order to compare this with the electromagnetic results we must extract the VV contribution from (21). It is usually assumed that VV= AA in magnitude; let us be more general and write AA = g^2 VV in which case

$$\int (F_2^{\nu n} + F_2^{\nu p})_{VV} \, \frac{d\omega}{\omega^2} = (0.55 \pm 0.16) \times \frac{2}{1 + g^2} \quad \overset{\text{Define}}{\equiv} \quad \nu N \tag{22}$$

to be compared with the electron data (where we have assumed naive Regge behaviour at large ω)

$$\int (F_2^{ep} + F_2^{en}) \, \frac{d\omega}{\omega^2} = 0.28 \pm 0.04 \quad \overset{\text{Define}}{\equiv} \quad eN \tag{23}$$

and so for the integrated data

$$\frac{eN}{\nu N} = (0.51 \pm 0.15) \times \left(\frac{1 + g^2}{2} \right) \tag{24}$$

The first question is to ask what constraints are imposed by CVC for the weak structure functions. The weak current is solely isovector whereas both

---

*Propane contains 26 protons and 18 neutrons. Since $\sigma^{\nu n} \neq \sigma^{\nu p}$ a correction must be applied before (21) can be extracted. We took $\sigma^{\nu n} = 3/2 \, \sigma^{\nu p}$ which yielded a 4% effect which has been included in (21). For further discussion see ref.

isovector and isoscalar pieces are present in the electromagnetic case. By looking at the sum of proton and neutron, then the isoscalar-isovector interference does not contribute and we may write

$$F^{ep} + F^{en} \equiv F(1) + F(0)$$

$$\left[F^{\nu p} + F^{\nu n} \right]_{VV} \equiv \tilde{F}(1) \xrightarrow{CVC} 2F(1)$$

(24)

and so

$$\frac{eN}{\nu N} = 0.5 + \frac{F(0)}{2F(1)} \geqslant 0.5$$

(25)

In general one would not expect the isoscalar contribution to be absent and it is interesting to compute the typically expected size of isoscalar to isovector content in the electron data. In SU(3) the photon transforms as the third and eighth components of an octet

$$\gamma \sim \rho + \frac{1}{\sqrt{3}} \omega_8$$

and hence

$$\frac{F(0)}{F(1)} = \frac{1}{3} \quad \text{yielding} \quad \frac{eN}{\nu N} = 0.66$$

(26)

While this is probably true for diffraction where $F^{en} = F^{ep}$, for non-diffraction things are different, in particular the "ϕ"-nucleon cross section is purely diffractive. Hence if we uncouple the "ϕ" piece of the photon (i.e. use magic mixing or in a quark picture where $\gamma = 2/3 \, p\bar{p} - 1/3 \, n\bar{n} - 1/3 \, \lambda\bar{\lambda}$ we throw away the $\lambda\bar{\lambda}$ contribution) then one has $\frac{F(0)}{F(1)} = 1/9$ and so far non-diffraction finally[*]

$$\frac{eN}{\nu N} = \frac{5}{9}$$

(27)

The empirical value of $(0.51 \pm 0.16) * \left(\frac{1 + g^2}{2} \right)$ suggests that the non-diffraction is dominant(unless $g^2 > 1$), which is consistent with the small value for $\frac{R}{L}$ (which in a parton model suggests that the antiquarks - which are assumed relevant only

---

[*]In the quark-parton model this result obtains[21] when strange quarks in the nucleon are ignored. This is of course very similar in essence to our approach but note that partons are not necessary in order to derive the ratio (27).

to the diffractive scattering - are unimportant) and also with the fact that the cross section (eq.18) is probing the small ω region where diffraction is believed negligible (see also P.V. Landshoff these proceedings). It is encouraging that out of the a priori infinite range of possibilities for the eN/νN ratio, empirically it appears close to our theoretical prejudices. Much more data is required to be able to determine this ratio as a function of ω and see how much diffraction or non-diffraction is important. It might even be that the CVC constraint is being strained unless $g^2 > 1$.

Finally it is amusing to note that for diffraction $F^{en} = F^{ep}$ and $\frac{eN}{\nu N} = \frac{2}{3}$ in which case (assuming $g^2 = 1$)

$$\left[F_2^{\nu n} + F_2^{\nu p} = 6 F_2^{ep} \right]_{ND} \tag{27a}$$

Similarly for non-diffraction one expects $F^{en} = \frac{2}{3} F^{ep}$, and $\frac{eN}{\nu N} = \frac{5}{9}$ and again

$$\left[F_2^{\nu n} + F_2^{\nu p} = 6 F_2^{ep} \right]_{D} \tag{27b}$$

and so this relation should hold irrespective of the relative importance of diffraction to non-diffraction[22]. However, since $F_2^{en} < \frac{2}{3} F_2^{ep}$ as $\omega' \to 1$ it is probable that this relation (27) is violated as $\omega' \to 1$. It will be interesting to see in what way it is violated.[14]

4   DOES EVERYTHING SCALE IN ω_W ?

In section 2 we discussed the observed scale invariance of νW_2 (W^2, Q^2) for $Q^2 > 1$, $W^2 > 4$ (GeV)^2. Historically this scaling was originally noted in the variable $\omega = \frac{2M\nu}{Q^2}$ and the data plotted against $\omega' = \frac{W^2}{Q^2} + 1$ in fig. 1 would be essentially the same when plotted against ω since $W^2 = 2M\nu + M^2 - Q^2$ and hence for $W^2 \gg M^2$ with Q^2 large then $\omega' \simeq \omega$. However, for small W^2, e.g. in the resonance region, there is a significant difference between ω' and ω.
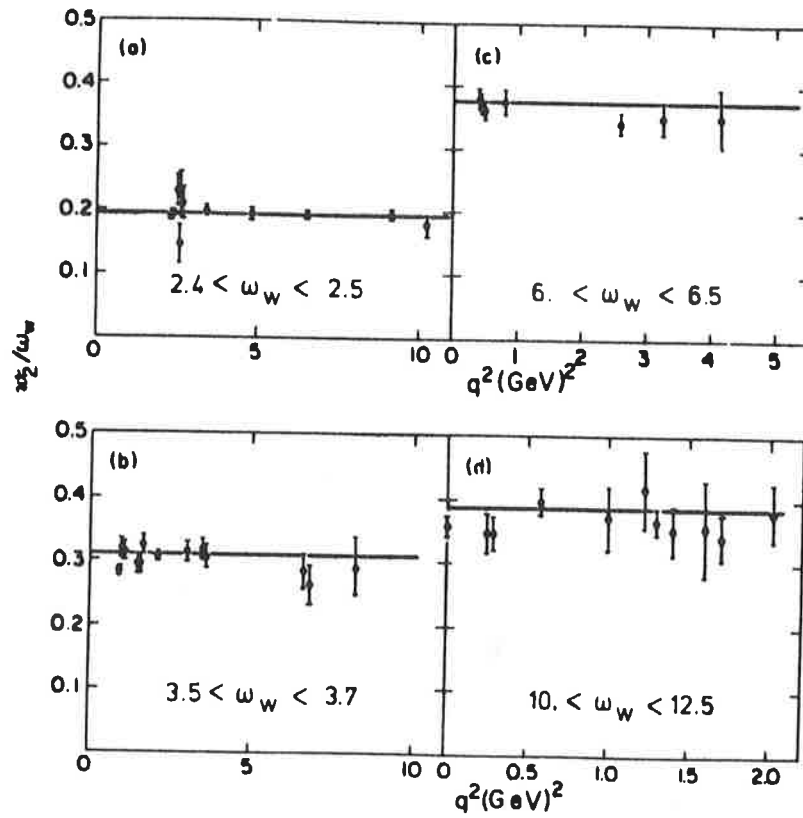
Fig.16   Constancy of $\dfrac{\omega_\nu W_2}{\omega_W}$ at fixed ω_W (ref.23)
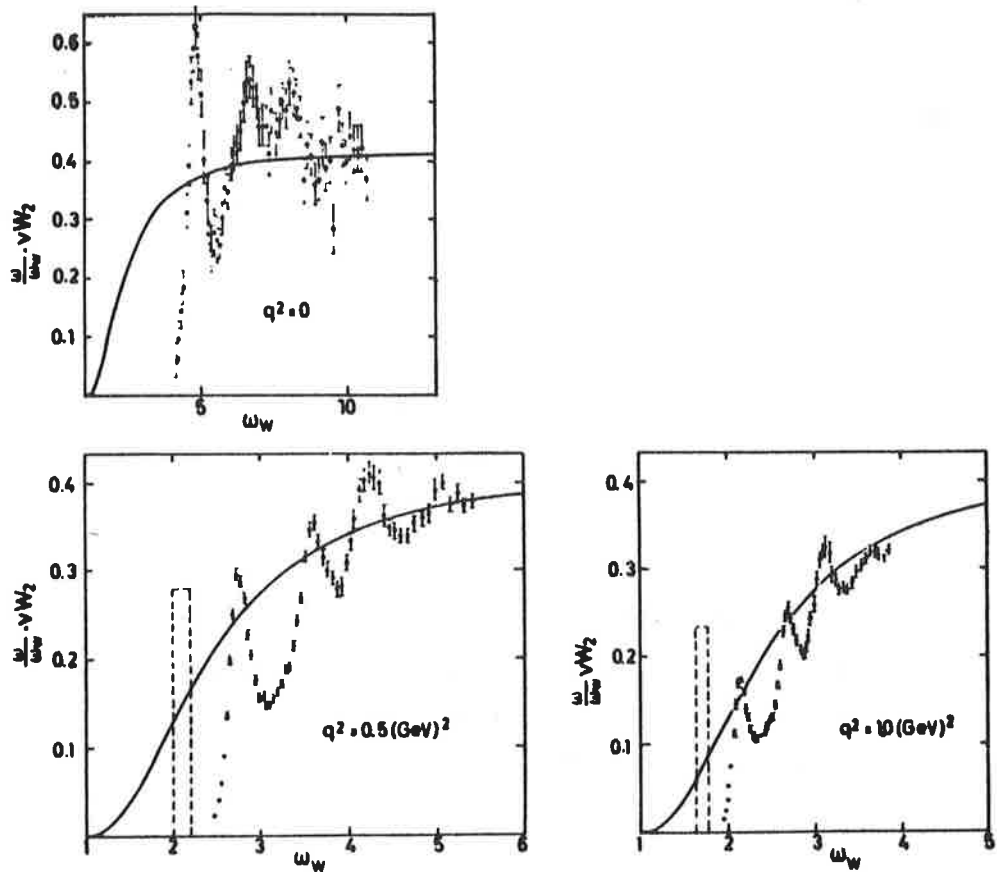
Fig.17   Comparison of $\dfrac{\omega_\nu W_2}{\omega_W}$ in the resonance region with the scaling limit

curve. The dashed rectangles represent the δ-function contribution
of elastic scattering (ref. 23).
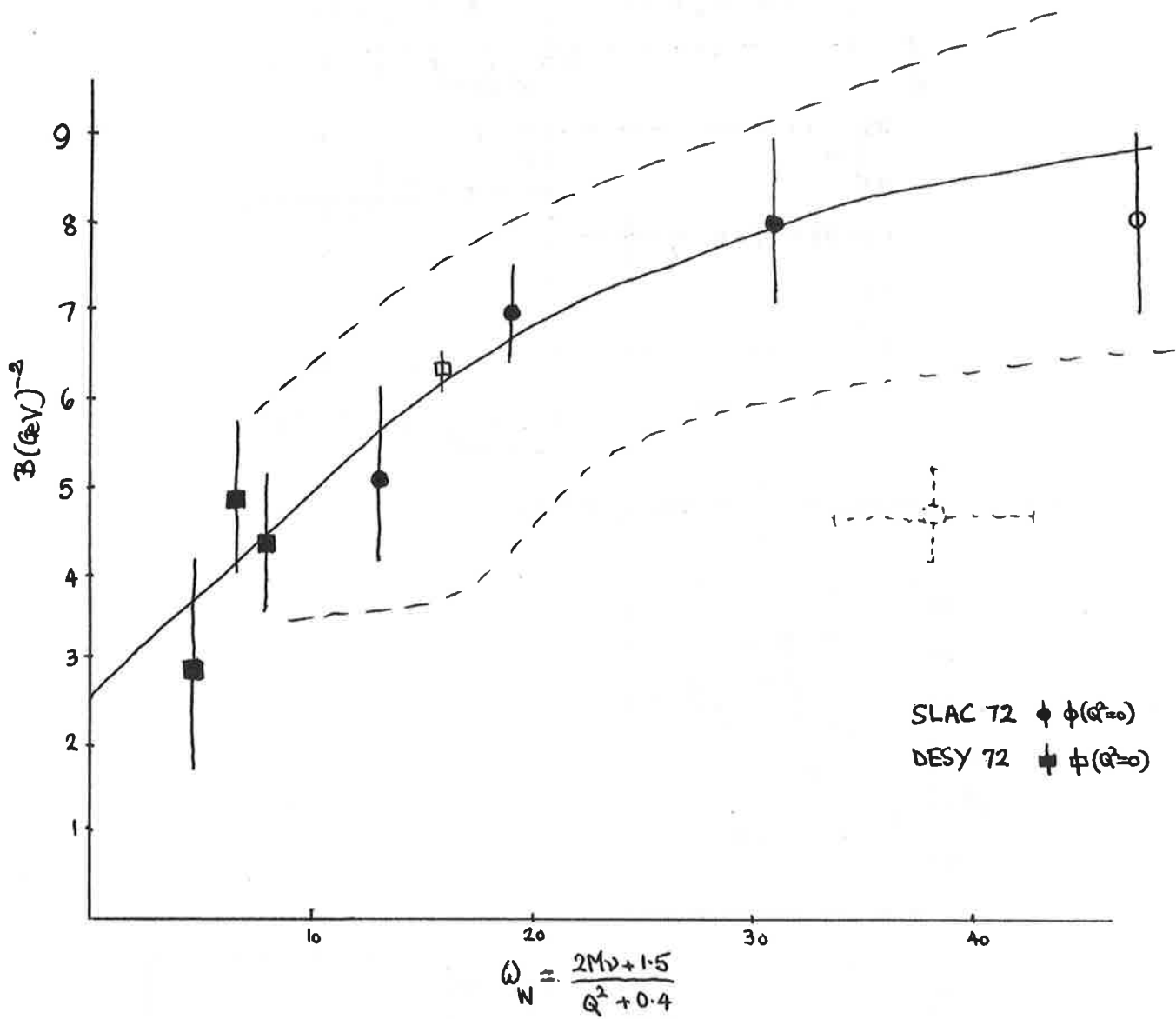
Fig.18   Slope B in ρ photo- and electroproduction, $\frac{d\sigma}{dt} \sim e^{Bt}$, plotted as a function of ω_W. Data from ref. 26. The dotted line is a rough indication of the range of B in photoproduction. The solid curve is an arbitrary eyeball fit going to B = 2.5 at small ω_W (see text).

The observation of scaling at small W^2 noted in fig. 10 would not obtain in terms of ω. Thus we conclude that the plotting of data in ω' extends the scaling* to smaller values of W^2 than when plotted against ω. This does <u>not</u> extend the scaling to smaller values of Q^2.

If one introduces[6] a variable $\omega_W \simeq \dfrac{2M(\nu + m_\rho)}{Q^2 + m_\rho^2}$ then for $Q^2 \gg m_\rho^2$ this $\simeq$ ω or ω'. Hence scaling at large Q^2 will obtain in ω, ω' or ω_W with equal facility. For $Q^2 \lesssim m_\rho^2$ the choice of ω, ω' as against ω_W will be critical and it was found that the function $\dfrac{\omega}{\omega_W} \nu W_2$ exhibits scale invariance in ω_W even down to $Q^2 = 0$. This may be seen in fig. 16 where $\dfrac{\omega}{\omega_W} \nu W_2$ is independent of Q^2 for various values of ω_W while in fig. 17 the solid curve is the analogue of our scaling curve for large W^2, Q^2 (fig. 7) and we see the resonance region oscillating round the scaling curve even at $Q^2 = 0$ (compare fig. 10b).

Since the total structure functions appear to be universal in ω_W then do the contributions from the individual channels also scale in ω_W? Things are unlikely to be this simple since channel thresholds open up at fixed W^2 and hence at different ω_W as Q^2 varies[24].

It has been noted that in ρ electroproduction the differential cross section $\dfrac{d\sigma}{dt} \sim A e^{Bt}$ and that the slope B appears to decrease (i.e. the cross section broadens) as Q^2 increases[25]. However, the magnitudes of B at similar Q^2 in the two experiments[26] seem to be different (we are not considering the various experiments that detect missing mass and make no attempt to separate the ρ from ω and/or background). However, if we plot the slope B against ω_W we notice that the data sets of the two experiments intermesh nicely, in particular the $Q^2 = 0$ point from DESY meshes with the $Q^2 = 1.2$ (GeV)^2 from SLAC. The data are shown in fig. 18 and the dotted line represents the range of B in photoproduction - the wide range arising from the various ways of analysing the ρ. A similar plot has been made by G. Wolf[25]. The solid curve is an eyeball average which goes to B = 2.5 as $\omega_W \to$ small (i.e. $Q^2 \to \infty$) which is a typical result for B in a geometrical picture if the changing slope is due to the photon radius shrinking to zero as $Q^2 \to \infty$ (hence $B_{\gamma p} \sim \frac{1}{4} B_{pp} \sim 2.5$).

---

* on the average, i.e. modulo resonance enhancements fig. 10b.

To test whether B is really a function of ω_W it is probably best to vary Q^2 while holding ω_W fixed. At the high energies available at NAL and CERN II it will be interesting to see whether $B \sim 7$ and independent of Q^2 at $\omega_W \sim 30$ even when $Q^2 >> 1$ $(GeV)^2$. This would certainly contrast with the dramatic change in B even by $Q^2 \sim 0.5$ $(GeV)^2$ at the lower energies due to the associated decreasing of ω_W where one comes to the knee of the curve around $\omega_W \sim 25$ and below this value of ω_W the slope B falls from around 8 to as low as 2.5.

5   g-2 FOR PARTONS ?

If one takes the parton model seriously then it is likely that the parton, if spin 1/2, has an anomalous magnetic moment of order $\alpha/2\pi$ in the same way that the electron picks up such a term. It is amusing to consider what would result if one took account of such a term in the naivest parton model by inserting an intrinsic anomalous moment at the photoabsorption vertex. Then if the anomalous moment is K and $\mu = 1 + K$ one has

$$\frac{\nu W_2}{W_1} = \frac{2M\omega}{\mu^2}\left[1 - \frac{K^2 Q^2}{4M^2}\right] \xrightarrow{K \to 0} 2M\omega \qquad (28)$$

while

$$R \equiv \frac{\sigma_S}{\sigma_T} \xrightarrow[\omega \text{ fixed}]{Q^2 \to \infty} \frac{Q^2 \omega^2 K^2}{4\,\mu^2 M^2} + \frac{Q^2}{\nu\mu^2} \xrightarrow[K = 0]{} \begin{matrix} \longrightarrow \infty \\ \longrightarrow 0 \end{matrix} \qquad (29)$$

and when K = 0 we recover the familiar results of the naivest spin 1/2 parton model (these results can be modified in less naive models, e.g. see ref. 27).

The present data on R and on the scaling of νW_2 restrict $K \leq .03$. If $K \sim 10^{-3}$, as would be the expected order of magnitude for electromagnetic anomalous moments, then it could lead to interesting effects at large Q^2, ω (eq.28 and 29).

If one takes naive spin $1/2$ partons seriously then NAL or CERN II could tell you whether $R = Q^2/\nu^2$ or whether $K \sim 10^{-3}$ since at $\nu = 100$ GeV and $Q^2 = 1$ (GeV)^2 one has $\dfrac{Q^2\omega^2}{4M^2} \sim 10^4$ and a $K \sim 10^{-3}$ yields

$$R/(Q^2/\nu^2) \simeq 100$$

to be contrasted with a value of 1 for this ratio if $K = 0$. However one could not distinguish from a behaviour $R = $ const. which might be expected in Regge type models. To distinguish an anomalous moment behaviour from $R = $ const. one would need EPIC. If $R = $ const. $\simeq 0.2$ then one would need $\nu = 1000$ GeV at $Q^2 = 1$ in order to yield $R = 1$ with $K \sim 10^{-3}$ and distinguish between them. If $R = $ const. $\simeq 1$, one must go to $\nu = 3000$ GeV and $Q^2 = 1$ for which $R = 10$ with $K \sim 10^{-3}$.

Hence although it is unlikely that such a naive calculation has much relation to Nature it is amusing to see an example of how a small thing ($K \sim 10^{-3}$) can make a big effect at high energies. Thus one should not get depressed too quickly by scaremongers who suggest that NAL and EPIC will "merely confirm scaling at large ν, Q^2".

ACKNOWLEDGEMENTS

References

1. S.D. Drell and J.D. Walecka, Ann. Phys. 28, 18 (1964).

2. See for example W. Toner, Report at Oxford Int. Conference on High
   Energy Physics, April (1972) and H. Kendall, Electron Photon Symp.
   Cornell 1971, for recent reviews.

3. L. Hand, Phys. Rev. 129, 1834 (1963);
   F.J. Gilman, Phys. Rev. 167, 1365 (1968).

4. J.D. Bjorken, Phys. Rev. 179, 1547 (1969)

5. E.D. Bloom and F.J. Gilman, Phys. Rev. Letters 25, 1140 (1970) and
   Phys. Rev. D4, 2901 (1971).

6. V. Rittenberg and H.V. Rubinstein, Phys. Letters 35B, 50 (1971).

7. For a summary of elastic scattering and resonance excitation see, for
   example, J.C. Rutherglen and also A.B. Clegg in 4th Int. Conf. on
   Electron Photon Interactions, Daresbury 1969; R. Wilson, 5th Int. Conf.
   Cornell, 1971.

8. See F.J. Gilman, Int. Conf. on Duality and Symmetry in Hadron Physics,
   Tel-Aviv 1971 and SLAC-PUB-896;
   Data from M. Briedenbach et al., Phys. Rev. Letters 23, 935 (1969),
   E.D. Bloom et al., ibid 930, M. Briedenbach, Ph.D. Thesis MIT
   G. Miller, SLAC-PUB-815.

9. See E.D. Bloom et al., SLAC-PUB-796 (contributed to Kiev Int. Conf. 1970).

10. F.W. Brasse et al., DESY 71/2 (1971).

11. The meaning of "equally" here needs expansion. If one uses SU(6)
    symmetry and sums over all the available resonances and imposes the
    constraints from no exotic t-channel exchanges then one obtains 2/3 for
    the n/p non-diffractive ratio. Suppressing all Δ would reduce this to a
    minimum of 4/9 (CGK, ref. 12). In SU(3) one can attain 1/4 if Δ are
    suppressed and fortuitons F/D couplings imposed (PR, ref. 12). This
    extra freedom is absent in SU(6).

12. S. Pallua and B. Renner, Phys. Letters 38B, 105 (1972).
    F.E. Close, F.J. Gilman and I. Karliner, Phys. Rev. D6, 2533 (1972).

13. R.P. Feynman "Photon Hadron Interactions", W.A. Benjamin, New York.

14. F.E. Close, DNPL/P146, to be published in Physics Letters.

15. See also the remark by P. Kessler in 4th Int. Conf. on Electron-Photon Interactions, Daresbury 1969 (p.191).

16. For more detailed discussion and further references on neutrino interactions see C.H. Llewellyn-Smith, Physics Reports $\underline{3C}$, 264 (1972).

17. J.D. Bjorken, Phys. Rev. $\underline{179}$, 1547 (1969).

18. See, for example, G. Myatt and D. Perkins "Further Observations on Scale Invariance in Neutrino Interactions" (Oxford 1970) and also ref. 16.

19. W. Venus, these proceedings.

20. D. Gross and C.H. Llewellyn Smith, Nucl. Phys. $\underline{B14}$, 337 (1969).

21. See ref. 16 and report by C.H. Llewellyn-Smith at the Oxford Int. Conf. April, 1972 (SLAC-PUB-1039).

22. See ref. 14 and also F.E. Close and F.J. Gilman, SLAC-PUB-1103.

23. F.W. Brasse et al., DESY 71/68 (1971).

24. But see also K. Berkelman, Report at XVI Int. Conf. on High Energy Physics, NAL (1972), CLNS-194.

25. For review see G. Wolf, DESY 72/61.

26. J.T. Dakin et al., SLAC-PUB-1154;
    V. Eckardt et al., DESY 72/67.

27. J.E. Mandula, CALT-68-356;
    H. Osborn and G. Woo, (DAMTP Preprint in preparation).

HIGHLY INELASTIC NEUTRINO REACTIONS

AT ACCELERATOR ENERGIES

W A Venus (RHEL)

1. Introduction

This talk gives an account of the data at present available from the CERN bubble chamber experiments on the inclusive reactions

$$\nu + N \rightarrow \mu^- + \text{hadrons}$$
$$\bar{\nu} + N \rightarrow \mu^+ + \text{hadrons}.$$

The experiments consist in firing a wide-band neutrino beam into a heavy liquid bubble chamber and measuring only the vector momentum $\vec{p}_\mu$ of the secondary muon and the total outgoing hadronic energy ν in each event. (The events occur in heavy nuclei, so details of the secondary hadron system are largely obscured by secondary interactions). From these quantities one calculates the primary neutrino energy E and the square of the 4-momentum transfer to the hadrons q^2:

$$E = E_\mu + \nu$$
$$q^2 = 4EE_\mu \sin^2 \frac{\theta_{\mu\nu}}{2}$$

The dimensionless variables x and y in terms of which scaling is supposed to be manifest in the "deep" inelastic region or Bjorken limit (q^2 and $M\nu$ both $\gg M^2$) are then given by

$$x = q^2/2M\nu \qquad 0 < x < 1 \quad (x = \frac{1}{\omega})$$
$$y = \nu/E \qquad 0 < y < 1$$

However, most of the events lie in what one might call the "shallow" inelastic region. Average values are $\bar{E} \sim 2\text{-}3$ GeV, $\bar{q}^2$ and $\bar{\nu} \sim 1$ GeV. Consequently one is obliged, as in the SLAC electroproduction experiments, to look for scaling behaviour in terms of slightly different dimensionless variables x' and y' that tend to x and y in the Bjorken limit.

The main experimental problems, apart from that of maximising the low high-energy event rate, are the identification of the muon, the determination of corrections for unseen hadronic energy (e.g. neutrons and gammas from π^0's), and the determination of the neutrino and antineutrino fluxes. The question of whether or not there are many neutrino events with <u>no</u> secondary muon (due to neutral currents) is largely unanswered but lies outside the scope of this talk (see earlier talk by Cundy).

The data presently available, ignoring events of energy below 1 GeV, consists of

(a) 740 neutrino events from the 1.2 metre bubble chamber (half from the 1963/1964 freon experiments and half from the 1967 propane experiment); and

(b) a preliminary analysis of the first 1117 neutrino events together with 1105 antineutrino events from the first runs (in 1971) of the current Gargamelle experiment in freon.

For these Gargamelle data, the absolute neutrino fluxes are only known to about the same precision (±15%) as for the 1967 experiment. But the <u>ratio</u> of neutrino and antineutrino fluxes is much better known (±5%) because of the cancellation of most sources of systematic error. And the corrections for unseen hadronic energy are very substantially smaller than in previous experiments because Gargamelle is much bigger. The absolute fluxes for the later runs (in 1972) of this experiment will be better known (perhaps to ±5%).

2. <u>Theoretical Background</u>

Assuming that only spins 0 or 1 are transferred to the hadron system, the differential cross section $d^2\sigma/dq^2 d\nu$ is given by just three structure functions. These are necessarily functions of the only scalar variables characterising the hadron vertex, namely q^2 and pq. $pq = M\nu$ if ν is evaluated in the rest system of the target nucleon.

$pq = M\nu$
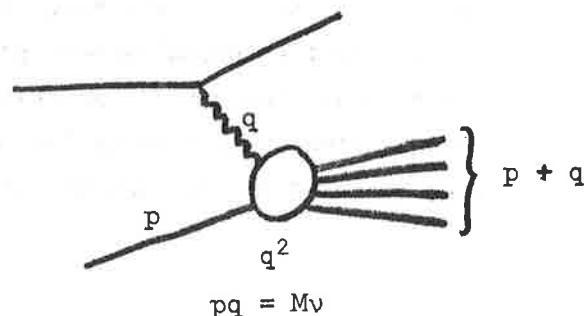
Assuming the leptonic weak current is point-like, and neglecting terms $O(M_\mu^2)$, the differential cross section can be written in the following form in terms of the variables x and y:

$$\frac{d^2\sigma^{\nu,\bar{\nu}}}{dx\ dy} = \frac{G^2ME}{\pi}\left[(1-y)F_2(pq,q^2) + \frac{y^2}{2}.2x\ F_1(pq,q^2) \pm (y-\frac{y^2}{2})x\ F_3(pq,q^2)\right] -(1)$$

where the F_i are simply related to the commonly-used W_i:

$$F_1 = W_1 \qquad F_2 = \frac{pq}{M^2}W_2 \qquad F_3 = \frac{pq}{M^2}W_3$$

This expression is analogous to the generalisation of the Rosenbluth formula which describes inelastic electron scattering. The only essential differences in the case of neutrino scattering are that

(i)   The change of coupling constant from α^2 to G^2 entails (basically for dimensional reasons because $G^2 \sim 10^{-5}/M_p^2$ is not dimensionless) the linear dependence on laboratory energy E_ν.

(ii) There is no propagator factor like $^1/_{q^4}$ because the interaction is assumed point-like.

(iii) The parity-violating F_3 term, which changes sign in going from ν to $\bar{\nu}$, is not necessarily zero.

The hypothesis of scale invariance is that there is no particular mass or length characterising the scattering. It implies that the only dimensionless variable available on which the F_i can depend is just the ratio of the two variables pq and q^2:

$$F_i(pq,\ q^2) \rightarrow F_i(x)$$

From fairly general arguments, Bjorken proposed that the limits as $\nu, q^2 \rightarrow \infty$ with x fixed of the $F_i(M\nu,q^2)$ should exist and be non-zero. And therefore that at least in the deep inelastic region the F_i should become functions of $M\nu/q^2 = x$ only, and therefore scale invariant. Parton models, in which deep inelastic scattering is regarded as incoherent elastic scattering off point-like constituents of the nucleon in the impulse approximation, provide a simple explanation of scale invariance. The partons are usually taken to be quarks or antiquarks (the nucleon consisting of "valence" quarks plus a "sea" of $q\bar{q}$ pairs corresponding to the virtual meson cloud).

The differential cross section (1) can be rewritten

$$\frac{d^2\sigma^{\nu,\bar{\nu}}}{dxdy} = \frac{G^2ME}{\pi}\left[(1-y) + \frac{y^2}{2}\left(\frac{\sigma_L + \sigma_R}{\sigma_L + \sigma_R + \sigma_S}\right) \pm (y - \frac{y^2}{2})\left(\frac{\sigma_L - \sigma_R}{\sigma_L + \sigma_R + \sigma_S}\right)\right] F_2 \qquad -(2)$$

where σ_L, σ_R and σ_S are the hypothetical absorption cross sections for left-handed, right-handed and scalar currents respectively. Using this form, one can see immediately that positivity of the cross sections (σ_L, σ_R, σ_S all ≥ 0) requires

$$F_2 \geq 2xF_1 \geq |xF_3| \qquad\qquad -(3)$$

In parton models, several important results are immediately obvious from (2) if the scattering is looked at in the Breit frame, in which absorbing the current reverses the parton momentum:

In this frame:

(i) Since the helicity of spin-$\frac{1}{2}$ partons is conserved by a V-A interaction they must absorb one unit of angular momentum along $\vec{q}$, implying $\sigma_S = 0$ and therefore

$$2xF_1 = F_2 \quad \text{(Callan-Gross relation)} \quad -(4)$$

(ii) Spin-0 partons cannot absorb angular momentum and therefore would give a contribution with $\sigma_L = \sigma_R = 0$ and

$$2xF_1 = xF_3 = 0$$

(iii) If the partons are spin-$\frac{1}{2}$ particles (e.g. "valence" quarks) only left-handed currents can be absorbed in a V-A interaction, implying

$$|xF_3| = 2xF_1 = F_2$$

While (iv) for the contribution of the quark-antiquark "sea", $\sigma_L = \sigma_R$ and therefore

$$|xF_3| = 0$$

3. Tests of Scale Invariance in Previous Experiments

If the structure factors F_i depend only
on x, the total cross section should
increase in proportion to the neutrino
energy. The data shown (from the 1967
propane experiment) fitted the linear
dependence

$$\sigma_{TOT} = (0.8 \pm 0.2) \times 10^{-38} E_{GeV} \, cm^2/nucleon$$

within the rather large statistical and
systematic errors.

Similarly, if the differential cross
section at energy E depends only on the
dimensionless variables $\dfrac{\nu}{E}$ and $\dfrac{q^2}{M\nu}$ as
predicted by scale invariance, the mean
value of q^2 should be proportional to

Fig. 1

E. As shown below, it was observed to increase linearly with E but with
non-zero intercept. This is consistent with scale invariance holding
for large values of q^2 and E but breaking down for small values.
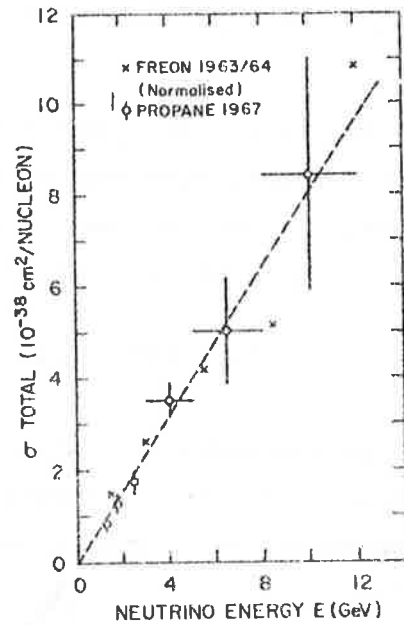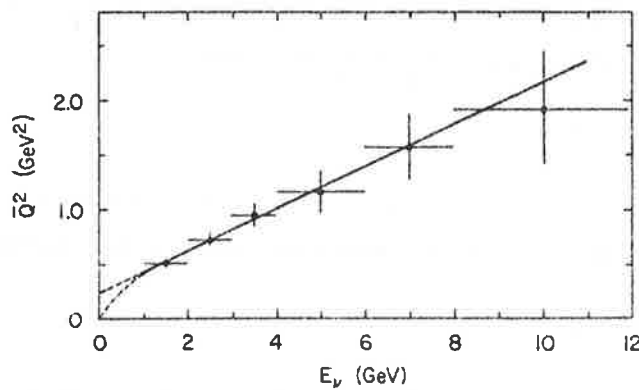
Fig. 2

Similarly the mean value of q^2 should be proportional to ν, and the data again showed
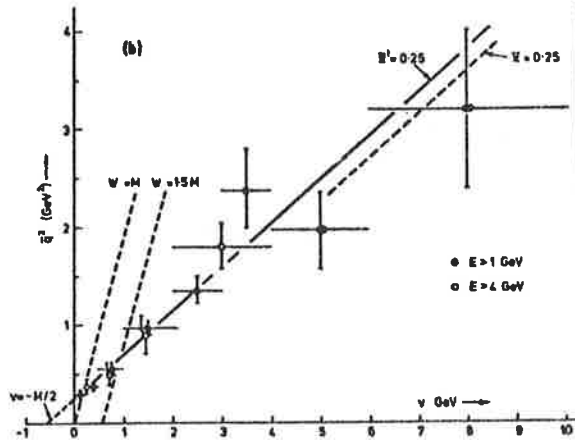
Fig. 3

a linear dependence with non-zero intercept. The line fitting the data in fact corresponds to scaling in the Bloom-Gilman parameter $x' = q^2/(2M\nu + M\nu)$ instead of in $x = q^2/2M\nu$. And the complete shapes of the q^2 distributions observed in various ranges of ν, not only the average values, fit such a scaling behaviour:
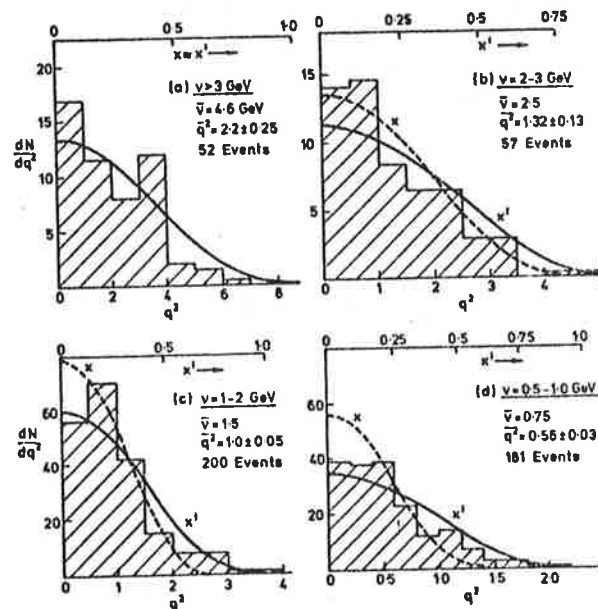
Distributions of q^2 for different ranges of energy transfer, ν. The dashed curves are normalized to the data, with the form $dN/dx \propto (1 - x^2)^3$ where $x = q^2/2M\nu$. This form has no physical significance and is merely to guide the eye. The full line curves are of the same form, but with $x' = q^2/(2M\nu + M^2)$ instead of x.

Fig. 4

These observations suggested that, in inelastic neutrino scattering as in electroproduction, scale invariance is approximately valid. And that structure factors determined in the deep inelastic region would fit the data rather well, at least in an average sense, even at low values of E, ν and q^2 if scaled in x' rather than x.

[Actually a complication has been glossed over in the above discussion, since a cut in ν will in general preferentially select certain regions of the y distribution and hence one or other of the F_i, which may have different distributions in x. However, it happens that the energy distribution of the events is approximately described by a steeply-falling power law, so that the selectivity in y is weak, and the observed x' distribution is anyway similar for all parts of the y distribution:
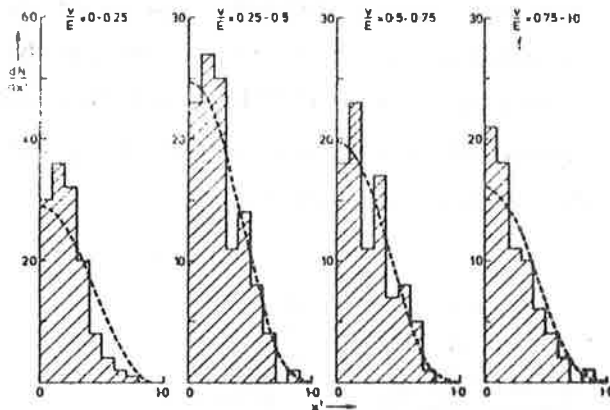
Fig. 5

Thus the complication can be safely ignored.]

4. The Present Neutrino Experiment in Gargamelle

The present experiment is a collaboration of seven groups at Aachen, Brussels, CERN, Ecole Polytechnique, Milan, Orsay and University College, London. One of its principal aims is a more detailed study of highly inelastic neutrino reactions. It will eventually yield an order-of-magnitude improvement in statistics with a harder neutrino energy spectrum, better known neutrino fluxes, and smaller systematic errors arising from statistical corrections to the visible hadronic energy — and also a substantial sample of inelastic antineutrino events.

The neutrinos are produced by the decay of pions and kaons produced by 26 GeV/c protons interacting in a long beryllium target and directed towards Gargamelle by two axially symmetric focussing devices, the so-called "horn" and "reflector". The production of $\pi^{\pm}$ and $K^{\pm}$ in beryllium at 24 GeV/c was measured over the whole range of secondary momenta and angles of interest and scaled up to 26 GeV/c. Two independently written Monte Carlo programs are used to calculate the neutrino flux through Gargamelle from this production spectrum and the focussing conditions. To monitor the beam and check the validity of the data input to these programs, the complete muon flux distribution is measured (and recorded continuously throughout the run) at six different depths in the shielding covering the whole energy range of interest. The measured muon fluxes are then compared in detail with the predictions of the programs. The muons are of course produced along with the neutrinos in pion decay, and at small angles to the pion direction. The measured muon distribution therefore directly reflects the spatial and angular distributions of the decaying pions, which in turn determine the neutrino flux through the detector. The muon measurements thus provide a sensitive means of checking that the beam is behaving according to calculation. They also fix the normalisation of the neutrino flux, since the muon detector signals can be normalised within a few per cent by track counting in nuclear emulsions while the overall normalisation of the π/K production spectrum is known only to ±15%.

The calculated flux error for the 1971 data is about ±8%. But because of problems due to an insufficiently homogeneous shielding and insufficient access to measure the whole of a slightly asymmetric muon flux distribution, a more conservative figure of ±15% is quoted. For the data taken in 1972 these problems were completely eliminated by rebuilding the shielding and the horn. The error will therefore be closer to ±5% than ±15%.

The neutrino/antineutrino flux ratio is much better known than the absolute fluxes because the muon flux distributions are closely similar in the two cases. Thus, to first order, the flux ratio is given directly by the ratio of muon counting rates.

Gargamelle was filled with freon (CF_3Br, ρ = 1.5 gm/cc, X_0 = 11 cms, λ_{INT} ~ 70 cms) in order to maximise the event rate. The visible volume is 4.8 metres long and 1.4 metres in diameter (volume 7 m^3). The fiducial volume chosen is 4 m long and 1 m in diameter (π m^3, 4.7 tons).

Muon momenta are typically measured to ±(5-10)%, hadron momenta to ±(10-15)%, and gammas to ±25%. Thus the visible energy in an event is typically measured to about ±10%.

Statistical corrections are necessary to allow for unseen gamma rays, unseen neutrons, the unseen energy in secondary neutron interactions, nuclear excitation energy (unseen evaporation prongs), and unresolved proton-π^+ ambiguities. The expected average correction to the total hadron energy ν is about 5-10%. This may be compared with 34% and 15% respectively in the previous propane and freon experiments in the 1.2 m chamber. In addition, Fermi momentum has the effect that the values of ν and E measured in the laboratory differ typically by ~10% from the values in the target nucleon rest system (but to the extent that the secondaries emerge in the forward direction the value of $y = \nu/E$ is unchanged).

5. Preliminary Results

Figure 6 shows the total neutrino and antineutrino cross sections determined from the present sample of events. They are consistent with the proportional increase of cross section with neutrino energy predicted by scale invariance. The proportionality constants are

$$\sigma_\nu = (0.69 \pm 0.14) \times 10^{-38} \, E_{GeV} \quad cm^2/nucleon$$

$$\sigma_{\bar\nu} = (0.27 \pm 0.05) \times 10^{-38} \, E_{GeV}$$

$$\sigma_\nu + \sigma_{\bar\nu} = (0.96 \pm 0.17) \times 10^{-38} \, E_{GeV}$$

$$= (0.62 \pm 0.11) \, \frac{G^2 ME}{\pi}$$

where the quoted errors include all systematic and statistical uncertainties. The cross section ratio is shown as a function of
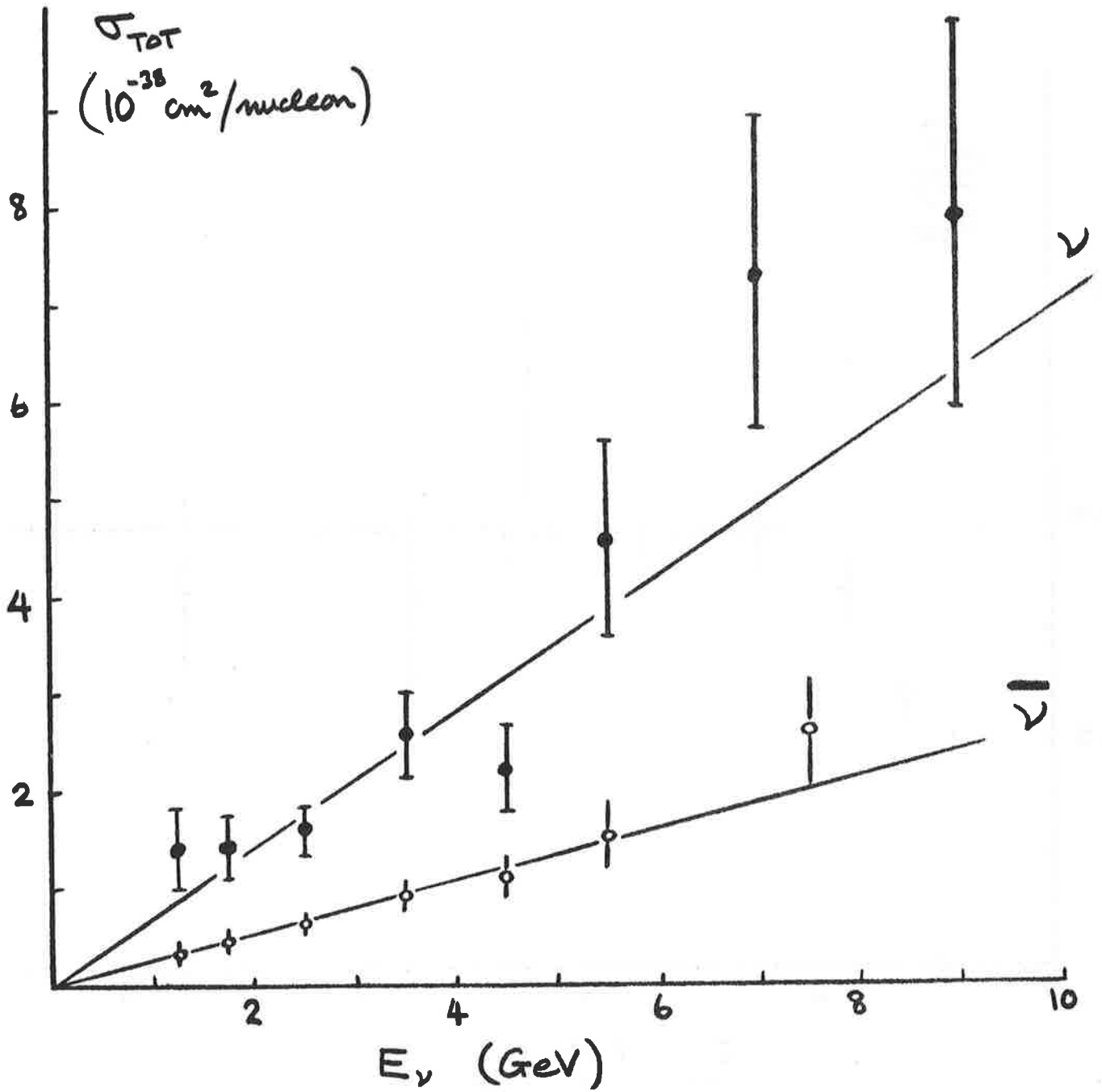
Fig. 6.   Preliminary neutrino and antineutrino total cross
sections measured in the CERN Gargamelle experiment.
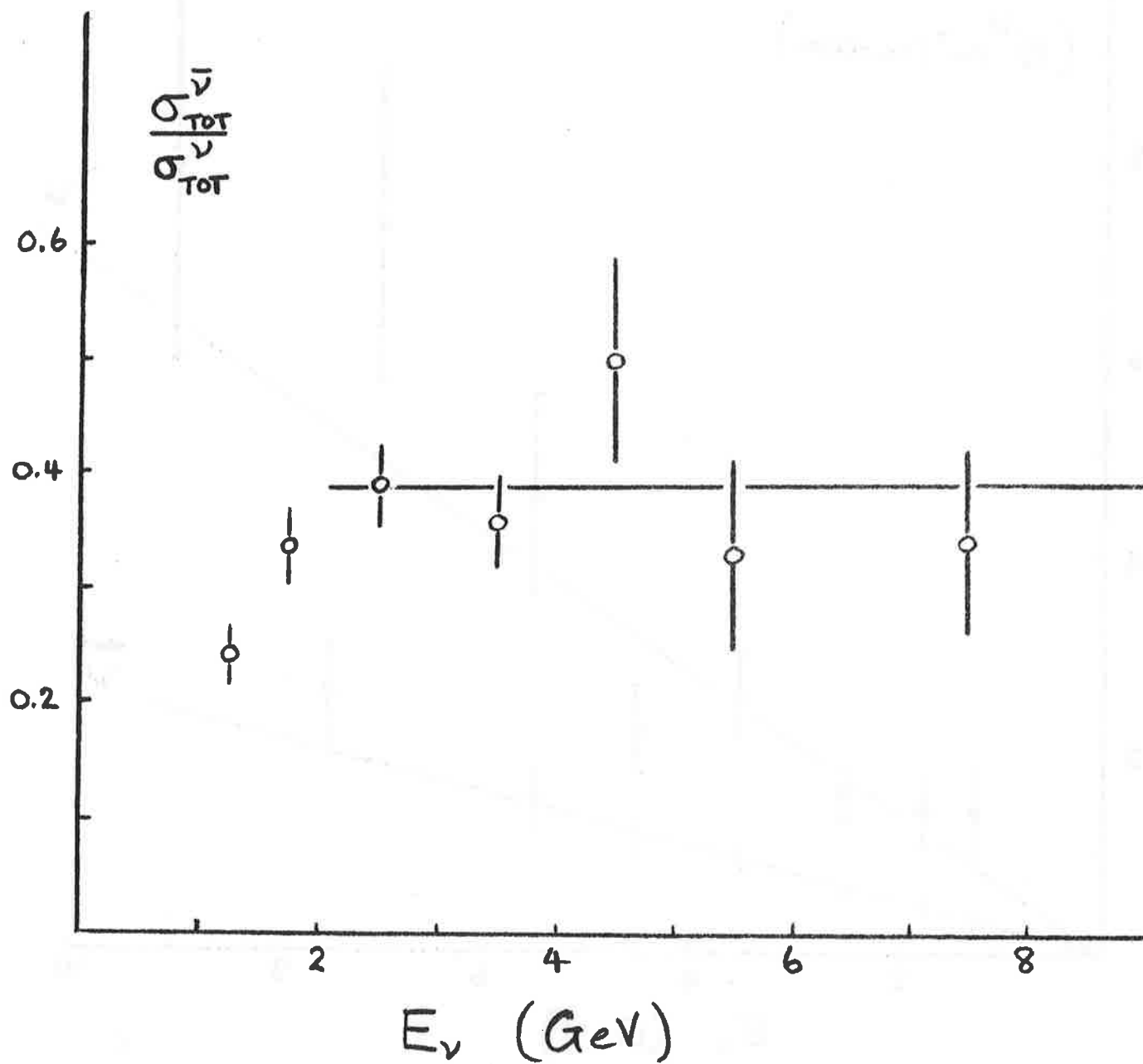
Fig. 7.   The ratio of the antineutrino and neutrino total
cross sections as a function of energy.

neutrino energy in figure 7. Above 2 GeV the data are consistent with a constant ratio

$$\frac{\sigma_{\bar{\nu}}}{\sigma_{\nu}} = 0.38 \pm 0.04$$

The measured cross section ratio shows that the F_1 and F_3 terms must be close to their maximum possible values, saturating the positivity conditions (3). Therefore the Callan-Gross relation is approximately satisfied, implying in parton models that the partons are predominantly of spin $\frac{1}{2}$. And parity violation is close to maximal, implying in a quark parton model, for example, that the contribution of the quark-antiquark sea is small.

To reach these conclusions we first note that the hypothesis of charge symmetry of the $\Delta Y = 0$ part of the hadronic current implies

$$F_i^{\nu p} = F_i^{\bar{\nu} n} \quad \text{and} \quad F_i^{\bar{\nu} p} = F_i^{\nu n}$$

and therefore that $F_i^{\nu N} = F_i^{\bar{\nu} N}$ for an essentially equal mixture of neutrons and protons (as in complex nuclei). Integrating the differential cross section (1) over x and y then gives

$$\sigma_{\text{TOT}}^{\nu,\bar{\nu}} = \frac{G^2 ME}{\pi} \left[\frac{3 + A \pm 2B}{6} \right] \cdot \int_0^1 F_2(x) dx$$

where $A \equiv \int_0^1 2x F_1(x) dx / \int_0^1 F_2(x) dx$

$$B \equiv \int_0^1 x F_3(x) dx / \int_0^1 F_2(x) dx$$

and both A and B have the same values for ν and $\bar{\nu}$ reactions.

The measured cross section ratio therefore gives

$$\frac{3 + A - 2B}{3 + A + 2B} = 0.38 \pm 0.04$$

and the positivity conditions (3) require

$$|B| \leqslant A \leqslant 1$$

These relations are not in principle sufficient to determine the values of A and B separately. However the range of allowed values is small. The minimum values of A and B occur for the condition A = B = 0.88 ± 0.10 and the maximum values are A = 1, B = 0.90 ± 0.10. Thus the data are close to saturating the positivity conditions and consistent with the Callan-Gross relation (A = 1) and maximal parity violation ($|B| = 1$).

The total cross sections can be compared with those measured in deep inelastic electroproduction at SLAC, since $F_2^{\nu N}$ can be related to $F_2^{\gamma N}$ via the CVC and chiral symmetry hypotheses. Adding the ν and $\bar{\nu}$ cross sections gives

$$\sigma_{\nu N} + \sigma_{\bar{\nu} N} = \frac{G^2 ME}{\pi} \left(1 + \frac{A}{3}\right) \int F_2^{\nu N}$$

Therefore $\int F_2^{\nu N} = (0.62 \pm 0.11)/(1.30 \pm 0.04) = 0.48 \pm 0.08$

The SLAC data give $F_2^{\gamma N} = 0.14 \pm 0.02$, where the error arises from extrapolating the measured F_2 values into the unmeasured region x < 0.08. We assume the extended CVC hypothesis (that the electromagnetic isovector and weak vector currents form an isotriplet), chiral symmetry ($|V| = |A|$), and a 10% isoscalar contribution in electroproduction (as in photoproduction). These assumptions predict

$$\int F_2^{\nu N} = 4 \int F_2^{\gamma N}(\text{isovector}) = 0.51 \pm 0.07$$

in excellent agreement with the measured value.

The ratios $\int F_2^{\nu N} / \int F_2^{\gamma N}$ and $\sigma_{\bar{\nu}}/\sigma_{\nu}$ can also be compared with the predictions of various quark-parton models. Table I, taken from Perkins' review at the Batavia Conference, shows such a comparison. The only model that fits both these ratios and also the ratio $F_2^{\gamma n}/F_2^{\gamma p}$ measured in electroproduction is the Gell-Mann/Zweig model in which three fractionally charged valence quarks dominate.

However, not all of the 4-momentum of the nucleon can be carried by weakly interacting quark-partons. If it were, the total cross section would equal that for elastic scattering off a point-like nucleon (i.e. $\int F_2^{\nu N}$ would equal 1). While $\lambda\bar{\lambda}$ pairs cannot contribute to $\Delta S = 0$ interactions, their presence alone cannot explain the discrepancy. If the $q\bar{q}$ sea is assumed to be SU3-symmetric, their contribution is similar to that of $n\bar{n}$ and $p\bar{p}$ pairs, which is measured by the value of (1 - B) and is small. Thus one is obliged to assume the existence of weakly and

TABLE I

Quark Model Predictions (all spin $\frac{1}{2}$)

Model	Nucleon Built From :—	$\dfrac{\int F_2^{\nu N} dx}{\int F_2^{\gamma N} dx}$	$\sigma^{\bar{\nu}}/\sigma^{\nu}$	$F_2^{\gamma n}(x)/F_2^{\gamma p}(x)$ $x=1 \rightarrow 0$
Gell-Mann/Zweig	3 fractional charge quarks	$3.6 \ (=\frac{18}{5})$	$\frac{1}{3}$	$\frac{1}{4} \rightarrow 1$
	3 valence quarks + many $Q\bar{Q}$ pairs	~ 3.0	~ 1.0	~ 1
Han-Nambu	3 integral charge triplets	$\leqslant 3.3$	$\frac{1}{3}$	$\frac{1}{2} \rightarrow 1$
Integral charge (eg Sakata, GIM)	Integral charge triplet or quartet	$\leqslant 2.0$	$\frac{1}{3}$	$0 \rightarrow \infty$
Experiment		$\underline{3.4 \pm 0.7}$	$\underline{0.38}$	$\underline{\sim 0.25 \rightarrow 1}$

electromagnetically neutral particles ("gluons") with $Q = Y = I = 0$
carrying a large fraction ϵ of the 4-momentum of the nucleon. The value
of ϵ is given by

$$1 - \epsilon = (1 + \frac{1-B}{2}) \int F_2^{\nu N}$$

Therefore $\epsilon = 0.50 \pm 0.08$

Such gluons are necessarily present in renormalisable field theories of
interacting quarks.

The above results come purely from the measured total cross sections.
An experimentally independent way of extracting the values of A and B
is from the shape of the y distributions. Integrating the double
differential cross-section (1) over x only, we have

$$\frac{d\sigma^{\nu, \bar\nu}}{dy} = \frac{G^2 ME}{\pi} \left[(1 - y) + \frac{y^2}{2} \cdot A \pm (y - \frac{y^2}{2}) \cdot B \right] \int F_2$$

For $A = B = 1$ this gives

$$\frac{d\sigma^\nu}{dy} = \frac{G^2 ME}{\pi} \cdot \int F_2$$

and

$$\frac{d\sigma^{\bar\nu}}{dy} = \frac{G^2 ME}{\pi} \cdot (1 - y)^2 \int F_2$$

which may be compared with the
differential cross sections for
neutrino-electron scattering.
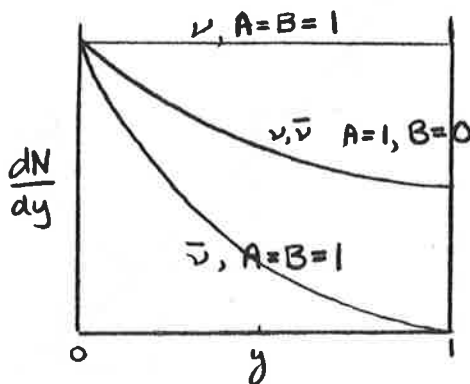
Thus for A and B close to unity we expect an almost flat y distribution
for neutrinos, as was
observed in previous
neutrino experiments
(Fig. 8). And the
distribution for
antineutrinos should
go nearly to zero for $y \sim 1$.
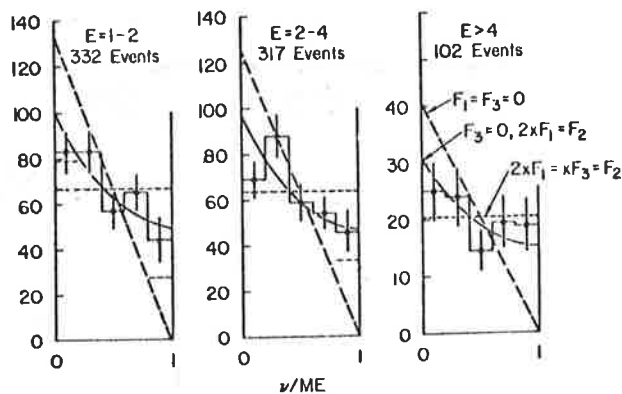
Fig. 8
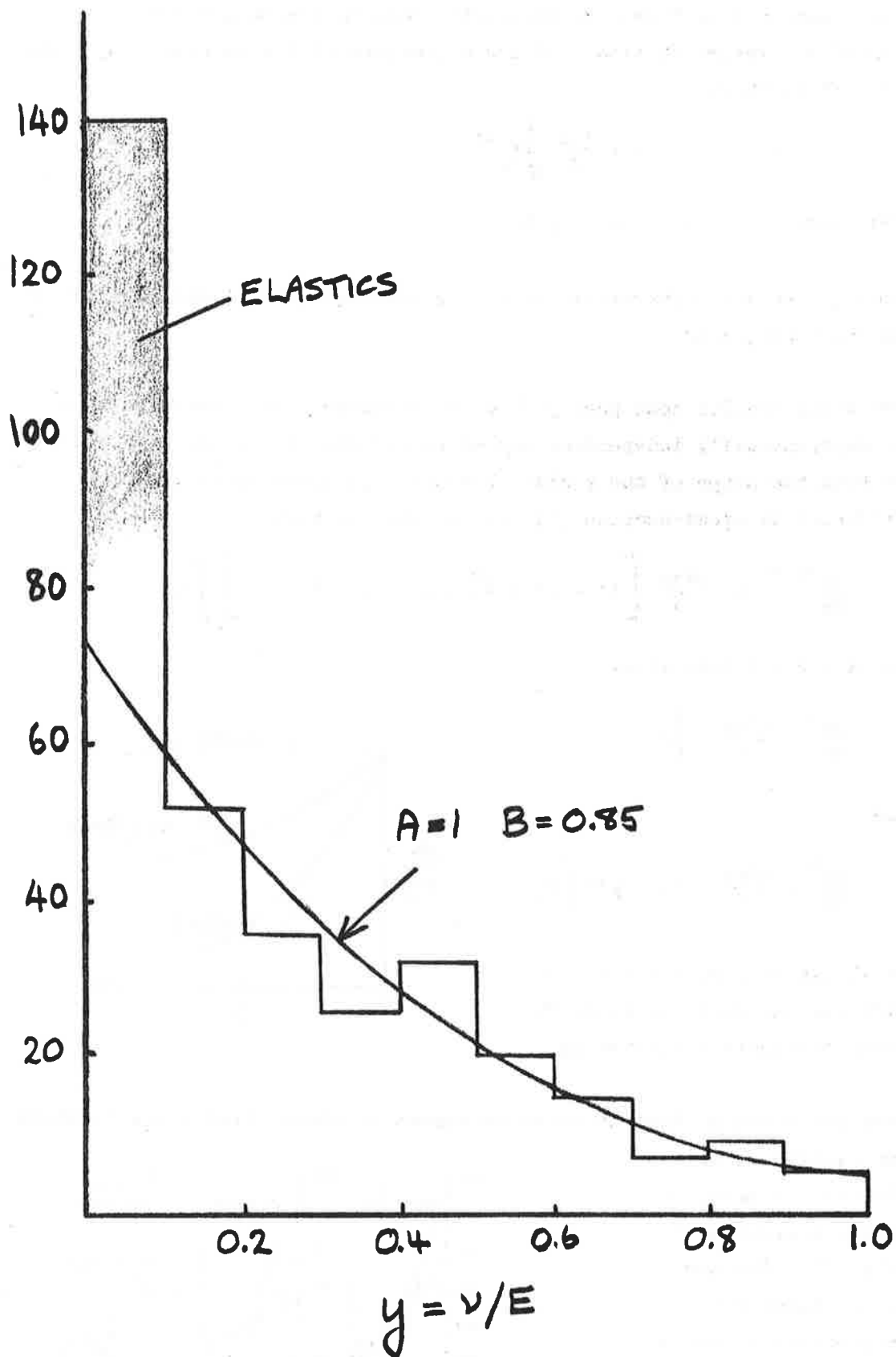
Fig. 9. Very preliminary y distribution for antineutrino events with energy above 3 GeV.

A very preliminary y distribution for the antineutrino events observed
in the Gargamelle experiment is shown in figure 9. There is an excess
of elastic and quasi-elastic events in the first bin, for which scaling
$F_i(x,yE) \to F_i(x)$ is least likely to be valid. Otherwise the shape of
the distribution is consistent with the scaling hypothesis. From the
above expression for the differential cross section, the ratio of the
cross section value at y = 1 to the value at y = 0 is

$$\left(\frac{d\sigma}{dy}\right)_{y=1} \bigg/ \left(\frac{d\sigma}{dy}\right)_{y=0} = \frac{A \pm B}{2}$$

The non-zero antineutrino cross section observed near y = 1 therefore
corresponds to A − B = 0.15 ± 0.04. The implication is that parity
violation is not quite maximal (B ≠ 1) because there is a measurable
contribution from the $q\bar{q}$ sea. But further analysis is needed.

Before leaving this discussion, it must be pointed out that, for simplicity
of presentation, several minor complications which must be taken into
account in a correct analysis of the data have been totally ignored
above. In particular,

(a) the kinematic ranges of x and y are not quite 0 → 1 at finite
     energies and the coefficient of the F_2 term in equations (1) et seq
     is $(1 - y/y_{max})$ rather than $(1 - y)$;

(b) similarly the positivity conditions (3) are more correctly written

$$F_2 \left(1 + \frac{2Mx}{\nu}\right) \geqslant 2xF_1 \geqslant \sqrt{\left(1 + \frac{2Mx}{\nu}\right)} \cdot |xF_3|$$

     at finite energies;

(c) much of the discussion in fact refers only to the ΔS = 0 part of
     the cross section so that ΔS = 1 events should be removed or
     corrected for and G^2 replaced by $G^2 \cos^2\theta_{Cabibbo}$;

(d) the ratio of neutrons to protons in CF_3Br is 1.19, not 1.0.

However, taking these small effects into account would not materially
alter any of the conclusions drawn at the present time.

6. Future Developments

A complete analysis of the x and y distributions will allow the F_1, F_2 and F_3 terms to be separated and their separate x (or x' or x_w) distributions obtained. Basically the neutrino-antineutrino difference yields the F_3 term; and the sum yields $F_1 + F_2$, which is dominated by F_2 at small and moderate y values and by F_1 at large y values. This is particularly interesting for evaluating the F_3 sum rule predicted by the quark model

$$-\int \frac{d\omega}{\omega^2} (F_3^{\nu p} + F_3^{\nu n}) = \int (F_3^{\nu p} + F_3^{\nu n}) \, dx = 6$$

and because the F_3 term is predicted to vanish for small x because of dominance by the $q\bar{q}$ sea contribution or Pomeron exchange.

This is not yet possible because backgrounds, lost-energy corrections and particle identification ambiguities are far more important in such an analysis than in the determination of the total cross section. However, analyses of these effects is currently in progress and results may be anticipated in the next few months.

In the slightly longer term, the statistics will be very substantially improved ($\bar{\nu}$ statistics x 2, ν statistics x 10). And most of the improvement will come from the data acquired in 1972 for which, as a result of beam improvements, the ν and $\bar{\nu}$ fluxes will be substantially better known. Also the background of ν events in the $\bar{\nu}$ film is reduced by the order of magnitude (eliminating much of the background and ambiguity problem).

Eventually still more data may be anticipated from (i) the proposed $\bar{\nu}$ experiment intended mainly to look for more ν_μ-electron scattering candidates and from (ii) the proposed ν, $\bar{\nu}$ experiment using propane. In propane ~15% of nucleons are free protons and one will be able to look at neutron-proton differences and details of the secondary hadron systems.

However, the CERN experiments are about to be upstaged by NAL. Many bubble chamber experiments using wide-band ν or $\bar{\nu}$ beams have been proposed. The mean values of E, ν and q^2 will be ~10 times larger. And the neutrino program has high priority. This poses the question of the strategy to adopt in preparing second generation experiments at the SPS.

Most thinking (at least for bubble chamber experiments) is currently towards installing a scaled up version of the present wide-band beam and exploiting the possibility of determining the neutrino fluxes better, and perhaps installing a TST, in order to compete with NAL on favourable terms. However, potential wide-band event rates are roughly two orders of magnitude higher at the SPS than at the PS (x10 for proton intensity, x10 for proton energy). This is probably too high for most bubble chamber experiments to cope with because of associated background and correlation problems.

The reduction in potential high energy event rate by switching to narrow-band systems with broad momentum bite ($\Delta p/p \sim \pm 10\%$) would be only a factor ~3-5. The data obtained would be much cleaner (fewer background problems), analysis much faster and easier, and fluxes more precisely and reliably determined. Thus a very strong case can be made for basing the SPS bubble chamber program for neutrino physics on the use of narrow-band beams.

References

The author has drawn heavily on the review articles by C H Llewellyn Smith (Physics Reports, Volume 3C, number 5 (1972), p 261) and D H Perkins (review talk at the Batavia Conference, September 1972) to which the reader is referred for detailed references. The relevant data on previous CERN bubble chamber neutrino experiments is published in the papers by I Budagov et al (Physics Letters 30B (1969) 364) and G Myatt and D H Perkins (Physics Letters 34B (1971) 542), from which figures 1-5 and 8 have been taken.

QUARKS AND DEEP INELASTIC PROCESSES

P.V. Landshoff

Department of Applied Mathematics and Theoretical Physics

University of Cambridge.

The assumption that nucleons in some sense consist of quarks provides the most successful model that we have so far for correlating the presently available data[1] for the following deep inelastic processes:

$$
\begin{aligned}
&\text{(a)} \quad eN \longrightarrow eX \\
&\text{(b)} \quad \nu N \ \text{ or } \ \bar{\nu} N \longrightarrow \mu X \\
&\text{(c)} \quad e^+ e^- \longrightarrow X \\
&\text{(d)} \quad NN \longrightarrow \mu^+\mu^- X \\
&\text{(e)} \quad NN \longrightarrow \pi X \ .
\end{aligned}
\tag{1}
$$

In each case, X denotes a system of hadrons. In process (e) the pion has large transverse momentum. Using what one learns from the processes (1), one can make quantitative predictions for certain other processes, such as $eN \longrightarrow e\mu^+\mu^- X$, for which there are no data; I shall not discuss these here.

The theory that lies behind what I have to say may be formulated[2] using three apparently different languages:

(i) Feynman's parton approach

(ii) Covariant field theory softened at large momentum (or short distance)

(iii) Light cone algebra

Provided that the parton model is made sufficiently general, it is precisely equivalent to the softened field theory. Both of these approaches lead to the same results as the light-cone algebra, when the latter is applicable. However, it seems that the light-cone approach is less powerful than the other two; for example, it is unlikely to be applicable to process 1(d).

The experimental result that the ratio σ_L/σ_T in electroproduction is small is most easily explained by supposing that the partons or, equivalently, the fields to which the electromagnetic and weak currents couple, have spin $\frac{1}{2}$. The most economical assumption is that they are quarks, so that the electromagnetic current is

$$\frac{2}{3}\bar{p}\gamma^\mu p - \frac{1}{3}\bar{n}\gamma^\mu n - \frac{1}{3}\bar{\lambda}\gamma^\mu\lambda \tag{2}$$

and in the approximation where the Cabibbo angle is set equal to zero, the weak current is

$$\bar{p}\gamma^\mu(1-\gamma_5)n. \tag{3}$$

Introducing quarks obviously poses theoretical problems, unless quarks are actually found in Nature. These problems have not been solved. A possibility, suggested long

ago by Gell-Mann, is that the quarks are bound very tightly to their parent hadrons, and cannot escape. There have been attempts recently[3] to understand whether this is theoretically possible. I shall not discuss them since, in any case, the first thing to do is to see whether the quark hypothesis leads to results that agree with experiment.

Electroproduction

Here, because of the optical theorem, if none of the final-state hadrons is observed one needs the imaginary part of the forward virtual Compton amplitude. In the deep inelastic limit, the parton approach, the softened field theory approach and the light cone approach all agree that the dominant contribution corresponds to the two electromagnetic currents coupling to the same quark (or quark field). See **Figure 1.**
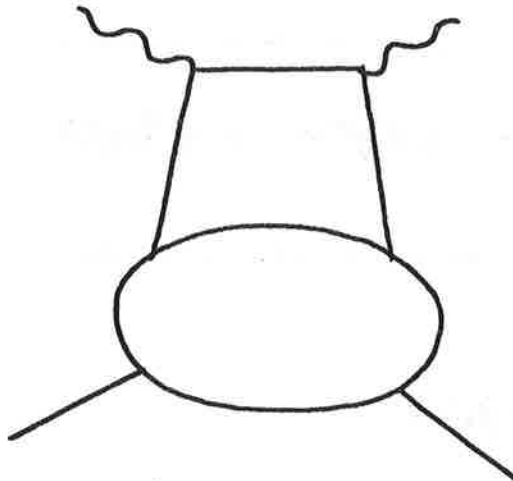

Figure 1

1. The dominant contribution to the virtual Compton amplitude in the deep inelastic limit. The internal line is a quark or an antiquark.

This quark can be either p, n, λ or $\bar{p}$, $\bar{n}$, $\bar{\lambda}$: as we shall see, the proton is not supposed to consist just of the three quarks p p n of the naive quark model, but in addition there is a "sea" or "core" of quark-antiquark pairs. Thus, if we write in explicitly the factors at the vertices arising from the quark charges, the proton structure function is a sum of six terms:

$$F_2^{eP}(\omega) = \left(\tfrac{2}{3}\right)^2 \left[F^p + F^{\bar{p}}\right] + \left(\tfrac{1}{3}\right)^2 \left[F^n + F^{\bar{n}} + F^{\lambda} + F^{\bar{\lambda}}\right] \tag{4}$$

Each of the six functions $F^q(\omega)$, $F^{\bar{q}}(\omega)$ is associated with the probability that the proton emits the corresponding virtual quark or antiquark, that is it is associated with the bubble in figure 1. Notice that the quark that is emitted by the proton and then struck by the current is virtual; one can show that the momentum that it carries is spacelike.

By charge symmetry, the amplitude for the emission of, say, an n quark by the proton is equal to that for the emission of a p quark by the neutron. Thus we may write the neutron structure function in terms of the same six proton functions:

$$F_2^{eN}(\omega) = \left(\tfrac{2}{3}\right)^2 \left[F^n + F^{\bar{n}}\right] + \left(\tfrac{1}{3}\right)^2 \left[F^p + F^{\bar{p}} + F^{\lambda} + F^{\bar{\lambda}}\right] . \tag{5}$$

For both proton and neutron figure 1 gives $F_1(\omega) = \tfrac{1}{2} \omega F_2(\omega)$, corresponding to $\sigma_L / \sigma_T \rightarrow 0$.

The structure functions F_1, F_2, F_3 for the scattering of ν or $\bar{\nu}$ on P or N may also be written in terms of the same six functions.

In principle, one may test[4] whether the expressions for the various structure functions in terms of these six functions are correct, without making any further assumptions. First, they lead to a linear relation for all ω :

$$12 \left(F_1^{eP} - F_1^{eN}\right) = F_3^{\nu P} - F_3^{\nu N}, \tag{6}$$

but this is hard to use because the functions F_3 are not easily extracted from the data. Secondly, each of the six functions F^q , $F^{\bar{q}}$ is positive, and this

results in inequalities for the structure functions, such as

$$F_2^{eP} + F_2^{eN} \geq \frac{5}{18}(F_2^{\nu P} + F_2^{\nu N}).$$

(7)

There is no evidence that these inequalities are violated, but of course an inequality is not a very sensitive test. Lastly, one can derive conditions that ensure that the proton has the correct charge, baryon number and strangeness:

$$\int_1^\infty \frac{d\omega}{\omega}(F^P - F^{\bar{P}}) = 2$$

$$\int_1^\infty \frac{d\omega}{\omega}(F^n - F^{\bar{n}}) = 1$$

$$\int_1^\infty \frac{d\omega}{\omega}(F^\lambda - F^{\bar{\lambda}}) = 0.$$

(8)

These lead to sum rules for the structure functions, such as the Adler sum rule and the Gross-Llewellyn Smith sum rule:

$$\int_1^\infty \frac{d\omega}{\omega}(F_2^{\nu N} - F_2^{\nu P}) = 2$$

$$\int_1^\infty \frac{d\omega}{\omega^2}(F_3^{\nu N} + F_3^{\nu P}) = -6.$$

(9)

It seems likely that large values of ω are important in the integrals, so these sum rules are slow to converge and so hard to test.

These tests involve only the assumption that the partons are quarks. To go any further, it is necessary to introduce some dynamics. So far, nobody has a way of doing this outside the quark framework, so one cannot easily discuss how the results that I give from now on would differ if the partons were something else.

Similar dynamical assumptions have been made[5] independently by Landshoff and Polkinghorne, and by Kuti and Weisskopf. They are closely connected with the widely accepted two-component theory of duality in strong-interaction physics. Suppose that

the baryons are made up of three "valence" quarks, p p n in the case of the proton, together with a "sea" of quark-antiquark pairs. This sea will be supposed to be the same for each baryon in the nucleon octet, and the sea for each antibaryon is assumed to be the same as that for the baryon. That is, the sea is an SU_3 singlet of even signature. We do not enquire further into the structure of the sea; the number of quark-antiquark pairs, in so far as one can give meaning to the number of highly virtual particles, is almost certainly infinite. It may be that some of the pairs are bound together to form neutral "gluons".

Write each $F^q(\omega)$, $F^{\bar{q}}(\omega)$ as a sum of contributions from valence quarks and from the sea:

$$F^q(\omega) = V^q(\omega) + S^q(\omega).$$ (10)

The valence quark contributions $V^q(\omega)$ are thought to be primarily associated with direct-channel resonances or the exchange of ordinary Reggeons, while the contributions $S^q(\omega)$ from the sea are pictured as being mainly diffractive, corresponding to pomeron exchange.

Because of the assumptions about the sea

$$S^p = S^n = S^\lambda = S^{\bar{p}} = S^{\bar{n}} = S^{\bar{\lambda}}$$

$$= S(\omega) \quad \text{say} .$$ (11a)

Also, since the valence quarks are p p n ,

$$V^\lambda = V^{\bar{p}} = V^{\bar{n}} = V^{\bar{\lambda}} = 0 .$$ (11b)

Introduce the further assumption that V^p and V^n have the same shape as functions of ω . This may well be wrong, particularly near $\omega = 1$, but so far there is no other natural assumption to replace it. The relative normalisation of V^p and V^n is determined by (8):

116.

$$V^n = \tfrac{1}{2} V^p$$
$$= V(\omega) \quad \text{say} . \tag{12}$$

Then all the structure functions are expressible in terms of the two functions $V(\omega)$ and $S(\omega)$. For example

$$F_2^{eP} = V + \tfrac{4}{3} S$$

$$F_2^{eN} = \tfrac{2}{3} V + \tfrac{4}{3} S .$$

The function $V(\omega)$ may be extracted directly from the data[1a] for the difference $[F_2^{eP}(\omega) - F_2^{eN}(\omega)]$. This is shown in figure 2. I shall suppose that the curve represents the best fit; it is actually a curve that Polkinghorne and I calculated from a Veneziano-like model.[6] The curve satisfies the sum rule

$$\int_1^\infty \frac{d\omega}{\omega} \left[F_2^{eP} - F_2^{eN} \right] = \tfrac{1}{3} , \tag{13}$$

which follows from (8) and the subsequent assumptions. The data for larger values of ω (not shown in figure 2) fall somewhat below the curve. There are uncertainities in the data, arising particularly from the fact that F_2^{eN} must actually be extracted from data for a deuterium target, but if it continues to appear that the integral (13) is rather less than $\tfrac{1}{3}$, some modification of the model will be needed.

Now that I have $V(\omega)$, it can be plotted with the data for $F_2^{eP}(\omega)$ figure 3. The difference between the curve and the data is then, by (13), $\tfrac{4}{3} S(\omega)$. Although it appears that $S(\omega)$ is negative for $\omega \lesssim 2.5$, this cannot be, which is why I said that it may be necessary to modify the assumption (12) near $\omega = 1$. I shall assume that $S(\omega)$ is essentially zero for $\omega < 2.5$. Because $S(\omega)$ is dominated by pomeron exchange, we expect that for large ω, $S(\omega) \sim \omega^{\alpha_P(0)-1}$ = const; it will be of great interest to see what this constant is, and whether it is non-zero, when data become available at large values of ω . Being dominated by tensor-meson exchange at large ω , $V(\omega)$ goes to zero like $\omega^{\alpha_T(0)-1} = \omega^{-\frac{1}{2}}$ at large ω.
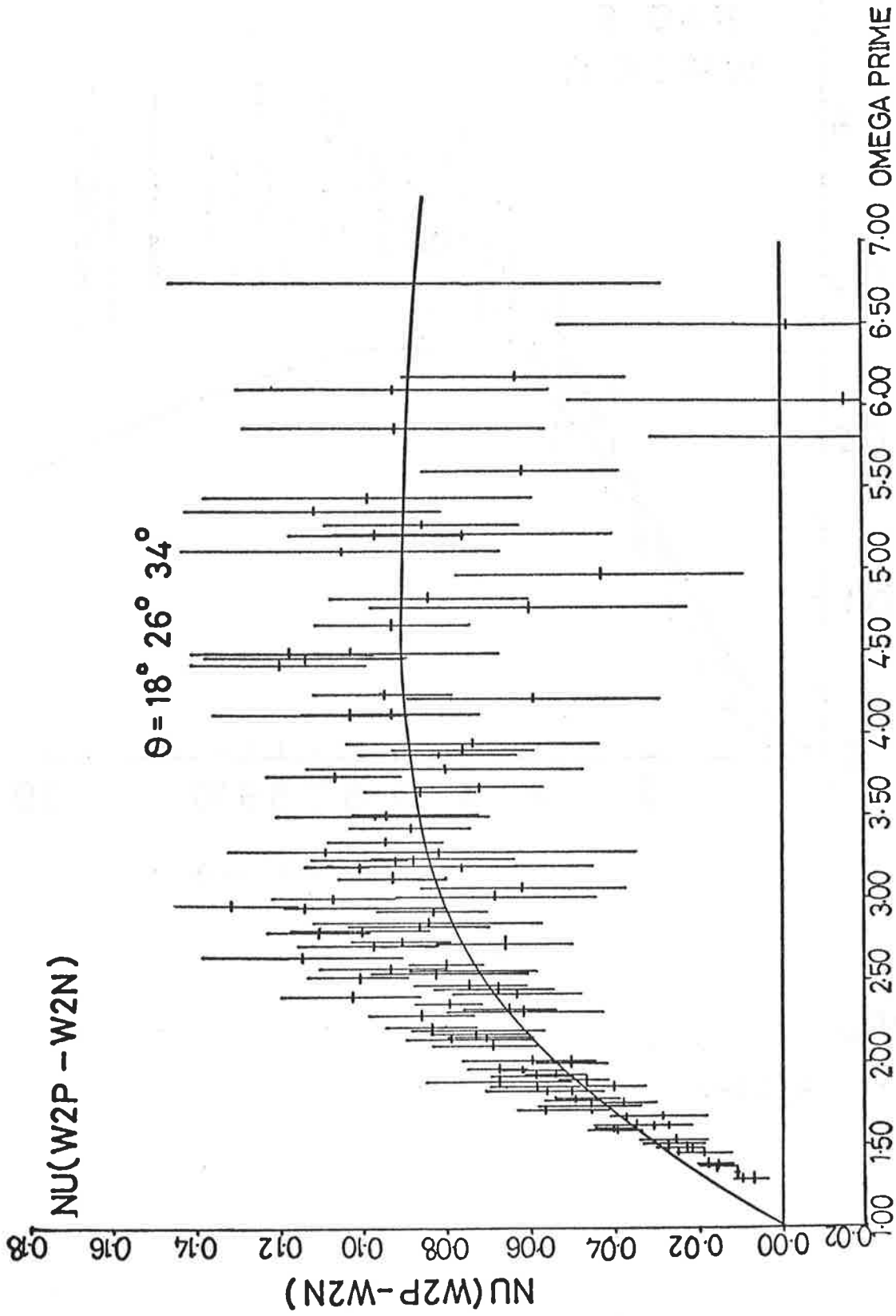
Figure 2

Data for $\left[F_2^{eP}(\omega) - F_2^{eN}(\omega)\right]$, with the curve $\frac{4}{3}V(\omega)$ that is taken to be the fit to it.
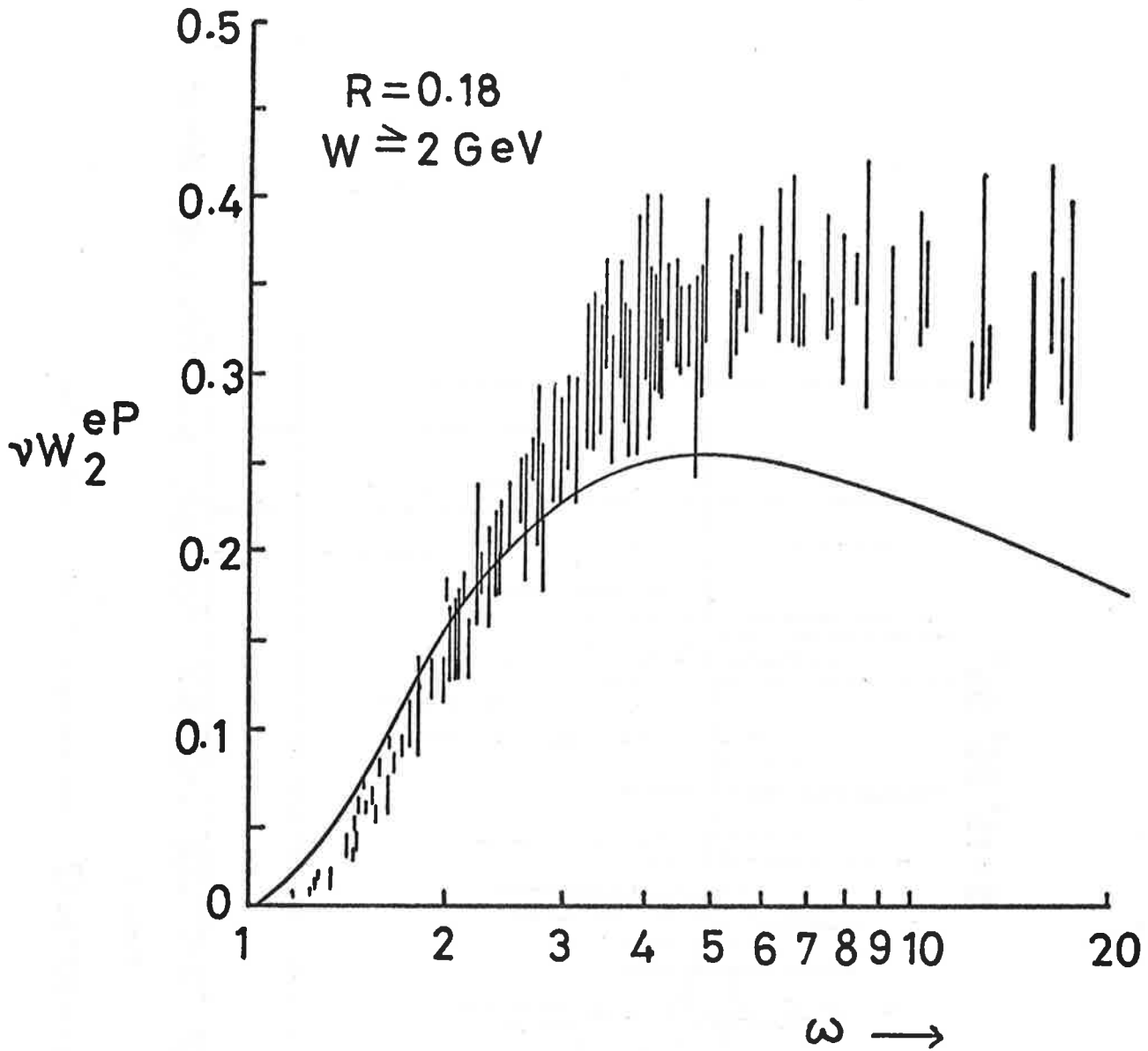
Figure 3.

Data for $F_2^{eP}(\omega)$, with the curve $V(\omega)$. The difference is identified with the contribution $\frac{4}{3} S(\omega)$ from the sea.

Neutrino Experiments

Having determined $V(\omega)$ and $S(\omega)$, we may use these to make predictions for various other experiments, and compare them with data.

First, all the neutrino and antineutrino structure functions are expressible in terms of $V(\omega)$ and $S(\omega)$, so that when the data becomes available they can be tested for all ω. In the total cross sections, they come in integrated, $\int d\omega/\omega^2$. Because $S(\omega) \approx 0$ for $\omega < 2.5$, the contributions from the sea are small. in these integrals, even though we believe that $S(\omega)$ becomes larger than $V(\omega)$ at sufficiently large ω.

Writing

$$D = \int_1^\infty \frac{d\omega}{\omega^2} S(\omega) \quad , \qquad R = \int_1^\infty \frac{d\omega}{\omega^2} V(\omega) ,$$

one finds

$$\sigma^{\bar{\nu} P} = \frac{G^2 ME}{\pi} \left[\frac{4}{3} R + \frac{8}{3} D \right]$$

$$\sigma^{\nu N} = \frac{G^2 ME}{\pi} \left[4R + \frac{8}{3} D \right]$$

$$\sigma^{\nu P} = \frac{G^2 ME}{\pi} \left[2R + \frac{8}{3} D \right]$$

$$\sigma^{\bar{\nu} N} = \frac{G^2 ME}{\pi} \left[\frac{2}{3} R + \frac{8}{3} D \right] .$$

From our fit to the electroproduction data, Polkinghorne and I supposed that

$$R = \frac{1}{7} \qquad\qquad D = \frac{1}{40}$$

and so we calculated[7] that, for scattering of neutrinos on propane the cross-section per nucleon should be

$$0.47 \; \frac{G^2 ME}{\pi}$$

compared with the experimental value

$$(0.52 \pm 0.13) \ \frac{G^2 ME}{\pi} \ .$$

For heavy freon, we predicted that

$$\frac{\sigma(\bar{\nu})}{\sigma(\nu)} = 0.4 ,$$

which is to be compared with the data in figure 4. (If there were no sea, the expected ratio would be .315). We also calculate

$$\frac{\sigma^{\nu N}}{\sigma^{\nu P}} = 1.8 ,$$

while experiment gives for this ratio 1.8 ± 0.3 in the propane experiment and 1.1 ± 0.3 in the freon experiment. (The results in the two experiments should, of course agree. I understand that the propane result is more likely to be reliable.)

Muon-Pair Production

Drell and Yan[8] showed that a dominant contribution to the muon-pair production process (1d) corresponds to one nucleon emitting a quark and the other an antiquark; these then annihilate with each other, to produce the virtual photon that subsequently decays into the muon pair. This gives

$$\frac{d\sigma}{d\sqrt{q^2}} = \frac{8\pi\alpha^2}{3(q^2)^{3/2}} \sum_{\substack{quarks \\ a}} Q_a^2 \int d\omega_1 \, d\omega_2 \ \delta(\omega_1 \omega_2 - s/q^2) \ F^a(\omega_1) \, F^{\bar{a}}(\omega_2).$$

$$(14)$$

Here $\sqrt{q^2}$ is the invariant mass of the muon pair. The functions F^a, $F^{\bar{a}}$ are the same as in (4), so that they can be calculated from $V(\omega)$ and $S(\omega)$, and so $d\sigma/d\sqrt{q^2}$ may be calculated.[8] The result is shown in figure 5, together with the data.[1d] The experiment had a cut-off q_{min} on the momentum of the muon pair. This appears as an upper limit on the ω_1 integration in (14) and has an important effect. In particular, it means that one cannot apply any simple scaling law to the data, to

ANTINEUTRINO/NEUTRINO CROSS-SECTION RATIO (CERN GARGAMELLE)

1,105 $\bar{\nu}$ EVENTS
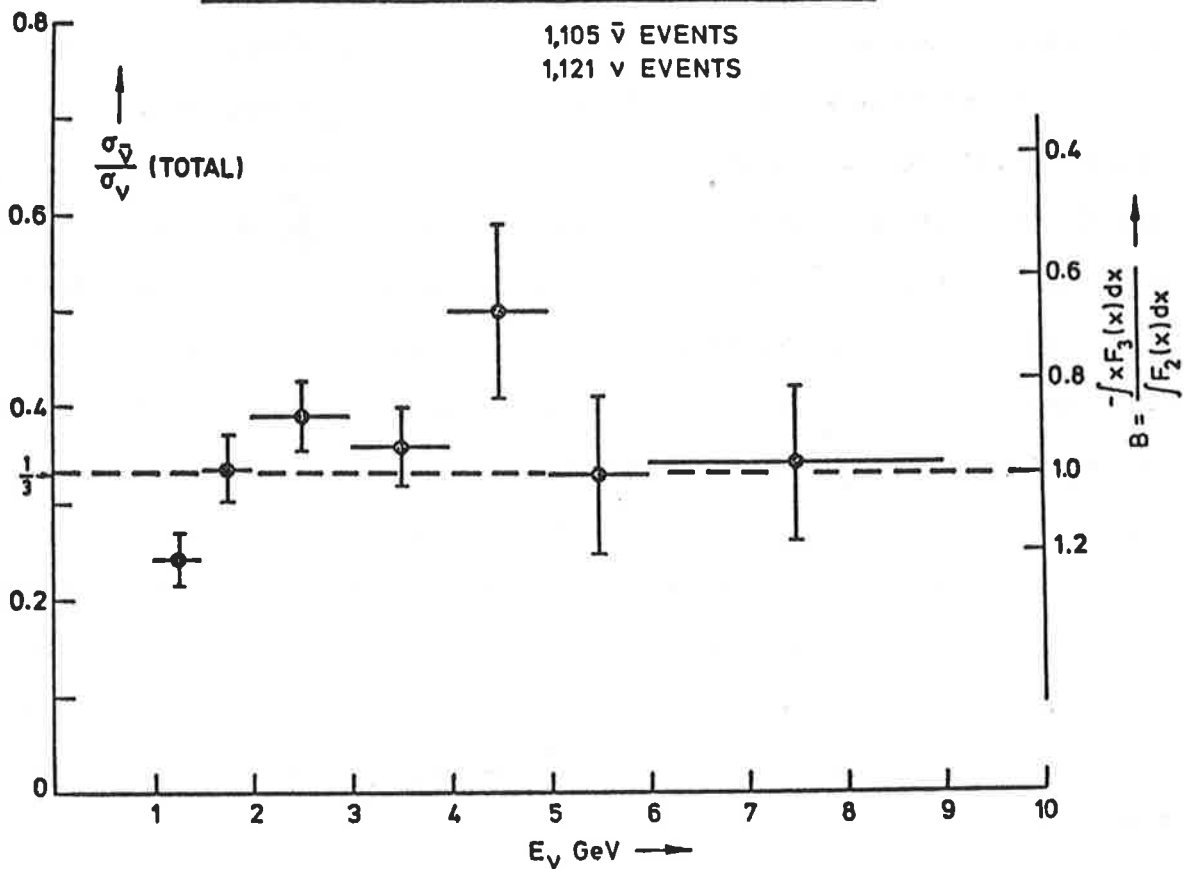1,121 ν EVENTS

Figure 4

Data for $\sigma(\bar{\nu})/\sigma(\nu)$ in heavy freon. The value $\frac{1}{3}$ is the approximate minimum allowed in quark models, and corresponds to $S(\omega) = 0$.
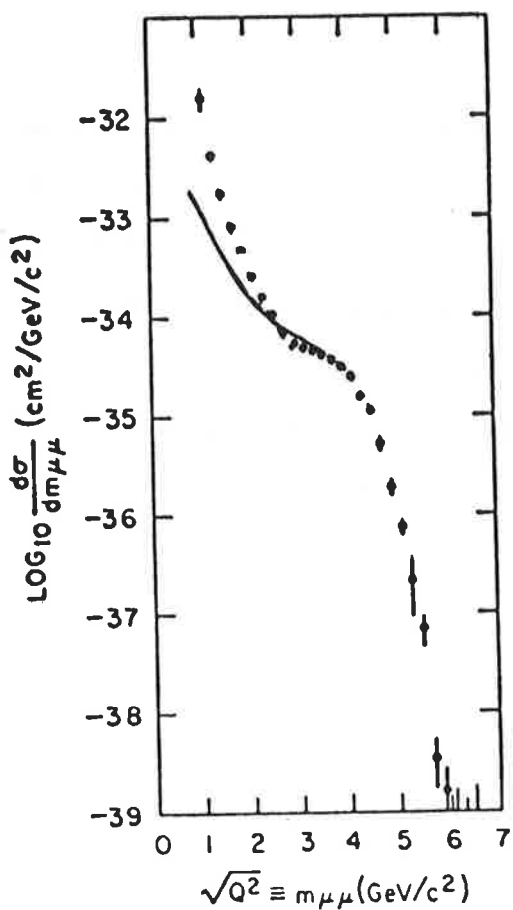

Figure 5

Data for muon pair production, with calculated curve.

predict what will happen in similar experiments at other energies; to make such predictions, a complete recalculation is necessary.[9] Note that the antiquark functions $F^{\bar{a}}(\omega)$ in (14) are just $S(\omega)$, and it is the fact that $S(\omega) \approx 0$ for $\omega < 2.5$ that is responsible for the turn-over at $\sqrt{q^2} \approx 4$ and the subsequent sharp fall. The details of this are highly sensitive to the way that $S(\omega)$ goes to zero as ω is decreased towards 2.5; in our calculation,[8] Polkinghorne and I assumed that $S(\omega)$ decreases very abruptly. The discrepancy between the data and the calculated curve for $\sqrt{q^2} < 3$ is presumably because in this region q^2 is not large enough for asymptopia to have set in. (Unlike in electroproduction, q^2 is timelike, so that electroproduction cannot be used to predict how large q^2 must be before other contributions have died away).

One may similarly calculate the cross-section for the production of a W boson, if such exists. It should be found at the ISR, provided that its mass is less than 15 to 20 GeV.

It will be interesting to have the results of muon-pair production experiments with other projectiles, so as to get information about the corresponding $F^a(\omega)$.

Mesons at large transverse momentum

I now digress from the discussion of weak and electromagnetic process, to mention a purely hadronic process that may perhaps be related to them. This is the production, in pp collisions, of mesons at large transverse momentum. In the case of the weak and electromagnetic processes, well-defined assumptions lead to firm conclusions about what are the dominant terms, but for the hadronic processes the present situation is that one decides what is the dominant term largely by guesswork. Polkinghorne and I have made such a guess,[10] as have other authors.[11] The guesses differ in detail, but all have the consequence that, at large p_T,

$$E \frac{d\sigma}{d^3p} = s^{-n} f(p_T/\sqrt{s}, \theta).$$

(15)
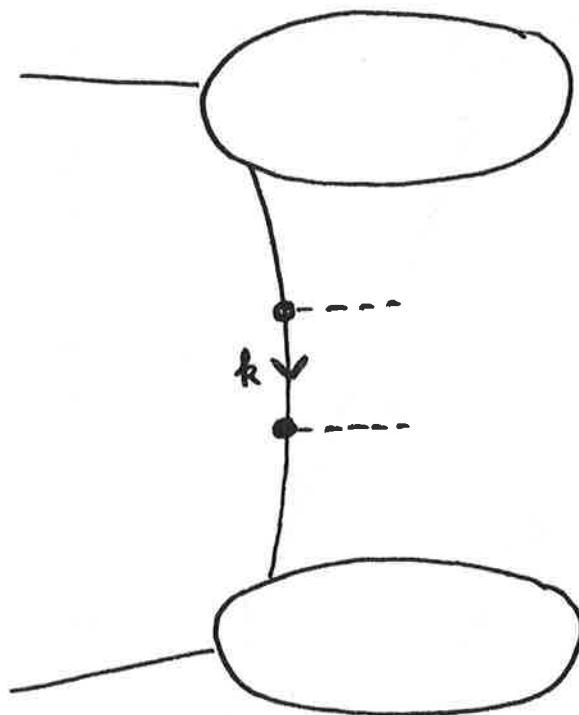
Fig 6

Guess for dominant contribution to production of large-transverse-momentum meson production. The internal lines are quarks.

π° production at 90°

$$\frac{E}{p^2} \frac{d^2\sigma}{dpd\Omega}$$

$\sqrt{s} = 44\,GeV$

$\sqrt{s} = 30 \cdot 6\,GeV$

10^{-32}

10^{-33}

10^{-34}

$\sqrt{s} = 53 \cdot 4\,GeV$

$0 \cdot 10$ $0 \cdot 20$ $p_T/\sqrt{s}$

Fig. 7

Data for π° production at 90°, with the curves calculated from the model of figure 6. The model contains two free parameters. The curves are parallel - there is constant vertical distance between them!

Our guess, which represents an attitude somewhere between those of Amati et al. and Blankenbecler et al., is that the mechanism is very similar to that for muon-pair production, and that the dominant contribution corresponds to figure 6. Both mesons emerge with large transverse momentum, that is we suppose that a large-transverse-momentum meson is always accompanied by another of nearly opposite transverse momentum (though their longitudinal momenta may differ, so that they do not emerge in opposite directions). The variable k^2 is large, but the squared momenta in the other two interna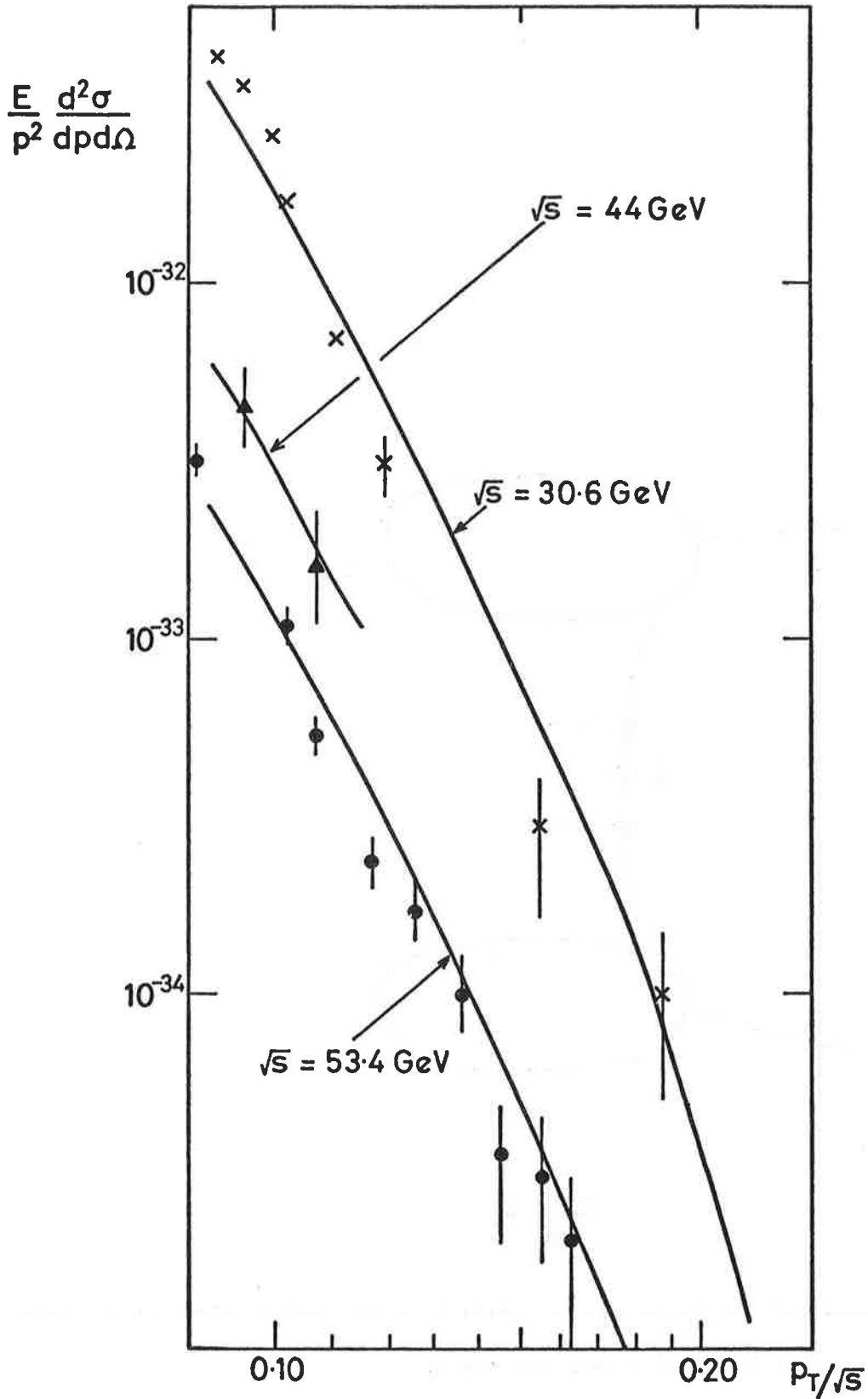l quark lines are not. We assume that only the mesons of the octet have an appreciable coupling to the quarks, that their coupling obeys SU_3 , and that it behaves like $(k^2)^{-\gamma}$ for large k^2 . Then it turns out that $n = 2 + 4\gamma$, and the function f is a certain integral involving F^a and $\bar{F}^a$. Since we know these functions, there are just two free parameters, the value of γ and the normalisation of the meson couplings. The result is shown in figure 7, together with the data. The constant γ determines the spacing between the curves; the best fit is $\gamma = \frac{1}{8}$, so that $n = 2.5$. The normalisation of the meson couplings fixes the position of one of the three curves, and the other two are then completely determined. For $p_T/\sqrt{s} > 0.25$ the curves fall sharply, and the cross-section is essentially zero by the time the value $p_T/\sqrt{s} = 0.3$ is reached; this is because $S(\omega) \approx 0$ for $\omega < 2.5$.

We predict that for $0.1 < p_T/\sqrt{s} < 0.2$ the relative numbers of large-transverse-momentum mesons produced at 90° are in the approximate ratios

$$\pi^+ : \pi^o : \pi^- : K^+ : K^- : \eta = 1.1 : 1.0 : 0.9 : 1.1 : 0.6 : 0.8$$

The authors[10,11] who consider large-transverse-momentum processes also discuss pp elastic scattering at large t . All agree that one should expect

$$\frac{d\sigma}{dt} \sim s^{-m} \mathcal{F}(\theta).$$

(16)

Provided that one imposes the condition $t > 2.5(GeV)^2$, the data[12] seem to confirm this,[13] even up to ISR energies (figures 8 and 9). One concludes that $m \approx 9.7$
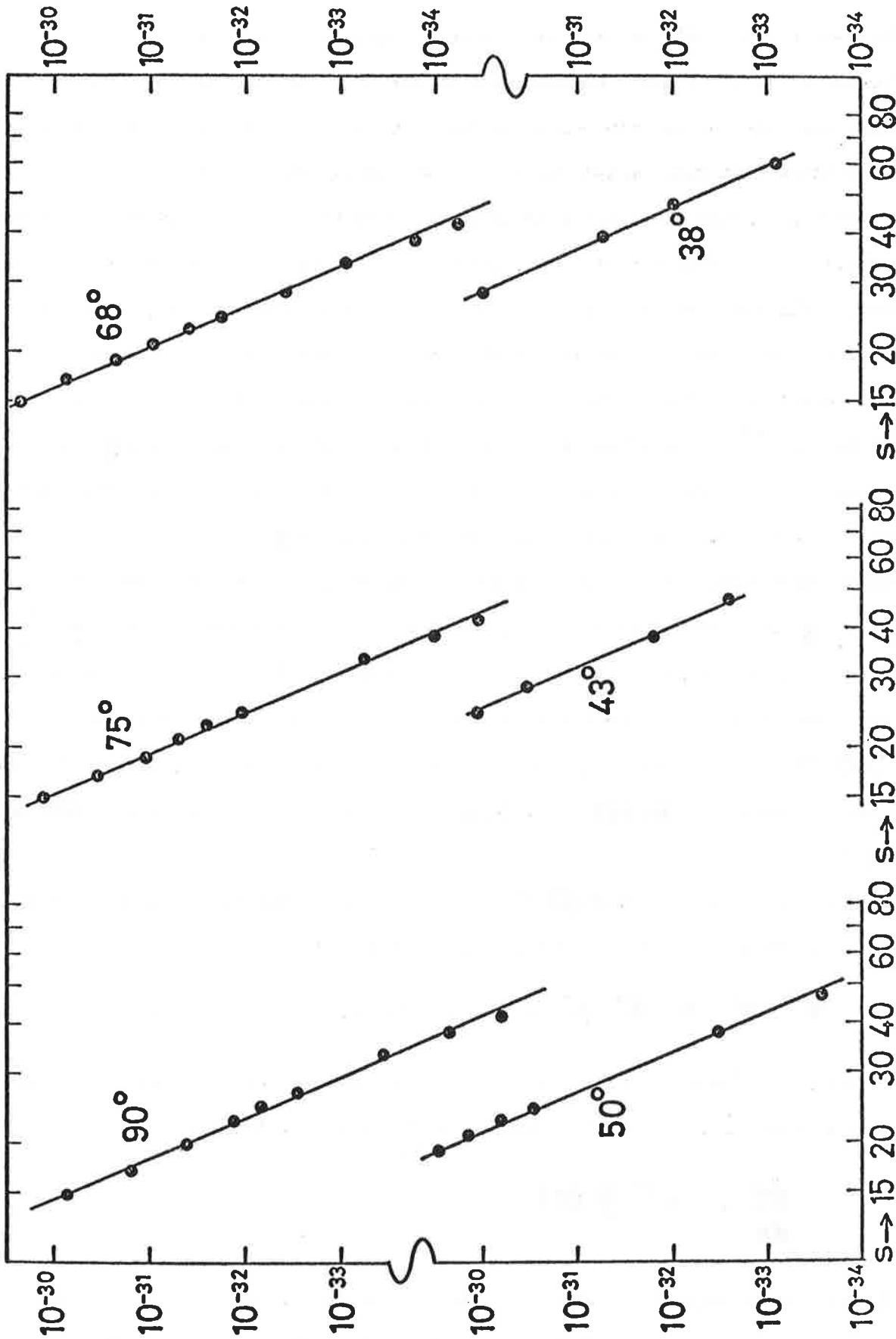
8. $d\sigma/dt$ against s for pp elastic scattering at various fixed angles, on log-log scales. The straight lines correspond to $s^{-9.7}$.
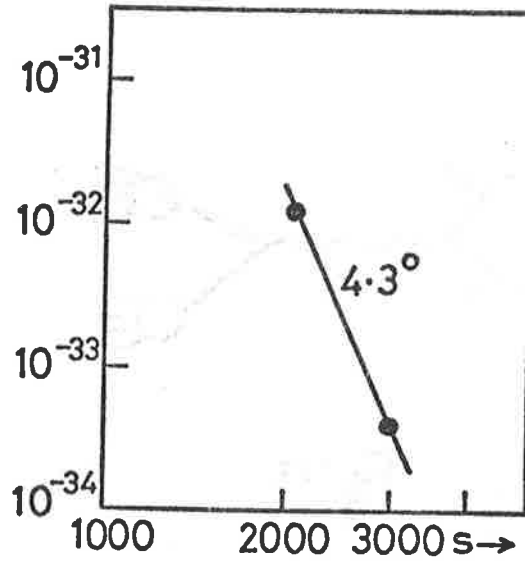
Figure 9

9. The same for the preliminary ISR data.

10. The angular dependence corresponding to the straight lines in figure 8. The straight line corresponds to $(\sin \Theta)^{-14}$.

11. As figure 8, but including also data points corresponding to $t < 2.5(\text{GeV})^2$.
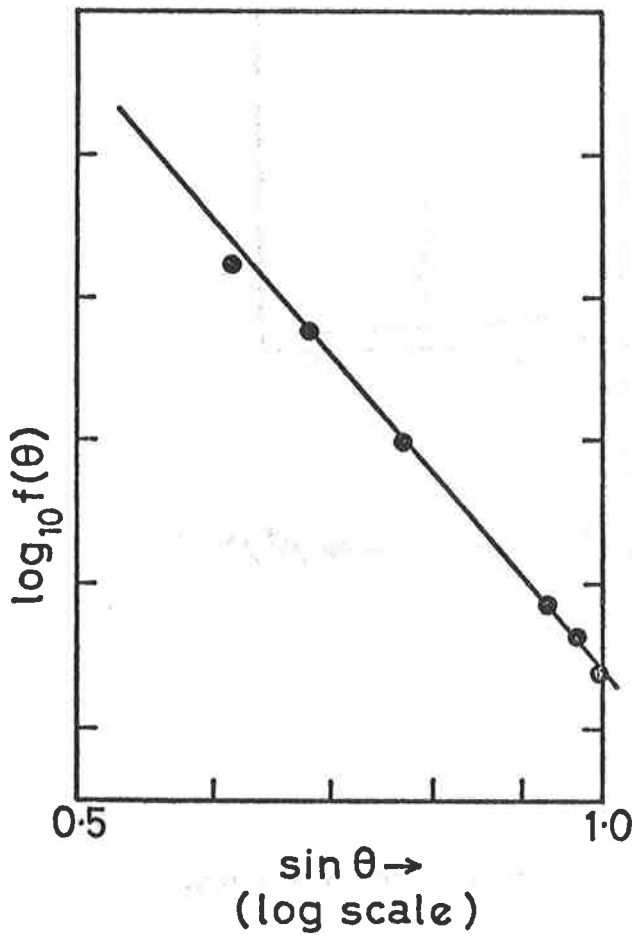
Figure 10
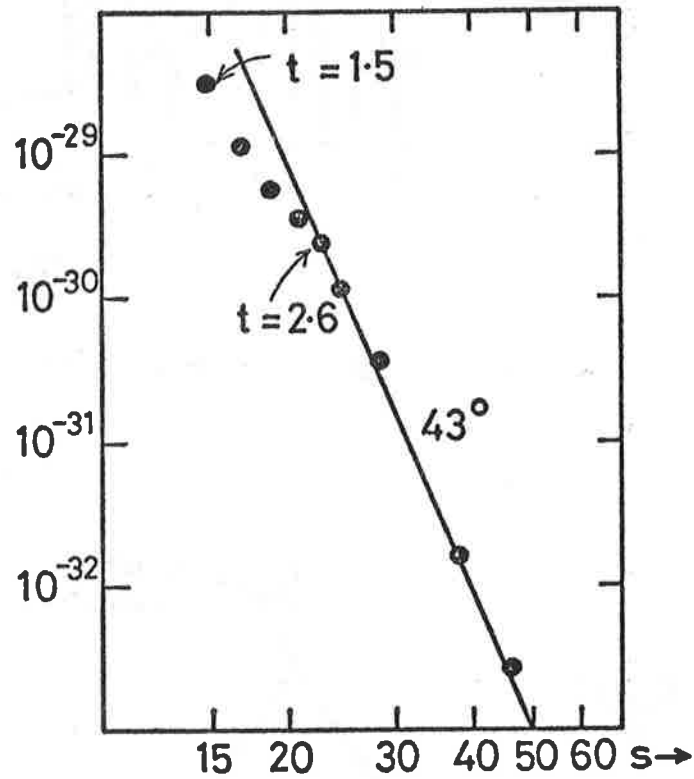
Figure 11
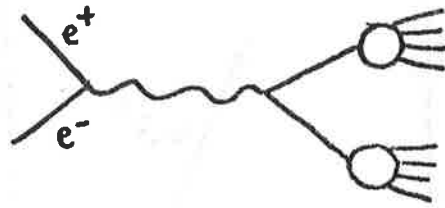
Fig 12

Dominant contribution to $e^+e^- \longrightarrow X$.
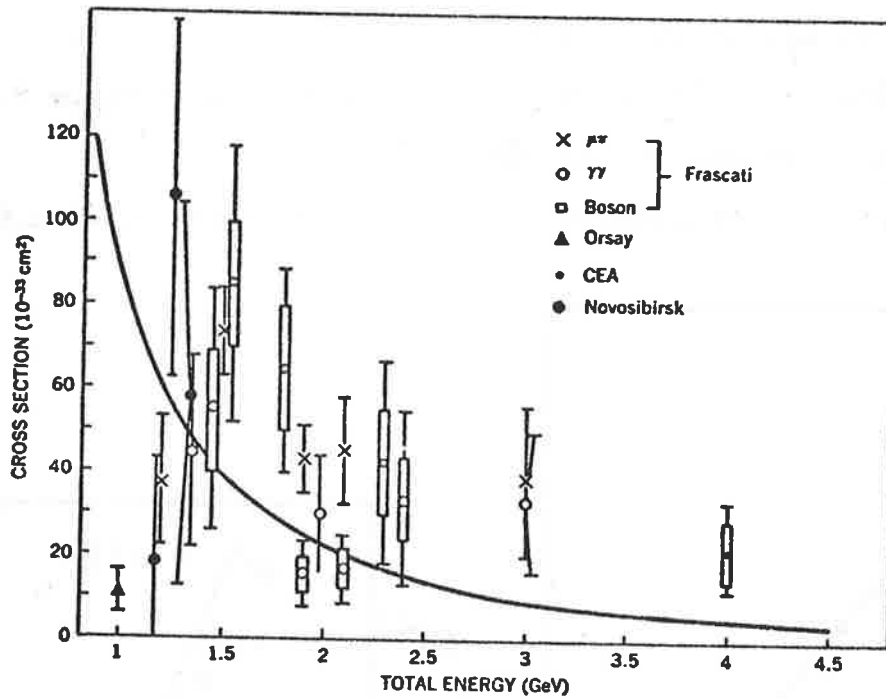
Fig 13

Data for $\sigma(e^+e^- \longrightarrow X)$. The curve is $\sigma(e^+e^- \longrightarrow \mu^+\mu^-)$.
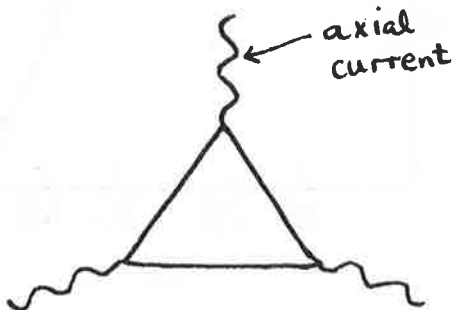
Fig 14

Adler-anomaly diagram.

and (figure 10) that for $90° < \theta < 40°$ a reasonable fit to $\mathcal{J}(\theta)$ is $(\sin \theta)^{-14}$. The importance of imposing the condition $t > 2.5$ is illustrated in figure 11; the region around $t = 2.5$ represents[13] the transition between the Regge régime and the "fixed angle" regime (16).

Electron-Positron Annihilation

I now return to electromagnetic interactions. The remainder of my discussion will not depend in any way on the dynamical assumption about valence quarks and the sea.

In particular, at sufficiently high energy the total cross-section for e^+e^- annihilation should depend just on the charges of the quarks. The expected mechanism is shown in figure 12, and results in[14] a cross-section falling like $1/s$, with

$$\frac{\sigma(e^+e^- \rightarrow X)}{\sigma(e^+e^- \rightarrow \mu^+\mu^-)} = \sum_a Q_a^2 \tag{17}$$

With quark partons, the sum of the squares of their charges is $\sum Q_a^2 = 2/3$. An SU_3 octet of partons would give $\sum Q_a^2 = 4$, and Gell-Mann's[2111] three triplets of quarks (see below) would give $\sum Q_a^2 = 2$. The data are shown in figure 13, together with the curve for $\sigma(e^+e^- \rightarrow \mu^+\mu^-)$. My own interpretation of the data is that asymptopia has probably not yet been reached.

$\pi^0 \rightarrow 2\gamma$

If one believes PCAC, the rate for this process can be calculated[15] from the Adler anomaly diagram, figure 14. Taking the internal lines to be quarks, one obtains a rate about 10% of that observed. There are two obvious ways out: either to argue[3] that PCAC goes wrong, or to introduce[2111] three identical triplets of quarks, so that the calculated rate acquires an extra factor of 9. The second way would not

change the relationship between electroproduction and the neutrino processes, but[15a] it would multiply the theoretical curve in figure 5 by an undesirable factor of $\frac{1}{3}$.

The final state in electroproduction and annihilation

So far I have supposed that the system X of hadrons for each process (1) is not examined. To investigate the composition of X is not only harder experimentally, it is also much more difficult theoretically, and the results are much more model dependent. Also, there are reasons for believing that asymptopia may be achieved later, that is at larger s, q^2, than for the completely inclusive processes.

However, the parton or softened field theory approach does lead one to expect some general features:

(i) In electroproduction, the final-state multiplicity should remain finite as s, $q^2 \longrightarrow \infty$ at finite ω. As $\omega \longrightarrow \infty$, it should increase as log ω.

(ii) In e^+e^- annihilation, the multiplicity should be finite.[16]

(iii) In electroproduction, there should be[17] two bunches of particles, one from target fragmentation and one from fragmentation of the virtual photon. At finite ω there should be nothing in between, that is no analogue of the pionisation found in hadronic processes. (This statement may need some modification if the partons are taken to be quarks, but quarks are not found as particles. In this case, there had better be some communication between the two bunches of particles, which may require a small amount of pionisation.)

(iv) In the semi-inclusive annihilation process

$$e^+e^- \longrightarrow hX \tag{18}$$

there should be scaling. The corresponding structure functions $\bar{F}_1(\omega)$ and $\bar{F}_2(\omega)$ are calculated from a diagram just like figure 1, but with the external hadron lines swung round so as to represent the detected final-state hadron h. The leading

behaviour of $\bar{F}_1 = \frac{1}{2}\omega\bar{F}_2$ at $\omega = 1$ is the same as that of $F_1 = \frac{1}{2}\omega F_2$ but because of complicated things that happen at $\omega = 1$ no simple relation is expected[16,18] between F_2 and $\bar{F}_2$ away from $\omega = 1$.

(v) In the semi-inclusive electroproduction process

$$eN \longrightarrow ehX \tag{19}$$

for the case where the detected final-state hadron h is in the photon fragmentation region, the differential cross section is proportional to[19]

$$\sum_a Q_a^2 \, F^a \, \bar{F}^a \tag{20}$$

where F^a are again the functions defined in (4) for inclusive electroproduction, and $\bar{F}^a$ are the analogous functions for the semi-inclusive annihilation process (18).

Various authors[20], beginning with Pantin, have tried to extend the dynamical ideas of valence quarks and a sea to the semi-inclusive processes (18) and (19). A general feature of their predictions is a π^+/π^- ratio, and also a K/π ratio, rather higher than is normally expected in hadronic reactions. The available[21] data support this. According to Pantin, the π^+/π^- ratio could be as large as 8 in the photon fragmentation region, though Kingsley[19] has argued that this value is sensitive to the input assumptions, and that a rather smaller value is more reasonable.

R E F E R E N C E S

1. (a) E.D. Bloom et al., Kiev Conference Report (1970); H. Kendall, Cornell Conference Report (1971).

   (b) G. Myatt and D.H. Perkins, Phys.Lett. 34B, 542 (1971); D. Cundy et al., Brookhaven and NAL Conferences (1972); See also the talk by Dr. Venus.

   (c) C. Bacci et al., Phys.Lett. 38B, 551 (1972).

   (d) J. Christenson et al., Phys.Rev.Lett. 25, 1523 (1970).

   (e) CERN-Columbia-Rockefeller Collaboration, NAL Conference (1972); Saclay-Strasbourg Collaboration (unpublished); British-Scandinavian Collaboration (unpublished).

2. For reviews, see (i) M. Gourdin, lectures at CERN School (1972);

   (ii) P.V. Landshoff and J.C. Polkinghorne, Physics Reports 5C, 1 (1972);

   (iii) H. Fritzsch and M. Gell-Mann, Tel-Aviv Conference Proceedings (1971).

3. K. Johnson, Phys.Rev. D6, 1101 (1972); S.D. Drell and K. Johnson, Phys.Rev. D6, 3248 (1972).

4. D.J. Gross and C.H. Llewellyn Smith, Nuclear Physics B14, 337 (1969); C.H. Llewellyn Smith, Nuclear Physics B17, 227 (1970).

5. P.V. Landshoff and J.C. Polkinghorne, Nuclear Physics B28, 240 (1971); Phys.Lett. 34B, 621 (1971); J. Kuti and V.F. Weisskopf, Phys.Rev. D4, 3418 (1971).

6. P.V. Landshoff, Springer Tracts in Modern Physics, Vol. 62 (1972).

7. P.V. Landshoff and J.C. Polkinghorne, Phys.Lett. 34B, 621 (1971).

8. S.D. Drell and T.M. Yan, Phys.Rev.Lett. 25, 316 (1970). P.V. Landshoff and J.C. Polkinghorne, Nuclear Physics, B33, 221 (1971); erratum B36, 642 (1972). It is also shown here that there is a term additional to the Drell-Yan term; it scales similarly,but probably it is rather smaller numerically.

9. The experiment should be feasible at the ISR: see P.V. Landshoff and J.C. Polkinghorne, Phys.Lett. 40B, 463 (1972).

10. P.V. Landshoff and J.C. Polkinghorne, Cambridge preprints DAMTP 72/43 and 72/48 and in preparation.

11. R. Blankenbecler, S. Brodsky and J. Gunion, Phys.Lett. 39B, 649 (1972); 42B, 461 (1972); Phys.Rev. D6, 2652 (1972); S.M. Berman, J.D. Bjorken and J.B. Kogut, Phys.Rev. D4, 3388 (1971); D. Amati, L. Caneschi and M. Testa, preprint CERN TH-1597; D. Horn and M. Moshe, Nuclear Physics B48, 557 (1972); preprint CALT-68-382.

12. C.W. Akerlof et al., Phys.Rev.Lett. 17, 1105 (1966); Phys.Rev. 159, 1138 (1967); J.V. Allaby et al., Phys.Lett. 25B, 156 (1967); 27B, 49 (1968); 28B, 67 (1968); 34B, 431 (1971);

    R.A. Carrigan, Phys.Rev.Lett. 24, 683 (1970);

    G. Cocconi et al., Phys.Rev. 138, B165 (1965);

    C. Rubbia, report to NAL Conference (1972).

    Some of the plotted points correspond to interpolations between observations at two neighbouring values of t .

13. P.V. Landshoff and J.C. Polkinghorne, preprint DAMTP 73/4.

14. N. Cabibbo, G. Parisi and M. Testa, Nuov.Cim.Lett. 4, 35 (1970).

15. This can be shown using softened field theory (P.V. Landshoff, Cargèse lectures 1972, preprint DAMTP 72/23) or using light cone techniques (R. Crewther, Phys. Rev.Lett. 28, 421 (1972)).

15a. R. Kingsley and C. Nash, Nuov.Cim.Lett. 4, 802 (1972).

16. P.V. Landshoff and J.C. Polkinghorne, preprint DAMTP 72/38.

17. S.D. Drell and T.M. Yan, Phys.Rev.Lett. 24, 855 (1970); P.V. Landshoff and J.C. Polkinghorne, ref.8.

18. P.V. Landshoff and J.C. Polkinghorne, preprint DAMTP 72/16; R. Gatto, P.Menotti and I. Vendramin, Nuov.Cim.Lett. 4, 79 (1972); A. suri, Phys.Rev. D4, 570 (1971).

19. S.M. Berman et al., ref. 11; R. Kingsley, preprint DAMTP 72/49; Altarelli and Maiani, Rome preprint

20. C.F.A. Pantin, Nucl.Phys. 46B, 205 (1972); M. Gronau, F. Ravndal and Y. Zarmi, preprint CALT-68-367; R. Kingsley, ref.19; M. Chaichian, S. Kitakado and H. Satz, Bielefeld preprint Bi-73/01.

21. J.T. Dakin et al., Phys.Rev.Lett. 29, 746 (1972).

EPIC Experiments

by

W.T. Toner

1. Introduction

This talk is by an enthusiast for the physics one can do at EPIC and not by an EPIC expert. They are in the audience.

EPIC is an idea [1] for an Electron Proton Intersecting Complex which could be built at a not impossible cost in a finite number of years, perhaps by 1981-1982. The range of parameters under consideration is summarised below:[2]

Possible Stored Beams

e^-	8 to 14 GeV in a ring with conventional magnets.
e^+	" in a second ring with conventional magnets.
p	70 to 200 GeV/c in a ring with Superconducting magnets.
or	
D	70 to 200 GeV/c in the same ring.

Possible Collisions at $S = 4E_1E_2$

e^+e^-	)		
	)	256 to 784	$(GeV)^2$
e^-e^-	)		
e^-p	)		
	)	2200 to 11,200	"
e^+p	)		
$e^-n(p)$	)		
	)	1100 to 5600	"
$e^+n(p)$	)		

All of these and more, e.g. pp, are in principle possible.

In the design of such a complex it will be necessary to balance likely costs against relative feasibility and physics interest. Dr G. Manning is setting up study groups to tackle this job. Like many of you, I have volunteered to help. In the High Energy Physics community, one task is to assign relative priorities: is one prepared to sacrifice some energy in the e^+e^- system in order to get more in the e^-p system? Would one be prepared to give up the possibility of, say, e^-e^- collisions in favour of e^-n? Such choices (not necessarily these) between desirable but different features will have to be made, for the supply of money cannot be infinite. The machine designers will have to show us what are the relative costs and feasibility, and find ways to extract the most for the least cost out of any proposed arrangement.

The parameter that determines the event rate in a colliding beam system is the Luminosity:

$$L\sigma = \text{counting rate}$$

For EPIC, a luminosity of $\frac{1}{4} \times 10^{32}$ cm^{-2} sec^{-1} in each of 4 separate interaction regions is considered to be a realisable goal. However, it may equally be an upper limit beyond which one cannot go. There are some things that money cannot buy, and this may be one of them.

Now, if anyone had been so rash as to suggest such a system ten years ago, the EPIC that would have sprung to mind would be:
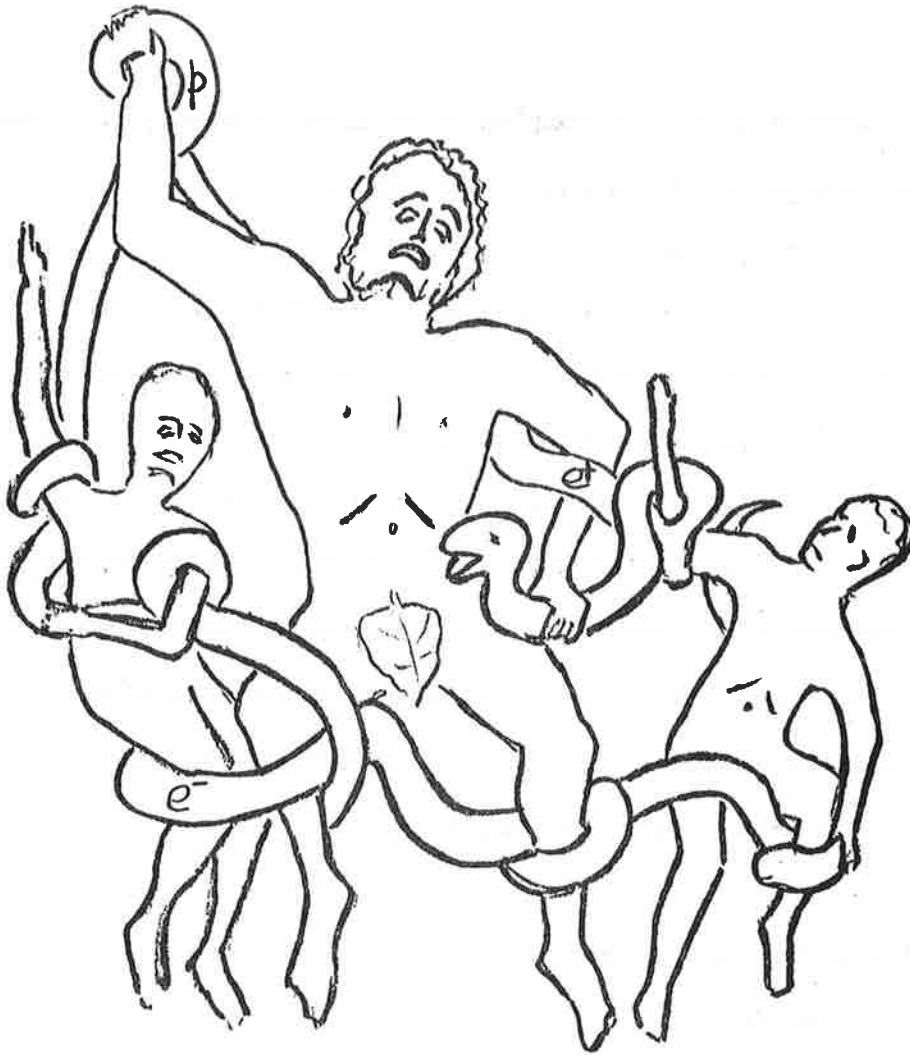
Figure (1) EPIC as visualised in 1963

Since then storage rings have been built and operated in many places,
usually with quite remarkable success:

ACO, Novosibirsk, ADONE, the ISR, CEA, and now SPEAR, soon DORIS.

The experiments carried out with them have likewise been most successful.

The physics has helped in a technical sense in the e^+e^- systems because

the very large cross-sections at large q^2 give reasonable counting rates at
achievable luminosities.

In fact, if one is thinking of snakes in 1973, the picture might look more like:

Figure (2) EPIC as visualised in 1973

Notice that there are now three snakes to one person.

Most important of all, new and unexpected fundamental physics has come from the experiments.

2.   General Survey of Physics

It is the importance of the physics which can come out of EPIC, not just technicalities, which is the motivation for considering such a system. Table I is a list of some of the measurements which could be made arranged partly by collision and partly by the type of physics. It is certainly not complete. Some of the items were only remembered at the last minute.

Table I   Physics with EPIC

e^+e^-	σ_T (one photon)
	Multiplicity, Correlations, Hadron Distributions
	Weak-EM interference
	Heavy Point Particles
e^-e^-	$\to e^-e^-\gamma\gamma \to e^-e^-$ hadrons
e^-p	$\to (e^-)\gamma \, {}^{p}_{D}$ Almost real photoproduction
e^-D	σ_{TOT}
	Vector Photoproduction
	Multiplicity, Correlations, Hadron Distributions
e^-p	$\to e^-$ Anything
e^-D	$\underline{\text{Small}}$ q^2 $\quad \omega \to \infty$ limit
	$\quad\quad\quad\quad \rho$ electroproduction
	$\underline{\text{Large}}$ q^2 $\quad$ Scaling Validity?
	$\quad\quad\quad\quad$ Final State Hadrons
	* Neutron and Proton Targets.
e^-p	Polarised Target - Polarised Beam.
e^-p	$\to e^-$ Anything: Weak-EM Interference.
e^+p	$\to e^+$ Anything: 2γ exch.
e^-p	$\to \left(\begin{matrix} e^- \\ \text{or} \\ \nu_e \end{matrix}\right) W^-$ Anything.
e^-p e^+p	$\to {\underline{\nu} \atop \nu}$ + Anything
$e^-n(p)$	Deep Inelastic Weak
$e^+n(p)$	> Deep Inelastic EM?

A few comments on some of them. In the e^+e^- system, as Landshoff [3] pointed out this morning, σ_T for one-photon annihilation can be regarded as measuring $\sum_i q_i^2$ where i runs over all the independently existing pairs of fundamental particles in the universe. Thus, 1 for $e^\pm$ plus 1 for $\mu^\pm$ plus **?** for the quarks or whatever other objects there may be, provided one is at sufficiently high energy that the binding between them does not distort things too much (as in ρ, ω, ϕ, ρ^1 etc). EPIC, if built, is likely to provide the highest e^+e^- energies anywhere.

If the multiplicities do not grow linearly with $\sqrt{S}$ - and various models predict that they will not [3] - then one is inevitably led to a situation where the final state pions will have large relative momenta, a very interesting state of affairs for a system with an overall angular momentum of 1. A detailed study of multiplicities, momentum distributions and correlations will be exciting.

Budny [4] will discuss possibilities for observing EM-weak neutral current interference effects in $\mu^+\mu^-$ production. Later in this talk, I will discuss possibilities for producing pairs of heavy leptons.

Collisions between e^-e^- (or e^+e^+) have a great deal of physics interest, for they give a pure sample of events for the process ee → ee $\gamma\gamma$ → ee + hadrons. A γ from the virtual photon cloud of one of the leptons collides with a γ from the cloud of the other lepton. The final state leptons will be hard to observe, for they continue almost undeflected though with some loss of energy. The physics here concerns Adler anomalies, $\pi\pi$ scattering and other topics and is extremely interesting. [5] The cross-sections can be quite large, and they grow roughly as the cube of the logarithm of the energy of the rings.

However, the cross-section is dominated by hadronic invariant masses
close to threshold, e.g. for the $\pi\pi$ system $\frac{d\sigma}{ds_{\pi\pi}} \sim s_{\pi\pi}^{-2}$

Most of the physics may therefore already have been studied at DORIS,
and the increased total rate at EPIC is not likely at first sight to open
up sufficient new physics in this field to make this the highest priority
item. However, it will be necessary at EPIC to measure the $\gamma\gamma$ processes
in e^-e^- (or e^+e^+) as they will be an important background to the one photon
annihilation in the e^+e^- system and must be subtracted to get clean one-
photon physics. There will presumably be difficulties with interference effects
even then (in the radiative corrections).

The next system is $e_D^p \rightarrow (e) \gamma_D^p \rightarrow$ photoproduced final states, where
the photon is almost real. One can describe these processes as the interaction
of a beam of almost real photons with the target hadrons. The "equivalent
radiator" [6] at EPIC energies is about 4×10^{-2} i.e. the effective photon flux
in the rest system of the target proton is $\sim 4\times10^{-2} \times \frac{dk}{k}$ where k is the
photon energy in that system. So, for $\frac{1}{e} < 2Mk/Smax < 1$, we have an effective
luminosity of $4\times10^{-2} \times \frac{1}{4} \times 10^{32}$ i.e. 10^{30} $Cm^{-2}sec^{-1}$ for high energy photons
on protons. This is to be multiplied by the real photon cross-section to
get the counting rate, which is 100 photoproduction events per second with
$S > \frac{1}{e}$ Smax. This is a healthy rate for the total cross-section, diffractive
photoproduction and inclusive studies. The new ISR pp results showing a
rising pp total cross-section increase the interest in $\sigma_{\gamma p}$: it is so
like the pion cross-section $\times \frac{1}{200}$ at low energies that one would like

to see if the photon-hadron correspondence holds also at these very high center of mass energies. In fact, photon-nucleon and nucleon-nucleon cross-sections will be the only ones we can reliably measure at these values of S.

In the vector meson photoproduction case, we should remember that if we tag these almost real photons, we measure their polarisation. Non-diffractive two body or quasi-two body channels will be unmeasurably rare.

Inclusive and semi-inclusive processes are also of interest. The experiments at EPIC will necessarily be different from those at the ISR, where the total interaction rate is some 1500 times greater. It will be essential to use a spectrometer with very large acceptance, and count for longer times, in order to reach into the large $p_\perp$ region which seems likely to be of interest. The apparatus described at the end of this talk might be a good starting point. One should remember that there will be large transverse momentum hadrons from high q^2 interactions, and the almost real photons will have to be tagged if one wants to examine the tail of the high $p_\perp$ region.

In almost-real-photoproduction, as in the inelastic ep case discussed below, it will be interesting to have deuterons both for $e(\gamma)n$ interactions and for $e(\gamma)D$ coherent interactions. [7]

Deep inelastic ep collisions at EPIC are important in two main regions.   There is the small but finite q^2, very small x (large ω) region where one would be interested in the structure functions for a limiting and very important case, [8] and also ρ^o electroproduction

which should be measurable. Secondly, in the large q^2 region there is the question of scaling of the structure functions (and the n-p difference) and the nature of final state hadrons. These topics are extensively reviewed in many places.[9] Llewellyn-Smith[10] mentioned the interference effects which might be observed were there a heavy "photon". Close[11] will discuss polarised lepton-polarised nucleon interactions at a later date at RHEL. The EPIC e$^-$ beam becomes polarised through synchrotron radiation and it may be possible to store polarised protons.

In all these cases, and especially for weak-EM interference, there will be questions raised as to the validity of one photon exchange, so that the availability of e$^+$p collisions to check for observable 2γ effects will be important.

The production of charged vector bosons is in principle possible either in pairs with e$^+$e$^-$ annihilation or singly in ep collisions via several diagrams of order $G\alpha^2$.[12] The much higher S available in ep collisions may be enough to compensate for the intrinsically lower cross-section, especially since only one heavy particle need be produced.

Finally in this survey we come to deep inelastic weak interactions, which I will discuss in some detail at the end of the talk. Here, it is appropriate to mention that should e$^-$p collisions yield measurable rates, which seems likely, there will be very great interest in comparing the results with e$^+$p, to get (V-A) and if at all possible with e$^\pm$n, to get the n-p differences.

It is a very impressive list of experiments of major scientific importance. We will now discuss two specific experiments in order to get a feel for the experimental problems that must be faced.

3. Heavy Leptons

The first experiment we consider is the detection of heavy leptons which do not have the same neutrinos as μ or e. These can in principle be observed in ep collisions at EPIC, by photo-pair production, or in one-photon annihilation of e^+e^-.
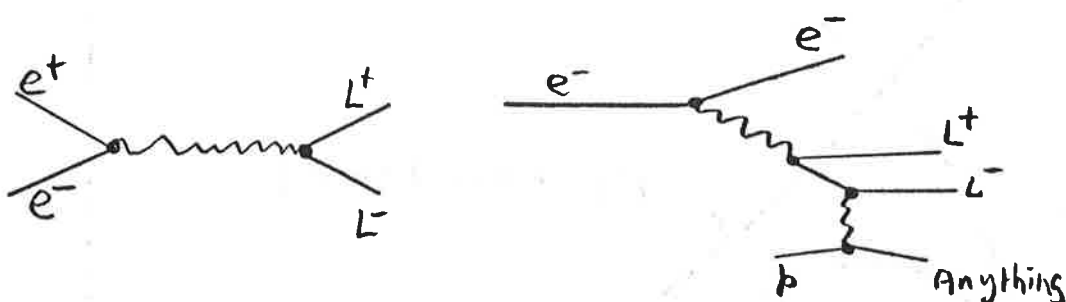
Kim and Tsai [13] have made extensive calculations of real photo-pair production, taking account of possible inelastic production, where the target proton breaks up. When multiplied by the effective photon flux of $4 \times 10^{-2} \, dk/k$, their cross-sections are very low indeed ($\sim 7 \times 10^{-37}$ for $M_L = 5 (GeV/c^2)$ at $S = 4000$). It seems clear that such particles will be found in e^+e^- annihilation if at all.

The cross-sections for heavy lepton and muon pair production by one-photon annihilation near threshold are shown in fig (3). If the total one-photon hadronic cross-section stays within a factor of 2 or so of the μ pair rate, it is clear that the signal to noise ratio will

144.

$$d\sigma = \frac{\pi \alpha^2}{2S}\left(1 - \frac{4M_L^2}{S}\right)^{\frac{1}{2}}\left[\left(1+\frac{4M_L^2}{S}\right) + \left(1 - \frac{4M_L^2}{S}\right)\cos^2\theta\right] d\cos\theta$$

$$\sigma = \frac{.87 \ 10^{-31}}{S} \ cm^2 \quad for \ M_L^2 \ll \frac{S}{4}$$

27 events /hour for 8.5 + 8.5
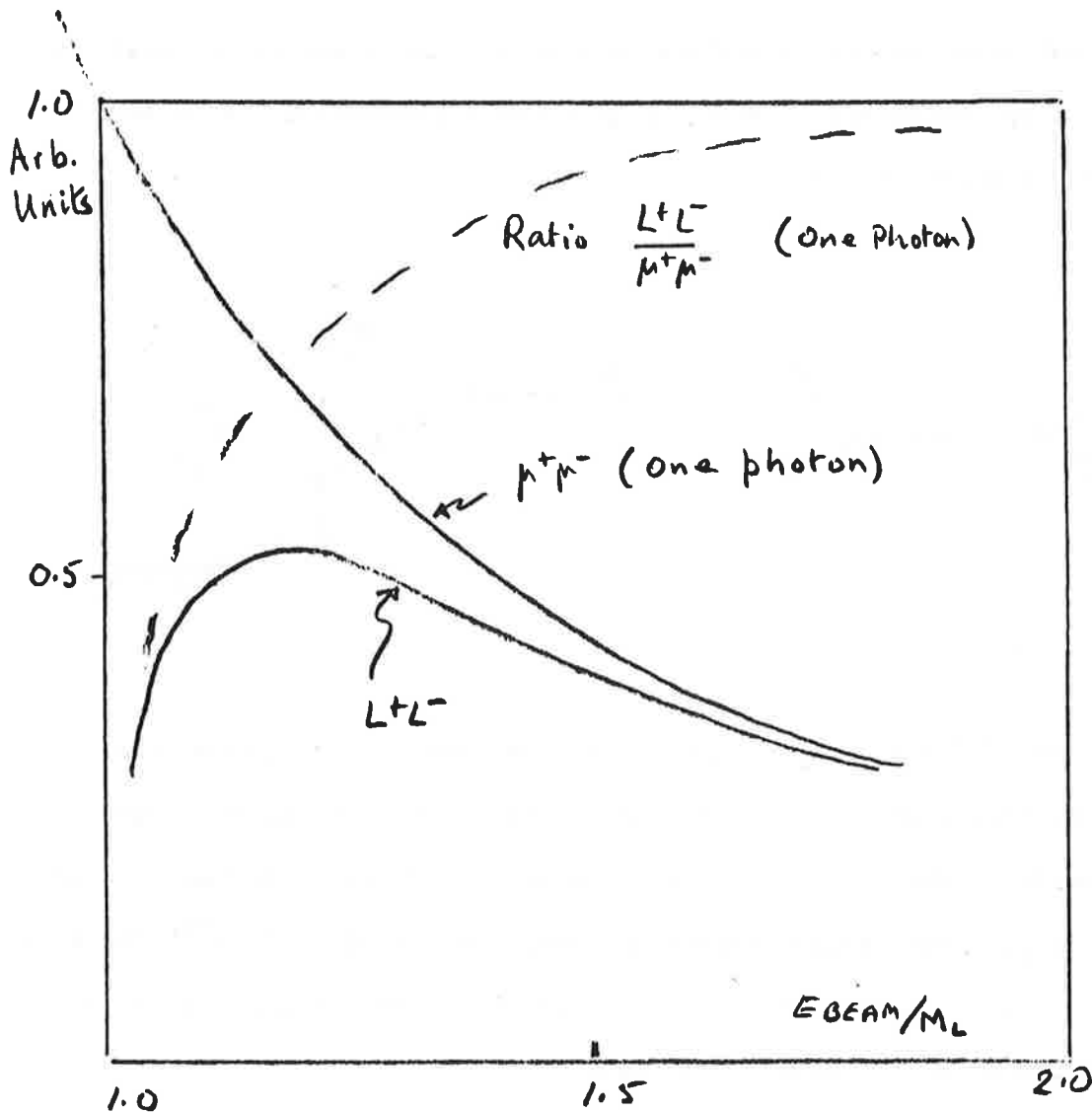
$$L = \frac{1}{4} \times 10^{32}$$

Fig. 3 Heavy Lepton Production by e^+e^- Annihilation

be excellent for M_L up to about 95% of E_{BEAM}. The overall production
rate is proportional to $\frac{1}{S}$, and is 27 per hour for $L = \frac{1}{4} \times 10^{32}$ with
8.5 GeV per beam.

Tsai [14] among others, has estimated that the branching
ratios for these types of particles, which cannot decay to $\mu\gamma$ or $e\gamma$,
should be

$$L \rightarrow \nu_L \mu \bar{\nu}_\mu : \nu_L e \bar{\nu}_e : \nu_L \text{ hadrons } :: \frac{1}{4} : \frac{1}{4} : \frac{1}{2}$$

Fairly uncontroversial assumptions about time-like scaling are involved
in making these estimates.

Thus, in $\sim \frac{1}{8}$ of the cases the production of L^+L^- will lead to an
electron (or positron) and a muon in the final state, with no other
observable particles, but with a large amount of missing energy ($\sim \frac{1}{3}$ of
the total), and with a large value for $(\bar{p}_{BEAM} \times \bar{p}_e) \cdot \bar{p}_\mu$. A truly spectacular
signal, as Llewellyn-Smith observed yesterday.

There will be roughly ten times the one-photon cross-section for the
production of $\mu^+\mu^-$ by the two photon mechanism. However, the $\mu^+\mu^-$ invariant
mass will be small and the events will be roughly coplanar with the beam,
though the muons will no longer be colinear. The amount of missing
transverse momentum will be very small. Therefore, the $\mu^+\mu^-$ and even the
e^+e^- combinations should be detectable, although the signal is less obvious.

A detector for the L^+L^- production will have to cover a large
solid angle, in order to collect as many of the events as possible and
also to demonstrate the absence of other particles. Positive identification
of both muons and electrons will be necessary. It seems **quite** conservative
to assume that in at least $\underline{1}$ of the μe decays, the geometry will be
3
favourable to unambiguous identification of both particles. The detection
rate for heavy leptons of mass 8 GeV at EPIC I would then be 1 per hour.
The background situation is excellent. One concludes that this is an
easy experiment. Until there is a satisfactory explanation for the seperate
existence of muons and electrons, a search for further lepton families will be
of the greatest importance.

4.   Could deep inelastic weak interactions be detected at EPIC?

The short answer is yes, but to arrive at it we must start by
examining the kinematics for

lepton + proton → lepton′ + any hadrons   (1)

in the unfamiliar situation where the proton in the initial state is
rapidly moving. It is amusing to note that the EPIC laboratory system
is a good approximation to the theorist's infinite momentum frame and also
contains as special cases two other theoretical reference frames one never
expected to see in the laboratory: the Breit or brickwall frame and the
rest frame of the final state hadrons. [15)

We use the notation of figure (4) below.

$$S = (E_\ell + E_p)^2 - (\vec{p}_\ell + \vec{p}_p)^2$$

$$q^2 = (E_\ell - E_{\ell'})^2 - (\vec{p}_\ell - \vec{p}_{\ell'})^2$$
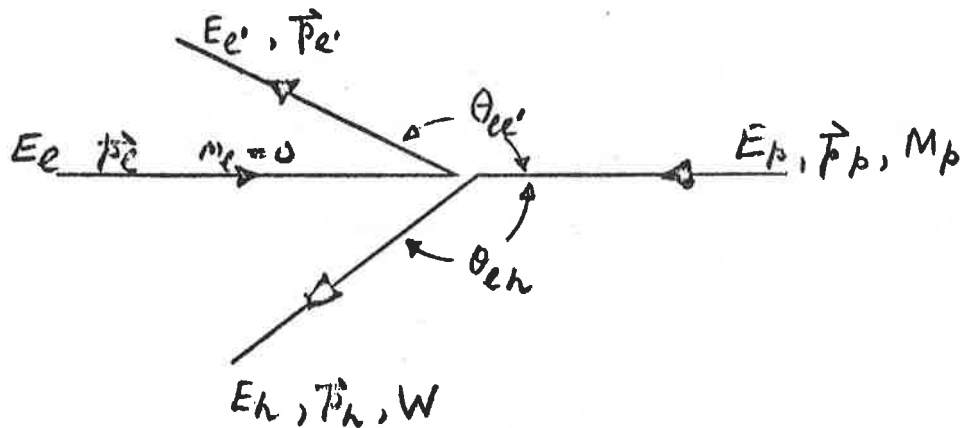
$$W^2 = (E_p + E_\ell - E_{\ell'})^2 - (\vec{p}_p + \vec{p}_\ell - \vec{p}_{\ell'})^2$$

Fig (4) Kinematics and Notation

If we sum over the final state hadrons so that only the overall $(E_h, \vec{p}_h, W)$ is determined, then the cross-section can be expressed in terms of the two invariants [16]

$$q^2 = -4E_\ell E_{\ell'} \, \sin^2 \frac{\theta_{\ell\ell'}}{2} \tag{2}$$

$$2M_p \nu = W^2 - M_p^2 - q^2 = S - M_p^2 - 4E_\ell \, p_p \, \cos^2 \frac{\theta_{\ell\ell'}}{2} - \frac{2M_p^2 E_{\ell'}}{E_p + p_p}$$

In the more usual case where the target proton is at rest ($p_p = 0$), (2) yields the familiar $2M_p\nu = 2M_p(E_\ell - E_{\ell'})$, as it should.

At EPIC energies it is easiest to work in terms of

$$x = -q^2/_{2M_p\nu} \quad \text{and} \quad y = \nu/_{\nu_{MAX}} \quad . \quad \text{Note that } xy = q^2/q^2_{MAX}$$

For our purposes, the $\dfrac{2M_p^2 E_{\ell'}}{E_p + p_p}$ can be dropped from (3), and it is

easy to show that $E_{\ell'} = xyE_p + (1-y)E_\ell$

$$\cos\theta_{\ell\ell}1 = -\left[\frac{xyE_p - E_\ell(1-y)}{xyE_p + E_\ell(1-y)}\right] \tag{3}$$

The kinematically allowed region for inelastic scattering is shown in fig (5) in terms of the invariants $-q^2$, $2M_p\nu$ with lines of constant W^2, x, y, xy indicated.
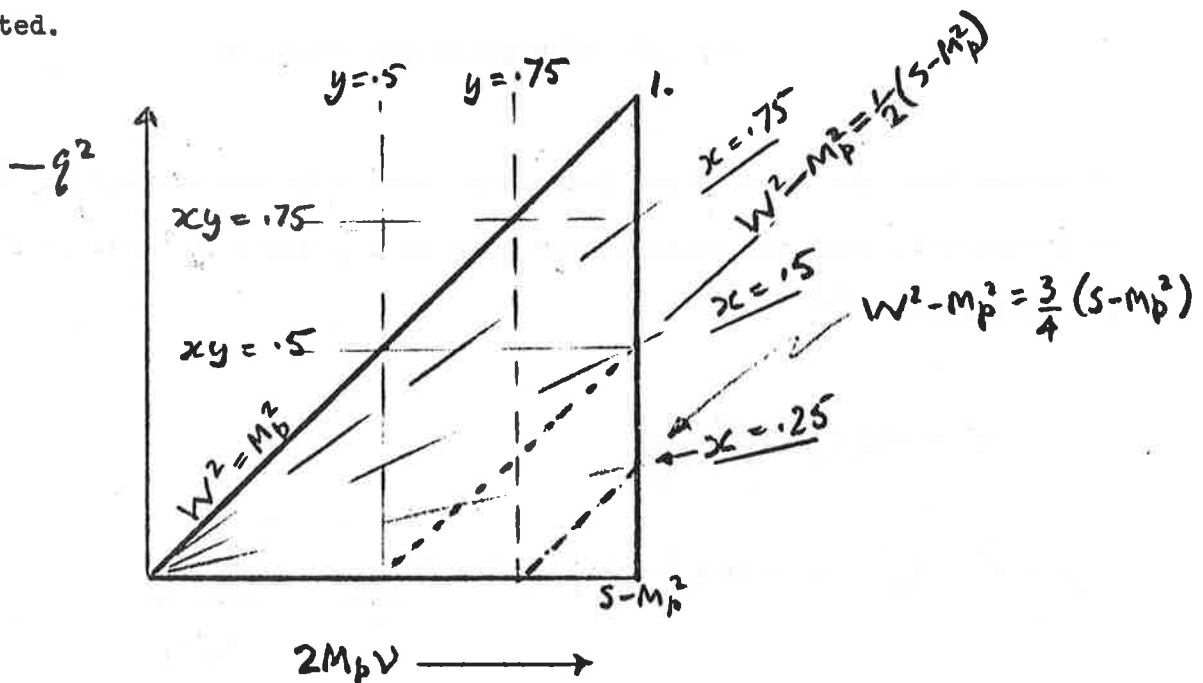

Fig. 5   Kinematic Invariants

The same region is shown in fig (7) in terms of the EPIC lab system parameters of the final state lepton and hadrons. In order to be specific, we have chosen $E_\ell = 8.5$ $E_p = 68$ $S \sim 2300$ which is at the lower end of the region under discussion for EPIC. We will discuss the lab kinematics in detail later.

It will be necessary to use some Simplistic Assumptions and Grandiose Apparatus in computing rates and designing an experiment.

The simplistic assumptions   are :-

    (a) Scaling continues to hold.

    (b) $F_2{}^\nu = 2xF_1{}^\nu = xF_3{}^\nu = 4F_2{}^\gamma = 8xF_1{}^\gamma$

        (Spin $\frac{1}{2}$ partons, no anti-partons, $|V| = |A|$ etc, neglect isoscalar part of $F_2{}^\gamma$)

    (c) $F_2{}^\gamma \simeq \frac{1}{3}(1-x^2)^3$
        (empirical, after Myatt and Perkins)

    (d) We will only consider $\Delta S = 0$ weak interactions.

Note that should this experiment become impossible due to the failure of these assumptions, EPIC physics will be the more interesting in other respects. From a general physics point of view the assumptions are pessimistic.

The differential cross-section for both weak and EM processes now become very simple when expressed in terms of x and y:[17]
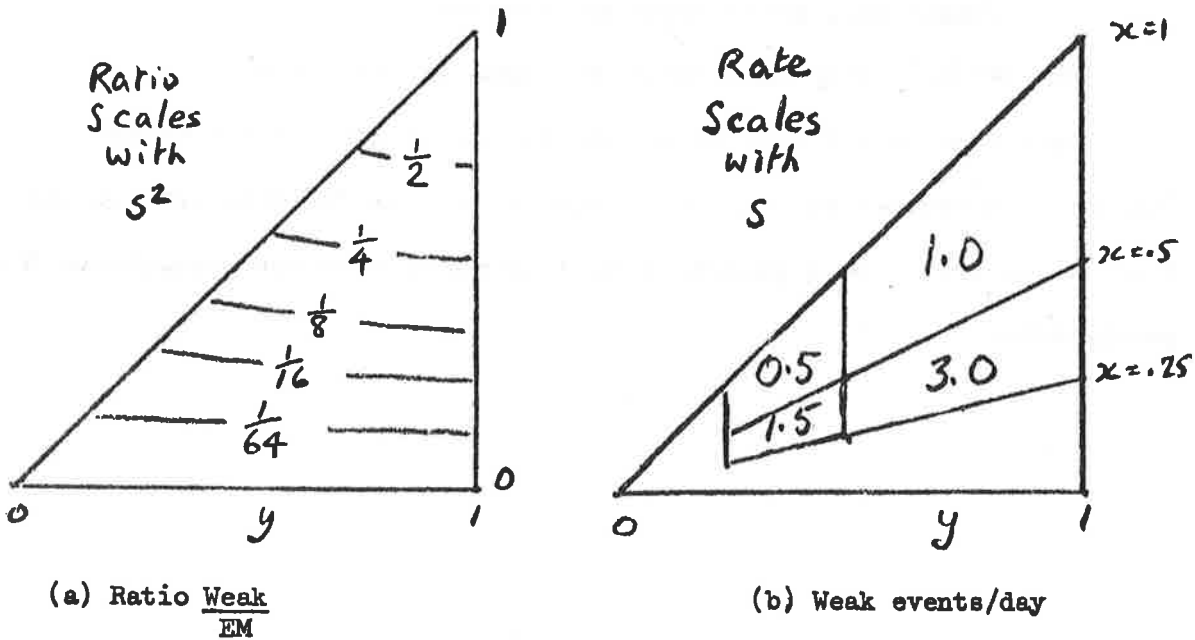
EM $$\frac{d\sigma^{\gamma}}{dxdy} = \frac{4\pi\alpha^2}{S} \quad \frac{q^4_{MAX}}{q^4} \quad F_2^{\gamma} \quad (1-y+y^2/2)$$

WEAK $$\frac{d\sigma^{\nu}}{dxdy} = \frac{G^2 S}{4\pi} F_2^{\nu} \left\{ \begin{array}{c} 1 \\ or \\ (1-y)^2 \end{array} \right\} \quad for \quad \left\{ \begin{array}{c} e^- \rightarrow \nu_e \\ e^+ \rightarrow \bar{\nu}_e \end{array} \right\}$$

and the ratio in the favourable case $e^- \rightarrow \nu_e$ is just

$$\frac{WEAK}{EM} = \frac{G^2 S^2}{4\pi^2\alpha^2} \quad \frac{q^4}{q^4_{MAX}} \quad \frac{1}{1-y+\frac{y^2}{2}}$$

Fig (6a) shows the ratio as a function of x and y for S ≃ 2800, where WEAK = EM at x = y = 1.

(a) Ratio $\frac{Weak}{EM}$ (b) Weak events/day

See Text for assumptions

Fig 6. Weak Interactions at S= 2800

For S $\approx$ 11,000 at the upper end of the conceivable EPIC range, the values

of the ratio would everywhere be X15 higher. The ratio is a reasonably well

behaved function of x and y so that we can have a good expectation of being

able to distinguish weak from EM processes over a large part of the allowed

kinematics, given the clear signature of missing transverse momentum in the

weak case, which we will discuss in detail below.

Weak interaction event rates are shown in fig (6) (b) above.

Unfortunately, the weak counting rates are not high at the assumed

luminosity of $\frac{1}{4}$ x 10^{32} : for S $\sim$ 2800, x > .5, y > .5 there are $\sim$ 1.0

weak events per day. At S $\sim$ 11,000 we are   4   times better off in rate

and in addition a larger piece of the triangle can be used because of the

15 -fold improvement in the weak/EM ratio.   A rate $\gtrsim$ 20 per day would seem

feasible. Although low, these rates are far from impossible, and there

would be no lack of physicists eager to try to observe weak processes in

the region where they are stronger than EM. Five days run at the upper limit

of S would yield as many events as were found in the famous two-neutrino

experiment, provided that our assumptions are valid.

We now return to the kinematics of the deep inelastic events in order to

design an apparatus.

In the process

$$e^- + \text{proton} \rightarrow \nu_e + \text{hadrons},$$

we must trigger on the hadrons and measure the total hadronic energy and

vector momentum. These must then be used to predict the energy and angle

of the supposed scattered lepton. Finally, we must prove that there is no

electron in the predicted region, or anywhere near it. (Of course, one would

be on the look out for violation of μ-e universality at the same time). The

relevant lab system kinematics are shown below in fig (7). They can

be obtained from equations (2) and (3).

(a) Scattered lepton

(b) Final Hadrons (Approx.)

$$p_\perp = \sqrt{Sxy(1-y)}$$
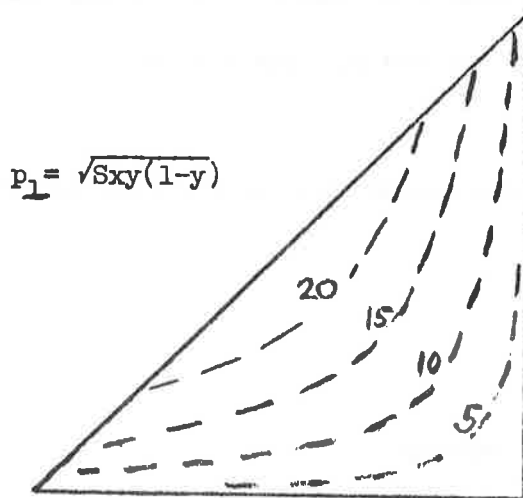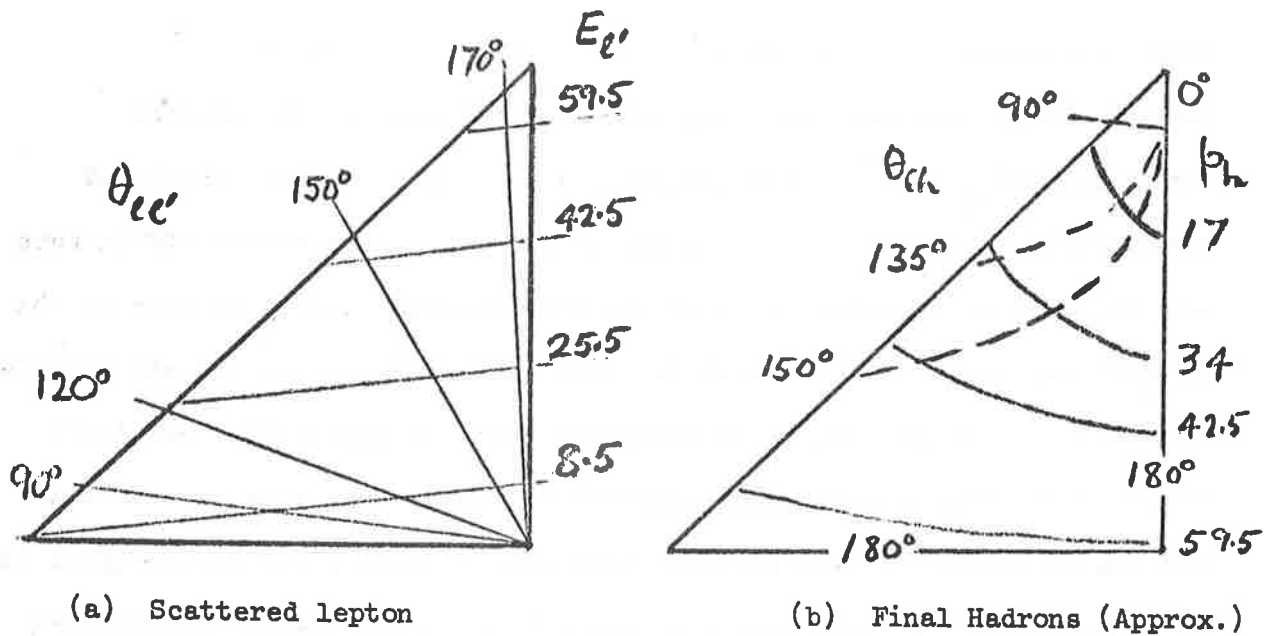
(c) Transverse Momentum

8.5 GeV leptons on 68 GeV protons

Fig 7   EPIC Laboratory System

The interesting region is at high q^2 - say $\gtrsim \frac{1}{4} q^2$ max - and it is immediately obvious from fig (7a) that the scattered lepton in these cases will be very easy to detect with high efficiency, if it is an electron. In only a small region of the kinematics does the scattered lepton come anywhere near the situation where it might be lost down the beam pipe. It always has a large energy and will give an unambiguous signal in a shower counter. The hadrons can be produced at somewhat smaller angles to the beam direction and one may sometimes loose a particle from the target fragmentation region. However, this will not introduce any error in the determination of the transverse momentum. A comparison of figs (7a) and (7c) shows that one needs only a good lower limit to the missing transverse momentum in order to predict a detectable lepton. If $\Sigma p_{\perp}$ > 10 GeV/c

hadrons

in the case we are considering, we can be certain of detecting the scattered lepton, if it is an electron.

In general, the hadronic system will have a moderate momentum, in the 20 to 40 GeV/c region, with a hadronic total energy of < 50 GeV. Typical hadron invariant masses are around 20 GeV/c^2 so that one can expect a multiplicity of say 6-10. Should multiplicity scale [18] with x in some way at very high energies rather than with W^2, one might have rather lower values. At any rate, a typical hadron will be $\sim$ 5 GeV/c, ranging up to $\sim$ 10 GeV/c. One can expect to find roughly one third of the final state lab energy in π^o mesons.

In fig (8) we show a possible detector which would have

    (a)   100% 2π coverage for $5^{\circ} < \theta < 175^{\circ}$ for all charged

           particles, with good momentum precision.

    (b)   100% (less cracks) coverage in the same angular region

           for γ rays, and for the identification of electrons.[19]

ΣE_{γ} and $\Sigma \vec{p}_{\gamma}$ for a total of 10 GeV going into γ-rays should be measurable to better than, say, $\pm$ 2 GeV. [20] For a field $\sim$ 20 kilogauss, charged particle momenta should be determined easily to a few per cent.

The axial field geometry is particularly good for complete azimuthal coverage of large transverse momenta, which is what we want. It is also compatible with operation of a very nicely balanced storage ring system. (A split field magnet would have to be designed in as part of the machine lattice).[21] Missing neutrons are a problem. In the discussion following the talk it was suggested that hadron calorimeters might be incorporated. This might be possible. In order not to destroy the very necessary good photon and electron resolution, they would have to be behind the lead glass counters. Since most of the missing neutrons and all of those at really large energies would be expected in the downstream direction from the incident proton beam (the target fragmentation region is close to that), such a hadron calorimeter need not be too big. However, roughly half of the events will not contain a neutron, so the problem is not critical. K^{o}_{L} would be another similar problem.
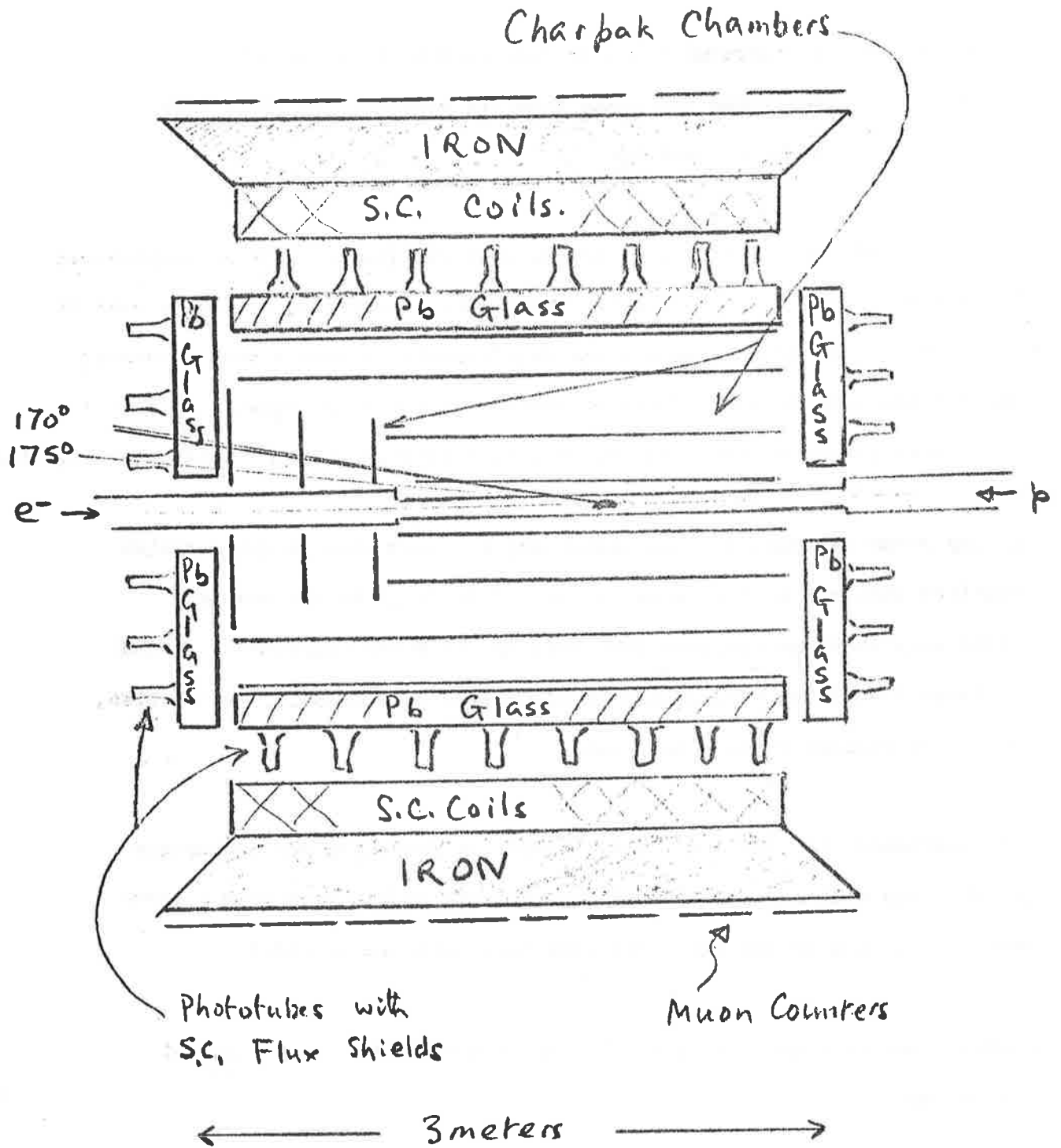
Fig. 8   SAGA Apparatus

A liberal use of superconductors is forseen both to produce the field, and to shield phototubes and beams from its effects. By 1981, these techniques [22] will be standard.

This is little more than a back of the envelope design, with no inhibitions about likely cost. It is, however, extremely encouraging to notice that it would be capable of meeting all the requirements to detect weak processes at EPIC and measure some of the properties of the final states, and yet it is no more grandiose than several devices currently in use or under construction.

A very rough estimate for the magnet and the lead glass counter system combined puts the cost at about £0.9m. This is quite reasonable, especially when one realises that many of the other experiments listed in Table I would be well suited to this detector. Clearly, in practise, one would economise where one could.

The conclusion is, then, that deep inelastic processes are measurable at EPIC and that several hundred events could be obtained if $S \sim 11000$ $(GeV)^2$, in a 20 day run. The experiment even seems easy!

References and Footnotes

1.   C. Pellegrini et al Proc 8th Intl. Conf. on High Energy Accelerators;
     CERN Sept. 1971 p 153.
     A.J. Egginton Proc. DNPL/RHEL working party Dec 1971 report
     RHEL/R 252 p 32.
     M. Allen et al Particle Physics with position-electron-proton
     colliding beams. April 1972. SLAC report 146/LBL report 750.

2.   At present, a scheme with missing RF power in its initial configuration
     is being examined. At first, the energies for ep collisions would
     be 12 GeV $e^{\pm}$, 100 GeVp. Later, with full RF power, collisions between
     14 GeV $e^{\pm}$ and 200 GeVp would be possible. G. Manning, remarks during
     discussion.

3.   e.g. P.V. Landshoff, this proceedings.

4.   R. Budny, this proceedings.

5.   see S.J. Brodsky Proc 1971 Intl. symposium on electron and photon
     interaction at high energies. Cornell University 1972, p14, for a review.

6.   K.J. Kim and Y.S. Tsai discuss the validity of the Weisäcker - Williams
     approximation in SLAC PUB 1106, Stanford Linear Accelerator Center, 1972.

7.   E. Gabathuler, this proceedings.

8.   F.E. Close, this proceedings.

9.   See, for example, J.D. Bjorken. Proc 1971 Intl. Symposium on electrons
     and photon interactions at high energies, Cornell 1972 p 282.
     K. Wilson, ibid, p 116.

10. C.H.Llewellyn Smith, this proceedings.

11. F.E. Close, Proc. Meeting on Polarised Targets Ed.Worden & Clark.
     RHEL Report, in preparation.

12. Ref 1, SLAC 146/LBL 750, gives results for the "photoproduction" of single W, i.e. For $\frac{S}{M_W^2} \gtrsim 8$, the cross-section is $\gtrsim 5 \times 10^{-37}$, which would give $\sim$ 1 event/day at EPIC luminosities. This is for S=4200.

13. J.K. KIM and Y.S. Tsai, SLAC PUB 1105, 1106. Stanford Linear Accelerator Center 1972.

14. Y.S. Tsai Phys. Rev D4, 2821 (1971).

15. The Breit frame is the frame in which the energy of the electron does not change. It coincides with the lab system for $\omega = \frac{2m\nu}{q^2} = p_p/p_\ell$

The final state hadrons are at rest in the lab for y=1, $q^2/q^2_{max} = \frac{p_p - p_\ell}{p_p}$ (see Fig. 7)

16. See F.E. Close, this proceedings.
and W. Venus " "

17. A factor of $\frac{1}{2}$ is included because the electrons are (longitudinally) unpolarised. See D. H. Perkins, Oxford Preprint 11/73. Should it be possible to precess the expected transverse polarisation of the EPIC electron beam into the longitudinal direction so that they have the correct helicity to produce neutrinos, the rates would be X2 larger.

18. There is experimental evidence (J. Dakin et al PRL 29, 746 (1972), J. Ballam et al SLAC PUB 1163 (1972)) that the multiplicity in inelastic ep scattering is somewhat less than in photoproduction at the same S. Most of the effect is due to a loss of diffractive ρ^o and is seen in the photon fragmentation region. For a summary of very high q^2 theoretical expectations, see J.D. Bjorken ref. 9, also P.V. Landshoff, ref 3.

19. Since the cylindrical spark chambers would have 100% azimuthal coverage, one could take into account any particles aiming at the edges of counters etc.

20. Lead glass counters are capable of substantially better precision. However, one should allow for the effects of non-uniformity for counter to counter in summing the energies of the γ-rays.

21. G. Rees, private communication.

22. F. Martin, S.J.St Lorant, W.T. Toner Nucl. Instr. Meth. <u>103</u>, 503 (1972).

ELECTRON-NEUTRON COLLIDING BEAM EXPERIMENTS

by

Erwin Gabathuler
Daresbury Nuclear Physics Laboratory

Recently, the possibility of doing experiments with colliding electron-proton beams to obtain very high values of S, the square of the total centre-of-mass energy has aroused a lot of interest. Storage ring systems under consideration are PEP (1) and ISABELLE (2) in the United States, and DORIS (3) and EPIC (4) in Europe.

It is important at this stage to note that storage rings can, in principle, store deuterons as well as protons provided (a) an injector is available to provide deuterons as well as protons and (b) the frequency range of the radio-frequency accelerating system is sufficiently wide to allow for the larger range of velocities. The spectator nucleon then provides a very simple method of tagging the electron-proton or electron-neutron reaction.

Experiments which are under way or planned at NAL and CERN II to study lepton-nucleon interactions are:

1. $\quad \ell^{\pm} + A \quad \rightarrow \quad \ell^{\pm}$ + hadrons (inclusive)

2. $\quad \ell^{\pm}$ + proton $\quad \rightarrow \quad \ell^{\pm}$ + hadrons (inclusive), $\pi^{\pm}$, $K^{\pm}$, etc.

   $\rightarrow \quad \ell^{\pm}$ + exclusive channels.

3. $\quad \ell^{\pm}$ + neutron $\rightarrow \quad \ell^{\pm}$ + hadrons (inclusive), $\pi^{\pm}$, $K^{\pm}$, etc.

   $\rightarrow \quad \ell^{\pm}$ + exclusive channels.

4. $\ell^{\pm}$ (polarised) + proton (polarised) $\rightarrow$ $\ell^{\pm}$ + hadrons (inclusive), etc.

$\rightarrow$ $\ell^{\pm}$ + exclusive channels.

These experiments will be capable of probing the structure of the nucleon for a value of S of the order of 500 GeV/c^2, which is equivalent to a 5 GeV electron incident on a 25 GeV/c proton. The very large increase in S obtained by colliding a 10 GeV/c electron on a 100 GeV/c proton will certainly probe a new range of the proton's structure. However if in addition the structure of the neutron could be probed if only to a value of S/2, then the range of physics of the facility could be greatly extended since the photon is a mixture of iso-scalar and isovector components and the proton and neutron have different charge constituents.

1   TOTAL PHOTON CROSS SECTIONS

$$\sigma(\gamma p) = \gamma + proton = I_0 + I_1 \quad \{isospin\ components\}$$
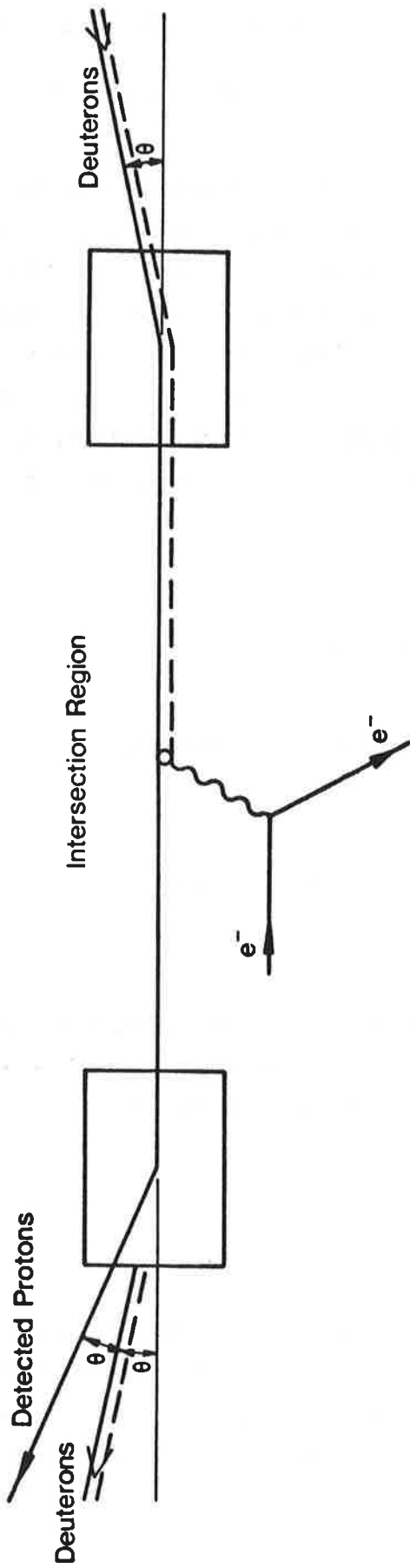
$$\sigma(\gamma n) = \gamma + neutron = I_0 - I_1$$

$$\sigma(\gamma p) + \sigma(\gamma n) = Pomeron\ (\alpha = 1) + P'\ (\alpha = 1/2)$$

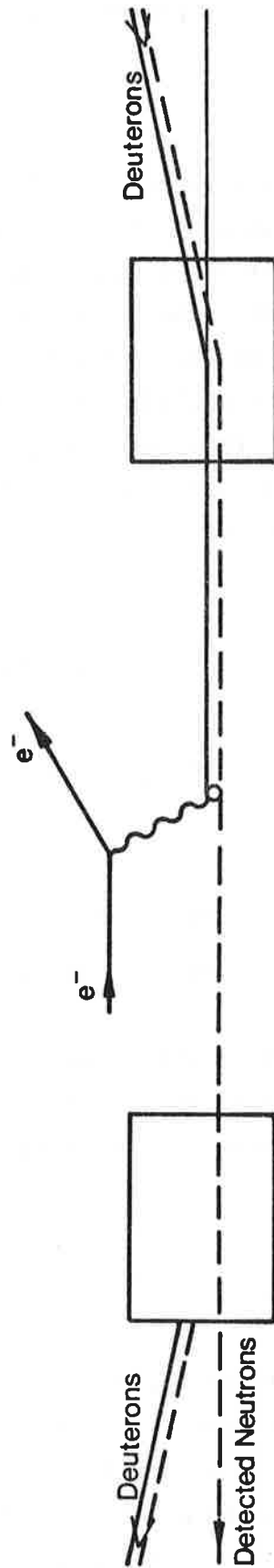$$\sigma(\gamma p) - \sigma(\gamma n) = A_2\ (\alpha = 1/2)$$

A direct comparison gives the amount of diffractive/non-diffractive cross section for large S. In addition with the facility to vary S over such a wide range, it should be possible to make a separation between P and P'.

2   STRUCTURE FUNCTIONS

For larger q^2, it is possible to take these ideas over to models which require the nucleon to consist of partons/quarks and give various predictions for the ratio of electron-neutron/electron-proton structure functions. There are also sum rules which relate the weak and electromagnetic interactions via their structure functions.

Deuterons

θ

Intersection Region

e⁻

e⁻

e⁻ + n ⟶ e⁻ + Tagged Proton Spectator

Detected Protons

Deuterons

θ   θ

Deuterons

e⁻

e⁻

e⁻ + p ⟶ e⁻ + Tagged Neutron Spectator

Deuterons

Detected Neutrons

Figure 1

3   WEAK INTERACTIONS

If it is assumed that the neutrino cross sections continue to rise linearly as S increases then it would be interesting to study and compare particle yields and correlations for

$$(a) \qquad e^+ + p \rightarrow \bar{\nu} + \text{Hadrons } (H^{++})$$

$$(b) \qquad e^- + p \rightarrow \nu + \text{Hadrons } (H^0)$$

$$(c) \qquad e^+ + n \rightarrow \bar{\nu} + \text{Hadrons } (H^+)$$

$$(d) \qquad e^- + n \rightarrow \nu + \text{Hadrons } (H^-)$$

If it was possible to achieve sufficient luminosity then the use of neutron targets provide a very clear test of $\Delta S = \Delta Q$ at these high energies since

$$e^- + n \rightarrow \nu + \Sigma^- \quad (\Delta S = \Delta Q)$$

$$e^+ + n \rightarrow \bar{\nu} + \Sigma^+ \quad (\Delta S \neq \Delta Q)$$

For all of these measurements, it would be very valuable if the experiment could be triggered or selected on an electron-proton or an electron-neutron interaction rather than to using a subtraction technique. A possible method of achieving this is illustrated for the electromagnetic interactions in fig. 1. Here the disadvantage of the shared momenta of the two nucleons in the deuteron in achieving high S is used to advantage in bending the spectator protons out of the storage ring. A direct ratio of electron-neutron to electron-proton cross sections can be measured by tagging the spectator neutron and the effect of the usual deuterium corrections can be minimised for absolute cross sections by a comparison with similar measurements on free protons. In the case where the outgoing hadron comes off along the direction of the spectator, then the number of electron-neutron plus proton coincidences can be measured as a function of proton momenta and the necessary corrections can be made for both outgoing neutrons and protons. In general the electron comes off at large angles, so that the coincidence between the spectator nucleon and the electron can be easily obtained.

REFERENCES

1.   Positron Electron Colliding Beams, SLAC-121, November 1970.

2.   J.P. Blewett et al., BNL Report CRISP 71-14, 1971.

3.   H. Gerke et al., DESY Report, H-72/22, 1972.

4.   D.A. Gray, RHEL/R.252, 1972.

EPIC Ways of Studying Weak Bosons

Robert Budny

Department of Theoretical Physics
University of Oxford

I wish to indicate the feasibility of studying weak inter-
actions with future electron-positron storage rings being considered
such as the EPIC II with beam energies of 14 GeV and luminosity of
10^{32}. For this I will consider weak boson effects in the reactions

$$e^+e^- \longrightarrow \mu^+\mu^- \qquad\qquad (1a)$$

$$e^+e^- \longrightarrow \nu\bar{\nu} \qquad\qquad (1b)$$

within the framework of Weinberg's[1] unified theory of weak and
electromagnetic interactions. In this theory the masses of the
charged and neutral intermediate vector bosons depend on a parameter,
the unifying angle

$$\theta_u = \tan^{-1}\frac{g'}{g}, \qquad\qquad (2)$$

whose value appears to be limited above by approximately 60° since
there is only one candidate event for the reaction $\bar{\nu}_\mu e^- \rightarrow \bar{\nu}_\mu e^-$
discussed earlier by Cundy[2]. Other evidence, such as the scarcity
of neutral neutrino pion production events[3] like $\nu p \rightarrow \nu p \pi^0$, suggests
that θ_u must be larger than roughly 40°.

The lowest order causes of reaction (1a) are given in Figure I.
Some of the two photon diagrams are infrared divergent, requiring
consideration of the bremsstrahlung diagrams in figure II. Together
they generate cross sections highly dependent upon the experimental
arrangement, and, possibly comparable to the cross section from
the one photon approximation. Examples with $q^2 \leq 25$ GeV^2 are given
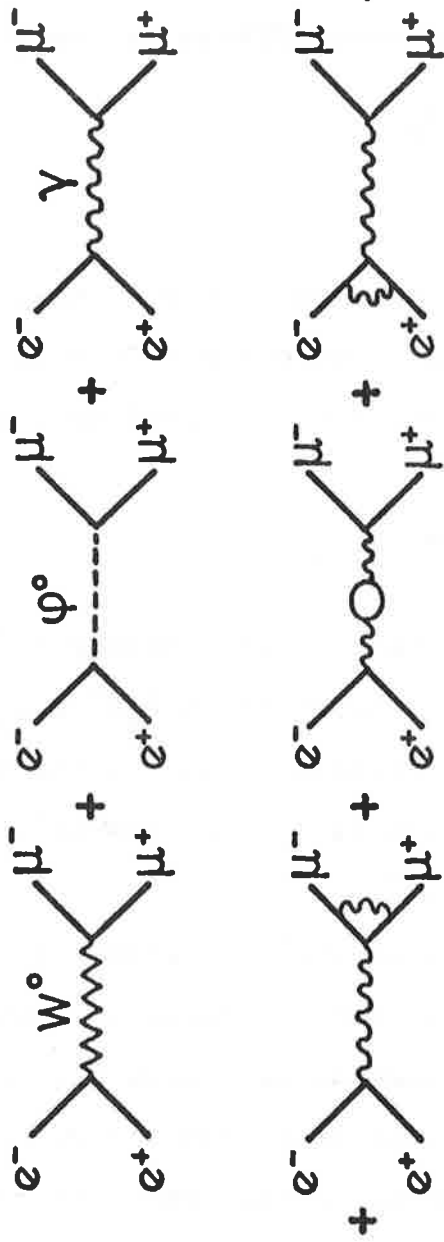by Berends et al.[4]. I will ignore this complication.
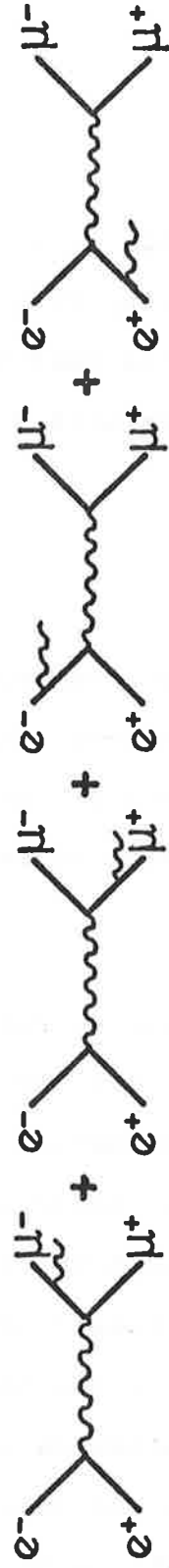
Fig.1   Diagrams for $e^+e^- \rightarrow \mu^+\mu^-$.

Fig.2   Diagrams for $e^+e^- \rightarrow \mu^+\mu^-\gamma$.

The amplitudes for the one γ, φ^0 and W^0 diagrams in Figure I, with the Bjorken and Drell conventions[5] are

$$\mathcal{M}_{W^0} = \frac{-i(g^{\alpha\beta}+\lambda q^\alpha q^\beta)}{q^2-M_0^2}\, \bar{u}_3\gamma_\alpha(g_V+g_A\gamma_5)v_4\bar{v}_2\gamma_\beta(g_V+g_A\gamma_5)u_1$$

$$\mathcal{M}_{\varphi^0} = \frac{-i\sqrt{2}\,Gm_em_\mu}{q^2-M_\varphi^2}\,\bar{u}_3v_4\bar{v}_2u_1 \tag{3}$$

$$\mathcal{M}_\gamma = \frac{-ie^2}{q^2}\,\bar{u}_3\,\gamma_\alpha\,v_4\,\bar{v}_2\,\gamma^\alpha\,u_1$$

where indices 1, 2, 3, 4 refer to e^-, e^+, μ^-, μ^+ and $q_\alpha=(p_1+p_2)_\alpha$. In the Weinberg theory the mass M_φ of the scalar Higgs particle is unspecified, but the masses of the vector bosons and the form factors are given by

$$M_0^2 = \frac{e^2}{\sqrt{2}G\sin^2 2\theta_u}$$

$$M_-^2 = \frac{e^2}{4\sqrt{2}G\sin^2\theta_u} \tag{4}$$

$$g_V = \frac{e(4\sin^2\theta-1)}{2\sin 2\theta_u}$$

$$g_A = \frac{e}{2\sin 2\theta_u}$$

For operating storage rings $\mathcal{M}_\gamma$ dominates $\mathcal{M}_{W^0}$ and $\mathcal{M}_{\varphi^0}$ since q^2 is small, but at higher q^2, contributions from $\mathcal{M}_{W^0}$ increase and eventually dominate. To see this consider the differential cross section of (1a) when the μ^- and μ^+ have helicities h_3 and h_4, and when the e^- and e^+ have spin polarizations $s_1^\alpha = (0,-s\hat{B}) = -s_2^\alpha$ along the field $\vec{B}$ of the bending magnets (as tends to happen in storage rings). The result from $\left|\mathcal{M}_\gamma + \mathcal{M}_{W^0}\right|^2$, neglecting lepton

masses and evaluating in the laboratory frame = center of momentum frame where $q^2 = 4E^2$, is

$$\frac{d\sigma}{d\Omega}(\mu^+\mu^-) = \frac{\alpha^2}{16q^2}\left\{(1-h_3h_4)\left[F_1(1+\cos^2\Theta)-F_2s^2\sin^2\Theta\cos2\varphi+F_3\cos\Theta\right]\right.$$

$$\left. +(h_3-h_4)\left[F_4(1+\cos\Theta)^2-F_5s^2\sin^2\Theta\cos2\varphi\right]\right\} \tag{5}$$

The scattering angle Θ and asymuthal angle φ from $\vec{s}_1$ are defined by $p_1 \cdot p_3 = E^2(1-\cos\Theta)$ and $s_1 \cdot p_3 = -sE\sin\Theta\cos\varphi$, and the Θ_u and q^2 dependant factors F_{1-5} by

$$F_1 \equiv 1+2g_V^2R+(g_V^2+g_A^2)^2R^2$$

$$F_2 \equiv 1+2g_V^2R+(g_V^4-g_A^4)R^2$$

$$F_3 \equiv 4g_A^2R\left[1+2g_V^2R\right] \tag{6}$$

$$F_4 \equiv 2g_Vg_AR\left[1+(g_V^2+g_A^2)R\right]$$

$$F_5 \equiv 2g_Vg_AR\left[1+(g_V^2-g_A^2)R\right]$$

$$R \equiv \frac{q^2}{e^2(q^2-M_0^2)}$$

The average helicity of the μ^-, given by $d\sigma(h_3) \equiv \sum_{h_4}\frac{d\sigma}{d\Omega}(\mu^+\mu^-)$, is

$$\langle h_3 \rangle \equiv \frac{d\sigma(+1)-d\sigma(-1)}{d\sigma(+1)+d\sigma(-1)} \tag{7}$$

$$= \frac{F_4(1+\cos\Theta)^2-F_5s^2\sin^2\Theta\cos2\varphi}{F_1(1+\cos^2\Theta)-F_2s^2\sin^2\Theta\cos2\varphi+F_3\cos\Theta}$$

Several special cases of $d\sigma(h_3)$ and $\langle h_3 \rangle$ have been published. Long ago Cabibbo and Gatto[6] considered the case where $s = 0$ and

$g_V = -g_A$. Their results are consistent with (5) but slightly inconsistent with (7), probably due to a typographical error. Recently Godine and Hankey[7] gave the case where the terms from $\left|\mathcal{M}_{W^0}\right|^2$ (the R^2 terms in F_{1-5}) are neglected. Their results agree in magnitude but disagree concerning the signs of $F_{3,4,5}$. They discussed the feasibility of testing Weinberg's theory with SPEAR at $q^2 = 36\ GeV^2$. Love[8] published an expression for $\langle h_3 \rangle$ when $\Theta = \frac{\pi}{2}$ and $\varphi = 0$ which is implied by (7). Cung et al.[9] have considered the case $g_V = -g_A$ and give results implied by (5) and (7).

When q^2 is negligible compared with M_0^2, the R dependent terms in F_{1-5} are negligible due to the limits

$$\frac{1}{q^2 - M_0^2} \begin{Bmatrix} g_V^2 \\ g_V g_A \\ g_A^2 \end{Bmatrix} \longrightarrow -\frac{G}{2/2} \begin{Bmatrix} (4\sin^2\Theta_u - 1)^2 \\ 4\sin^2\Theta_u - 1 \\ 1 \end{Bmatrix} \qquad (8)$$

The remaining contributions are the 1 terms in $F_{1,2}$ from $\left|\mathcal{M}_\gamma\right|^2$ which give the total cross section

$$\sigma_0 = \sum_{h_{3,4} = \pm 1} (1 - h_3 h_4)\ \frac{\pi\alpha^2}{3q^2} = \frac{4\pi\alpha^2}{3q^2} \qquad (9)$$

This generates 10^{-2} events/second with beams of 14 GeV and 10^{32} luminosity and is a convenient standard for comparing weak effects since, according to parton and current algebra models and measurements, it is comparable to the total rate for producing hadrons.

As q^2 increases towards $M_{W^0}^2$ the magnitude of R and thus of the W^0 contributions to (5) increase. For instance, the effects of W^0 interference on the rate, the $\cos\Theta$ asymmetry, and the μ helicity indicated by the second term in F_1, and the first terms in F_3 and F_4 respectively. Their percent values are given in figure III at $q^2 = (28\ GeV)^2$. In the range $40° \leq \Theta_u \leq 60°$ their magnitudes appear sufficiently large to be easily measurable.
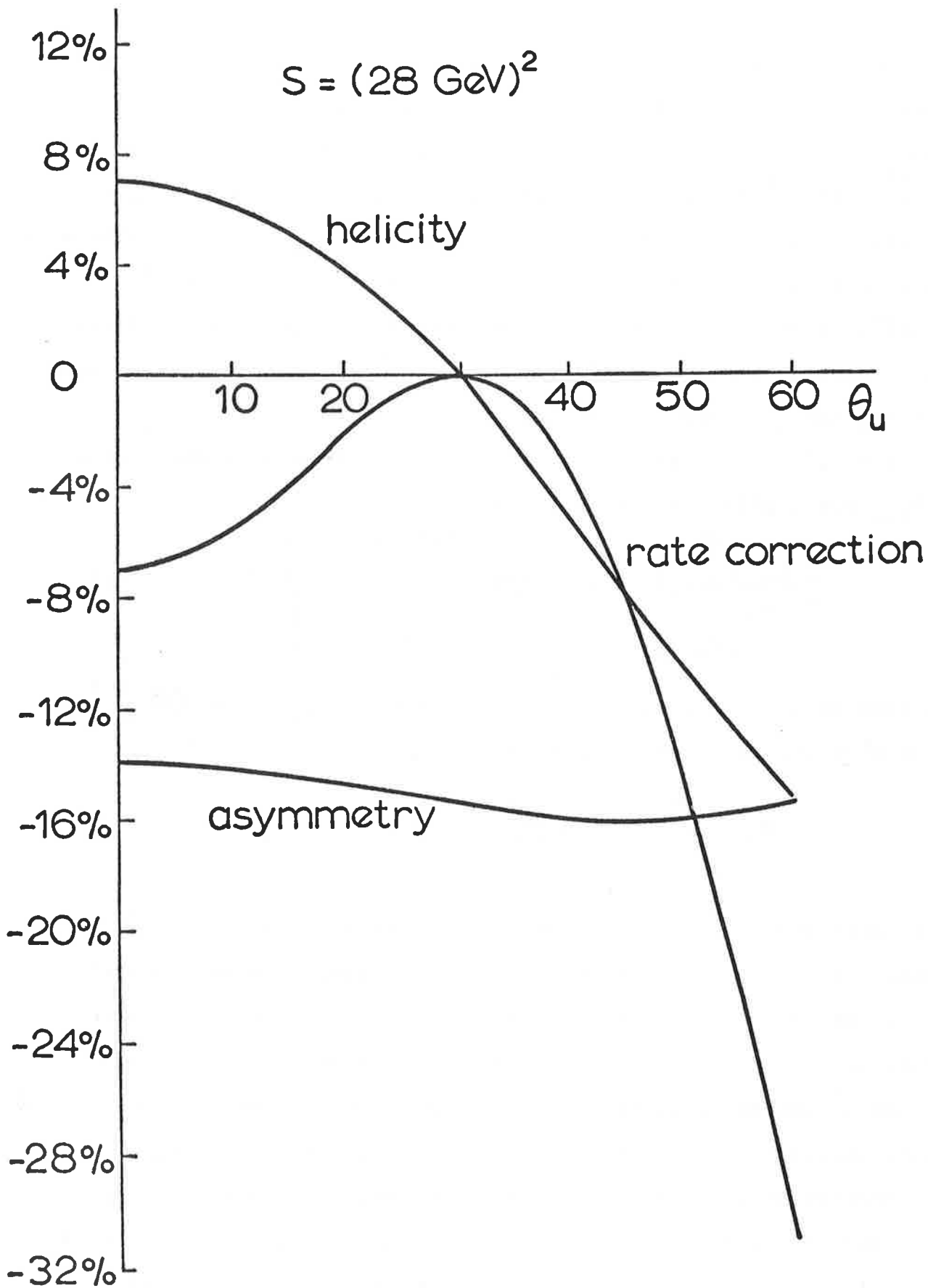
Fig. 3

Percent changes in the rate and amount of asymmetry
and helicity in $e^+e^- \rightarrow \mu^+\mu^-$ due to W^0 interference.

The effect of the Higgs particle can be estimated from the cross section corresponding to $\left|\mathcal{M}_\gamma + \mathcal{M}_{\varphi^0}\right|^2$. The result from (3), summed over $h_{3,4}$ and averaged over $s_{1,2}$ is

$$\sigma = \sigma_0 + \frac{G(m_e m_\mu)^2}{16\pi q^2 (q^2 - M_\varphi^2)} \left\{ \sqrt{2}^3 e^2 + \frac{Gq^4}{q^2 - M_\varphi^2} \right\} \tag{10}$$

The $(m_e m_\mu)^2$ factor, which results from the coupling of the φ^0, makes the φ^0 effect extremely small compared to σ_0 except possibly at the pole if the width of φ^0 is extremely narrow.

The beam depletion reaction (1b) is a curious novelty for storage rings. It is related by crossing to the reaction $\bar{\nu}_\mu e \to \bar{\nu}_\mu e$ discussed by Cundy. The lowest order diagrams for $\nu_e \bar{\nu}_e$ production are given in figure IV. For $\nu_\mu \bar{\nu}_\mu$ production the second does not contribute since $W^- \not\to e^- \bar{\nu}_\mu$. Their amplitudes are

$$\mathcal{M}_{\nu_e \bar{\nu}_e} = -i\bar{u}_3 \gamma_\alpha (1-\gamma_5) v_4 \bar{v}_2 \gamma^\alpha (G_{eV} + G_{eA}\gamma_5) u_1$$

$$\mathcal{M}_{\nu_\mu \bar{\nu}_\mu} = -i\bar{u}_3 \gamma_\alpha (1-\gamma_5) v_4 \bar{v}_2 \gamma^\alpha (G_{\mu V} + G_{\mu A}\gamma_5) u_1$$

$$G_{\mu V} \equiv \frac{1}{q^2 - M_0^2} \left[\frac{e^2 (4\sin^2\theta_u - 1)}{4\sin^2 2\theta_u} \right]$$

$$G_{\mu A} \equiv \frac{1}{q^2 - M_0^2} \left[\frac{e^2}{4\sin^2 2\theta_u} \right] \tag{11}$$

$$G_{eV} \equiv G_{\mu V} + T$$

$$G_{eA} \equiv G_{\mu A} - T$$

$$T \equiv \frac{1}{(k_3 - k_1)^2 - M_-^2} \left[\frac{e^2}{8\sin^2\theta_u} \right]$$

The cross sections, averaged on $e^- e^+$ spins, are given by

$$\frac{d\sigma}{d\Omega}(\nu\bar{\nu}) = \frac{q^2}{(8\pi)^2} \left\{ (G_V - G_A)^2 (1+\cos\theta)^2 + (G_V + G_A)^2 (1-\cos\theta)^2 \right\} \tag{12}$$
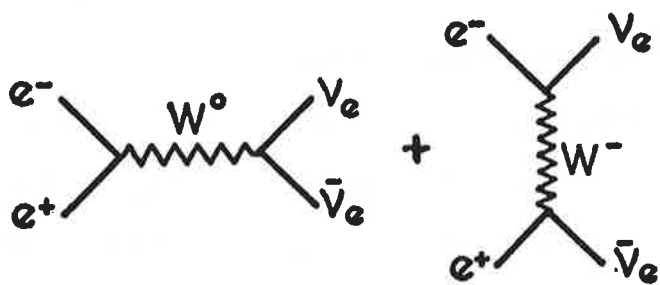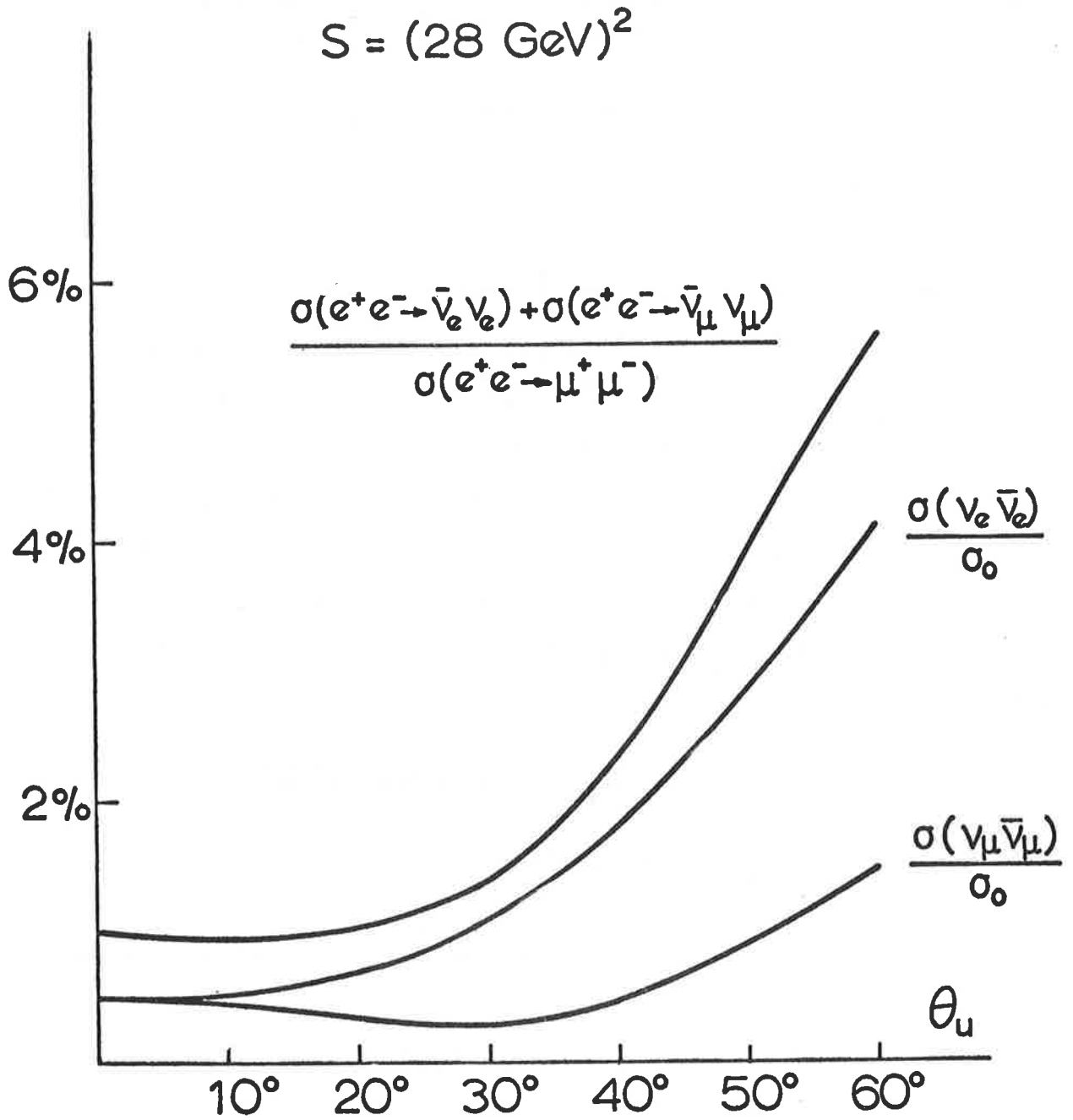
Fig.4

Diagrams for $e^+e^- \to \nu_e \bar{\nu}_e$.

$$S = (28 \text{ GeV})^2$$

$$\frac{\sigma(e^+e^- \to \bar{\nu}_e \nu_e) + \sigma(e^+e^- \to \bar{\nu}_\mu \nu_\mu)}{\sigma(e^+e^- \to \mu^+\mu^-)}$$

$$\frac{\sigma(\nu_e \bar{\nu}_e)}{\sigma_0}$$

$$\frac{\sigma(\nu_\mu \bar{\nu}_\mu)}{\sigma_0}$$

θ_u

Fig.5

Ratios in percent of $\sigma(e^+e^- \to \nu_\mu \bar{\nu}_\mu)/\sigma(e^+e^- \to \mu^+\mu^-)$,

$\sigma(e^+e^- \to \nu_e \bar{\nu}_e)/\sigma(e^+e^- \to \mu^+\mu^-)$, and their sum.

with the appropriate e or μ form factors. These integrate to

$$\sigma(\nu_\mu \bar{\nu}_\mu) = \frac{q^2}{6\pi}\left\{ G_{\mu V}^2 + G_{\mu A}^2 \right\}$$

$$\sigma(\nu_e \bar{\nu}_e) = \sigma(\nu_\mu \bar{\nu}_\mu) + \frac{q^2 a}{16\sin^2\theta_u}\left\{ (G_{\mu A} - G_{\mu V})I_1 + \frac{\pi a}{2\sin^2\theta_u} I_2 \right\}$$

$$I_1 \equiv \frac{4}{q^2}\left\{ 2(1+\frac{M_-^2}{q^2})\left[(1+\frac{M_-^2}{q^2})\ln(1+\frac{q^2}{M_-^2})-1\right] -1\right\}$$

$$I_2 \equiv -\frac{dI_1}{d(M_-^2)}$$

(13)

which are of the order of the $\left|\mathcal{M}_{wo}\right|^2$ terms in (5).

The ratios of $\sigma(\nu_\mu \bar{\nu}_\mu)$, $\sigma(\nu_e \bar{\nu}_e)$, and $\sigma(\nu_\mu \bar{\nu}_\mu) + \sigma(\nu_e \bar{\nu}_e)$ to σ_0 are given in figure V when $q^2 = (28 \text{ GeV})^2$. In the plausible range for θ_u the latter is at most 6% and thus not of practical interest or concern, but this ratio increases rapidly with q^2. For instance if $\theta_u = 60^\circ$, the masses of the W^0 and W^- would be 87 and 43 GeV and the propagators are still approximately real when $q^2 = (40 \text{ GeV})^2$. There $\sigma(\nu_\mu \bar{\nu}_\mu) = 0.08\,\sigma_0$ and $\sigma(\nu_e \bar{\nu}_e) = 0.18\,\sigma_0$. When $q^2 \gg M_0^2$, these have the limits

$$\sigma(\nu_\mu \bar{\nu}_\mu) \rightarrow \frac{\pi a^2}{6q^2}\left[\frac{16(\sin^2\theta_u - \frac{1}{4})^2+1}{\sin^4 2\theta_u} \right]$$

$$\sigma(\nu_e \bar{\nu}_e) \rightarrow \frac{a G}{2\sqrt{2}\sin^2\theta_u}$$

(14)

The first is comparable to σ_0, but since the second is independent of q^2, it eventually dominates.

To conclude, at $q^2 = (28 \text{ GeV})^2$ the Weinberg theory predicts W^0 interferences in $e^+ e^- \rightarrow \mu^+ \mu^-$ which can effect measurables by as much as 30%. The effects of the φ^0 appear very small, and beam depletion via $e^+ e^- \rightarrow \nu\bar{\nu}$ is not large enough to be a nuisance. The quantitative results are highly dependent on the specific form of the coupling of the weak bosons in the Weinberg theory, but similar results should hold for related theories. If such theories have not been disproven before EPIC-like storage rings are constructed, they will be abundant sources of grist.

References

1. S. Weinberg, Phys. Rev. Letters $\underline{19}$, 1264 (1967).

2. D. Cundy, these proceedings.

3. C. Albright, B. W. Lee, and E. A. Paschos, NAL-THY-86 (1972).

4. F. A. Berends, K. J. F. Gaemers, and R. Gastmans, Ref. TH.1562-CERN (1972).

5. J. D. Bjorken and S. Drell, Relativistic Quantum Mechanics, New York, 1964.

6. N. Cabibbo and R. Gatto, Phys. Rev. $\underline{124}$, 1577 (1961).

7. J. Godine and A. Hankey, Phys. Rev. $\underline{D6}$, 3301 (1972).

8. A. Love, Lettere al Nuovo Cimento $\underline{5}$, 113 (1972).

9. V. K. Cung, A. K. Mann, and E. A. Paschos, Phys. Letters $\underline{41B}$, 355 (1972).